Prediction of Draft Forces on Small-Scale Tillage Power in Different Soil Types using Mathematical Model

Thomas Gebre Lemma

A Dissertation Submitted to the Department of Mechanical Engineering
College of Mechanical, Chemical and Materials Engineering
Presented in Partial Fulfillment of the Requirement for the Degree of
Doctor of Philosophy

In

Agricultural Machinery Engineering

Office of Graduate Studies
Adama Science and Technology University

March, 2025
Adama, Ethiopia

Prediction of Draft Forces on Small-Scale Tillage Power in Different Soil Types using Mathematical Model

Thomas Gebre Lemma

Main Supervisor: Dr. Teshome Yitbarek (Associate Professor)

Co-Supervisor: Dr. Amana Wako (Associate Professor)

A Dissertation Submitted to the Department of Mechanical Engineering

College of Mechanical, Chemical and Materials Engineering Presented in Partial Fulfillment of the Requirement for the Degree of Doctor of Philosophy

In

Agricultural Machinery Engineering

Office of Graduate Studies

Adama Science and Technology University

March, 2025

Adama, Ethiopia

Declaration

I hereby declare that this Dissertation entitled “Prediction of Draft forces on small-Scale Tillage Power in different soil Types using Mathematical Model” is my original work. That is, it has not been submitted for the award of any academic degree, diploma or certificate in any other university. All sources of materials used for this thesis have been duly acknowledged through appropriate citations.

Name of student	signature	Date

Recommendation

We, the supervisors of this dissertation, hereby certify that we have read and revised the dissertation entitled “Prediction of Draft forces on small-Scale Tillage Power in different soil Types using Mathematical Model” prepared under our guidance by Thomas Gebre Lemma submitted in partial fulfillment of the requirements for the degree of Doctor of Philosophy in Agricultural Machinery Engineering. Therefore, we recommend the submission of the dissertation to the department for further review and defense.

Major Supervisor	Signature	Date
Co-supervisor	Signature	Date

Approval of Board of Examiners

We hereby certify that the recommendations and suggestions made by the board of examiners are appropriately incorporated into the final version of the dissertation entitled "Prediction of Draft forces on small-Scale Tillage Power in different soil Types using Mathematical Model" by Thomas Gebre Lemma.

Major Supervisor	Signature	Date
Co-supervisor	Signature	Date

We, the undersigned, are members of the Board of Examiners of the dissertation open defense by Thomas Gebre Lemma. We have read and evaluated the dissertation titled "Prediction of draft forces on small-Scale tillage Power in different soil types using mathematical model" and examined the candidate during the open defense. The dissertation approval has been to partial fulfillment of the requirements for the Doctor of Philosophy degree in Agricultural Machinery Engineering.

Chairperson	Signature	Date
Internal Examiner	Signature	Date
Dr Alemayehu Regassa Tolosa		03/04/2025
External Examiner 1	Signature	Date
Dr. Pankaj Gupta		18/03/2025
External Examiner 2	Signature	Date

Finally, approval and acceptance of the dissertation is contingent upon submission of its final copy to the Office of Postgraduate Studies (OPGS) through the candidate's Department Graduate Council (DGC) and College Graduate Committee (SGC).

Department Head	Signature	Date
College Dean	Signature	Date
Office of Postgraduate Studies, Dean	Signature	Date

AKNOWLEDGEMENT

The work carried out during the period 2019-2024 at the Department of Mechanical Engineering, Adama Science and Technology University, Adama, Ethiopia. I have many people to thank for their help and support in this. I would like to express my deep indebtedness to my main supervisor, Dr. Teshome Yitbarek (Associate Professor), Wolkite University, Ethiopia, for his guidance, support, and enthusiastic encouragement throughout the entire period of this research, which enabled me to complete this important milestone in my life. In addition, I would like to thank my co-supervisor, Dr. Amana Wako (Associate Professor), who assisted me in making this study possible by providing me with his professional skills and inspiration to overcome the challenges I faced during my PhD research work.

I extend my appreciation to the members of my doctoral committee Dr. Siraj K Busse, Dr. Getachew Alemayehu and Dr. Ramish Babu; whose valuable insights and constructive feedback have played a pivotal role in shaping the outcome of this research. Additionally, I would like to thank the mechanical engineering department for providing a good environment for academic growth.

Finally, I would like to thank my Mother Askale Badiy for all she had given me throughout my lifetime. I would also like to give special thanks to my wife Tsega G/Hiwot G/Mdehin for her support and sacrifice even if she is not in a good health condition. I am grateful to my brother Wolde Gebre lemma for his constant support and to all others who gave me the opportunity to complete the study.

TABLE OF CONTENTS

CONTENTS PAGE
Declaration III
Recommendation IV
Approval of Board of Examiners V
AKNOWLEDGEMENT vi
TABLE OF CONTENTS vii
LIST OF TABLES xi
LIST OF FIGURES xiv
Acronyms and Abbreviations xvi
Abstract xviii
CHAPTER ONE 1
INTRODUCTION 1
1.1 Background 1
1.2 Problem Statement 4
1.3 Objectives of the Research 5
1.3.1 General Objective 5
1.3.2 Specific Objectives 6
1.4 Expected outcomes of the study 6
1.5 Significance of the Study 6
1.6 Scope and Limitations of the Study 7
1.7 Structure of the Dissertation 7
CHAPTER TWO 8
LITERATURE REVIEW 8
2.1 Classification of Soil Types and Their Characteristics 8
2.1.1 Soil properties and soil mechanics 8
2.1.2 Soil Type 9
2.2 Soil Mechanics 11
2.2.1 Soil strength 12
2.2.2 Soil Mechanics Fundamentals 14
2.3 Tillage Tools 14
2.3.1 Tool geometry parameters 14

2.3.2 Mouldboard Plow 15
2.4 Operational Conditions 16
2.4.1 Operational speed 16
2.4.2 Working depth 16
2.5 Development of the Mathematical Model 16
2.6 Mathematical Model for Predicting Draft Force of Tillage Tools 17
2.7 Dimensional Analysis to Develop a Mathematical Model 18
2.7.1 Dimensional Analysis approach 19
2.7.2 PI-Buckingham theorem 20
2.7.3 Similitude 20
2.8 Draft Force Parameters of the Functional Variables 21
2.9 Socio-economic Approach of Smallholder Farmers in Ethiopia 22
2.9.1 Socio-economic characteristics of smallholder farmers 23
2.9.2 Socio-economic Benefit of small-scale tillage to Smallholder Farmer 23
2.10 Draft Force Measurement 23
2.11 Experimental Design (DoE) 24
2.11.1 Optimization of the Draft Force 24
2.11.2 Linear model 24
2.12 Validation and verification of models 25
2.13 Mathematical Models for Predicting Draft Force of Tillage Tools 26
2.14 Summary of key findings from the literature review 29
CHAPTER THREE 31
MATERIALS AND METHODS 31
3.1 Description of the Study Areas 31
3.2 Specifications of Tillage Tools 32
3.2.1 Ard Plow 32
3.2.2 Bottom Mouldboard Plow 32
3.3 Identification of Field Area Soil Textures 34
3.4 Determination Soil Physical Property 34
3.4.1 Soil moisture content 34
3.4.2 Soil bulk density 35
3.5 Determination Soil Mechanical Property 36
3.5.1 Soil shear strength: internal friction angle (φ) and cohesion (C) 36

3.5.2 Soil penetration resistance 37
3.6 Determination of Soil Shear Stress and Deformation 37
3.7 Predicting the Draft Force Using Dimensional Analysis 37
3.8 Modelling Assumptions 38
3.9 Modelling Approach 38
3.9.1 Modelling of the ard Plow 38
3.9.2 Application of Buckingham Pi theorem 41
3.10 Systematic Data Collection and Arrangements 47
3.10.1 Tillage treatments of ard plow 47
3.10.2 Experimental Instrumentation 49
3.10.3 Tillage treatments of walking tractor (scaled mouldboard Plow) 49
3.11 Quantitative Data Analysis 50
3.11.1 Statistical Design 50
3.11.2 IBM SPSS statistical software 50
3.11.3 Laboratory and Software Analysis 50
3.11.4 Field Sampling 50
3.12 Model Development of Shear Stress and Deformation in Soil Textural Class 52
3.12.1 Model Geometry 52
3.12.2 Loads and boundary conditions 53
3.12.3 Mesh generation 53
CHAPTER FOUR 54
RESULTS AND DISCUSSION 54
4.1 Soil properties in the study areas 54
4.1.1 Textural classes of soil in the Worden field 54
4.1.2 Textural classes of the Ewan Keble Texture Classification 56
4.2 Laboratory and Field Test of Soil Properties Results 58
4.3 Effects of Plow Geometry and Screening Variables on the Ard Plow Draft Force 59
4.3.1 Influence of distance (p) and operator operating angle (λ) on the draft force .. 59
4.3.2 Screened Variable Predictors of Ard Plow Draft Force in Soil Textures. 61
4.4 Effects of shear stress and soil texture deformation on the Ard draft force 70
4.4.1 Effects of shear stress on selected draft forces in silt clay and silt loam soil ... 70
4.4.2 Deformation in silt clay and silt loam soil 74

4.4.3 Prediction Draft Force of the Soil Texture 76
4.5 Prediction and Validation of Draft Forces of Scaled Model Moldboard Plow 79
4.5.1 Experimental draft force data for mouldboards in silt clay and silt loam. 80
4.5.2 Prediction draft force of ½-scaled and ¾-scaled mouldboard in silt clay 81
4.5.3 Prediction draft force of ½-scaled and ¾-scaled mouldboard in silt loam. 86
4.5.4 Statistical evaluation of ¾-scaled and ½-scaled draft force 89
4.6 Prediction and Validation of Draft Forces of Ard Plow 92
4.6.1 Prediction of Draft Forces of Ard Plow in Silt Clay 92
4.6.2 Draft Forces of Ard Plow in Silt Loam soil. 96
4.6.3 Validation of the Draft Forces of Ard Plow in Silt Clay and Silt Loam 98
4.7 Visual Basic Programming Language 101
5 CONCLUSIONS AND RECOMMENDATIONS 103
5.1 Conclusions 103
5.2 Future Research 107
REFERENCE 108
APPENDICES i
APPENDIX I: Samples of soil engineering properties, Ard Plow Geometry and Operating Conditions in silt clay soil i
APPENDIX II: Samples of soil engineering properties, Ard Plow Geometry and Operating Conditions in silt clay soil ii
APPENDIX III: Amount of shear stresses in silt soil on selected draft forces ii
APPENDIX IV: Amount of Shear stresses in the sand soil under selected draft forces iii
APPENDIX V Amount of deformation in silt soil on selected draft forces iii
APPENDIX VI Amount of deformation in the sand soil under selected draft forces iv

LIST OF TABLES

TABLE PAGE

Table 3.1. Specifications of the Ard Plow 32
Table 3.2. Mechanical properties of CK45 33
Table 3.3. The mechanical properties of soil particles 37
Table 3.4. Variables defining the draft force. 39
Table 3.5. Dimensional matrix 40
Table 3.6. Dimensionless variable 40
Table 3.7. Dimension of unrepeated variables. 40
Table 3.8. A summary of the dimensionless draft force 41
Table 3.9. Variables wanted to describe the draft force. 42
Table 3.10. Pi parameter dimensionless product groups. 45
Table 3.11. Prototype and model relationships among variables. 47
Table 3.12. A complete block randomized design 48
Table 3.13. Design of the block of plots 49
Table 4.1. Hydrometer analysis 54
Table 4.2. Experimental data for Sieve analysis with a disturbed sample size 55
Table 4.3. Soil data for Hydrometer Analysis 57
Table 4.4. Sieve analysis data. 57
Table 4.5. Properties of silt clay and silt loam soil 59
Table 4.6. Draft force (N) under the distance (p) and angle of the operator force (λ) 60
Table 4.7. Screened variables to predict the draft force of ard Plow in silt clay soil. 64
Table 4.8 ANOVA results for summery and parameter estimates of predictors 65
Table 4.9. Effect Summary 65
Table 4.10. Predictive variables of summer and Plow screening in silt loam soil 69
Table 4.11. Shear stress in silt clay soil 71
Table 4.12. Shear stress of loam Silt Soil 72
Table 4.13. Deformation of silt loam soil particles 75
Table 4.14. Repeat and non-repeat variables of parameters 77
Table 4.15. Predicted draft force of soil texture. 79
Table 4.16. Operating parameters of the full-scale Mouldboard Plow 80
Table 4.17. Values of soil cohesion and gravitational acceleration of silt clay and silt loam 80

Table 4.18 Measured parameters mouldboard Plow in silt clay soil. 81
Table 4.19. Selected pi groups for draft force for mouldboard Plow in silt clay soil. 81
Table 4.20. Coefficients of the measured draft force using a ½-scale mouldboard Plow in silt clay soil ($\pi 2$) 82
Table 4.21. Coefficients of the measured draft force using a ½-scale Mouldboard Plow in silt clay soil ($\pi 3$) 82
Table 4.22. Response of a ½-scale Mouldboard Plow 82
Table 4.23. Coefficients of the measured draft force using a ¾-scaled mouldboard Plow in silt clay soil ($\pi 2$) 84
Table 4.24. Coefficients of the measured draft force using a ¾-scaled mouldboard Plow in silt clay soil ($\pi 3$). 84
Table 4.25. Coefficients of the measured draft force using a ¾-scaled mouldboard Plow in silt clay soil ($\pi 4$). 85
Table 4.26. Coefficients of the measured draft force using a ¾-scale mouldboard plow in silt clay soil ($\pi 5$). 85
Table 4.27. Coefficients of the measured draft force using a ¾-scale mouldboard Plow in silt loam soil ($\pi 2$) 86
Table 4.28. Coefficients of the measured draft force using a ¾-scale mouldboard Plow in silt loam soil ($\pi 3$) 87
Table 4.29. Coefficients of the measured draft force using a ¾-scaled Mouldboard Plow in silt loam soil ($\pi 4$) 87
Table 4.30. Coefficients of the measured draft force using a ½-scaled Mouldboard Plow in silt loam soil ($\pi 2$) 88
Table 4.31. Coefficients of the measured draft force using a ½-scaled mouldboard Plow in silt loam soil ($\pi 3$) 88
Table 4.32. Coefficients of the measured draft force using a ½-scaled Mouldboard Plow in silt loam soil ($\pi 5$) 89
Table 4.33. ANOVA Table for the ¾-scaled mouldboard Plow 90
Table 4.34. ANOVA Table for ½ -scaled Mouldboard Plow 90
Table 4.35. Values of coefficients of a determinant for ¾-scaled Mouldboard Plow 90
Table 4.36. Values of coefficients of determinant for ½-scaled Mouldboard Plow 90
Table 4.37. ANOVA Table for ¾-scaled mouldboard Plow in silt loam 91
Table 4.38. ANOVA Table for ½-scaled mouldboard Plows. 92

Table 4.39. Values of coefficients of determinant for ¾-scale mouldboard Plow. 92
Table 4.40. Values of coefficients of determinant for ½-scaled mouldboard Plow. 92
Table 5.41. Prediction of the draft forces of functions (A, B, C, and D) 94
Table 4.42. Numerical values of x, y, z, and q 96
Table 4.43 Predictor vs. experiment draft force Model summary in Silt Clay..... 98
Table 4.44 Model summary of predictors vs. experimental draft force. 98
Table 4.45. Descriptive statistics of the measured draft force in silt clay soil. 100
Table 4.46. Errors in silt clay soil..... 100

LIST OF FIGURES

FIGURE PAGE

Figure 1.1 Total cultivated land cover by cereal crops in Ethiopia from 2011 to 2020 1
Figure 1.2 Human power and farm mechanization using small-scale tillage tools 4
Figure 2.1 Source of soil texture triangle source 10
Figure 2.2 Soil block separated from soil surface 12
Figure 2.3 Relationship between the internal friction angle and cohesion force 13
Figure 2.4 Tillage tool interactions with soil 15
Figure 2.5 Mouldboard Plow types 15
Figure 3.1 Map of the study area 31
Figure 3.2 ard plow geometry 32
Figure 3.3 Geometrical structure of the mouldboard 33
Figure 3.4 Experimental hydrometer readings 34
Figure 3.5 Soil moisture laboratory test equipment. 35
Figure 3.6 Soil samples from the field area to evaluate bulk density. 36
Figure 3.7 Soil specimen apparatus under first and corresponding stress conditions 36
Figure 3.8 Draft force components of the mouldboard Plow. 41
Figure 3.9 Experimental design of the field area 48
Figure 3.10 Draft force of the ard Plow drawn on the animal. 49
Figure 3.11 Geometry model 52
Figure 3.12 Boundary conditions. 53
Figure 3.13 Mesh of the model geometry. 53
Figure 4.1 Soil textural class of Worden Keble 56
Figure 4.2 Location of the soil texture of Ewan Keble in the soil textural triangle. 58
Figure 4.3 Draft force of Distance Stripe and Share, and operator operating angle. 60
Figure 4.4 Predictor “A” variable screening design of experiments. 61
Figure 4.5 Square least square regression model of the predictor “B” screening DoE 62
Figure 4.6 Square least regression model of the predictor “C” screening DoE……..63
Figure 4.7 Stepwise regressions modelling of the draft force. 64
Figure 4.8 Response of the draft force for screening variables of predictor “x” 66
Figure 4.9 Response of the draft force for screening the variables of predictor “y.” 67
Figure 4.10 Response of the draft force for screening the variables of the predictor “q.” .. 68
Figure 4.11 Response of the draft force to screening variables of predictor “z.” 69

Figure 4.12 Amount of shear stress in clay soil under different force 70
Figure 4.13 Contribution of silt clay soil on relation between draft force and shear stress. 73
Figure 4.14 Contribution of silt loam on relation between draft force and shear stress..... 73
Figure 4.15 Deformation of clay soil under selected draft forces 74
Figure 4.16 Deformation versus draft force 75
Figure 4.17 Measured and predicted values of the draft force in soil texture. 79
Table 4.18 Measured parameters using ¾-scaled and ½-scaled mouldboard Plow in silt clay soil 81
Figure 4.19 Relationship between measured and predicted draft forces (subtraction) 95
Figure 4.20 Relationship between the measured and predicted draft forces for the summation parameters..... 97
Figure 4.21 Relationship between the measured and predicted draft forces for the subtraction parameters (choice-2) 97
Figure 4.22 Scatterplot regressions standardized predicted Values and predicted functional values of silt clay soil. 99
Figure 4.23 Scatterplot regressions standardized the predicted values and predicted functional values of silt loam soil..... 99

Acronyms and Abbreviations

ANN	Artificial Neural Networks
ANOVA	Analysis of variance
ASABE	American Society of Agricultural and Biological Engineers
ASTM	American Society for Testing and Materials
ATA	Agricultural Transformation Agency
BHN	Brinell Hardness Number
CDA	Classical Dimensional Analysis
CRD	Complete Randomized Design
CRM	Confident of Residual Mass
DA	Dimensional Analysis
DAP	Draft Animal Power
DB	Dry Bulk
DEM	Distinct Element Method
DGC	Department Graduate Council
DOE	Design of Experiment
DW	Dry Weight
EAAP	European Association of Animal Production
EAP	Ethiopian Ard Plow
EDSWC	Ethiopian Design and Supervision Works Corporation
FEM	Finite Element Method
FFD	Full Factorial Design
FWI	Field Working Index
GA	Geometric Analogy
IBM	International Business Machines
MC	Moisture Contents
MLR	Multiple Linear Regression
OPGS	Office of Postgraduate Studies
RMSE	Root Mean Square Error
SEM	Structural Equation Modeling
SGC	School Graduate Committee

SPSS	Statistical Package for the Social Sciences
STI	Soil Texture Index
STM	Standard Test Method
TS	Theory of Similitude
USD	United States Department
USDA	United States Department of Agriculture
VGBT	Void age Grid Binning Technique
WPP	World Population Prospects
WW	Wet Weight

Abstract

Given its variable soil and limited resources, accurate prediction of the plowing force is crucial for efficient farming in Ethiopia. Smallholder farmers manage Ethiopia's tillage land. Even if Ethiopian smallholder farmers are interested in using appropriate farm power for their lands, they lack information about amount of force required for soil types, particular tool geometry and well-designed tillage tools. Prior researchers designed an effective distribution model for imported tools and suggested special policies for Ethiopian Banks to credit facilities for purchasing imported tools and machinery. They also designed and manufactured small-tillage tools without considering the complex nature of the soil. However, most farmers do not volunteer to use imported small-scale tillage tools as well as local manufactured tools because of the unfitness of tillage tools to till their soil. The objective of this study is to predict the draft forces acting on small-scale tillage power across various soil types using mathematical models. It solves the gap found in draft force models, which often cannot account for the heterogeneous soil conditions and the small-scale tool dynamics prevalent in agro ecosystems. Field experiments were conducted on Worden and Ewan Keble in the Central Ethiopia Regional State using common small-scale implements (ard plow and scaled moldboard plow) to measure the draft force under varying soil moisture, texture, and density conditions. The soil sample was tested and measured using tri-axial equipment, direct shear test equipment, and a Cone penetrometer. It identified the amount of soil strength (stress, deformation, and cone penetration), soil cohesion, and Soil friction angle. The design of experiments (DoE) approach was applied to study the factors affecting the draft force of small-scale tillage tools. The Buckingham Pi theorem (dimensional analysis) was used to reduce the number of variables by expressing them in dimensionless parameters. The JMP software was used to screen out the most significant variables that contributed to predicting the draft force. Integrating the selected soil mechanical properties, tool geometry, and operational parameters, a novel mathematical model was developed using visual basic programming language to predict the draft force across the identified Ethiopian soil types. The R-square, RMSE, Skewness, and Kurtosis were used for model evaluation and validation. This equation showed robust predictive accuracy when validated against empirical data, achieving an R^2 value range of 0.877 - 0.906, Root Mean Square Error value range of 0.093 - 0.246, and the skewness and kurtosis values range of 1.10 - 1.61, which is within the acceptable ranges for confirming the normality of the data. The research results highlight the model's capacity to guide tool selection and operational settings, enhancing energy efficiency and reducing labor for smallholder farmers. This research contributes to ard plow and scaled moldboard plow for sustainable tillage management, offering practical insights for farmers to select farm power and designers aiming to improve tillage practices in Ethiopia and similar contexts.

***Keywords**: Draft Force, Mathematical Model, Optimization, Prediction, Small-scale tillage tool.*

CHAPTER ONE

INTRODUCTION

1.1 Background

Ethiopia's agricultural sector relies heavily on traditional and small-scale tillage tools, with limited adoption of mechanized or improved technologies. Approximately 90% of smallholder farmers use the traditional marshal plow (animal-drawn) as their primary tillage tool (Kirchner, 2022). Only 12%–8% of farmers use modified tools such as the Berken Maresha (ripper plow) or ard plow (Ahmed, 2004). Less than 2% of smallholders use motorized tillage equipment (e.g., two-wheel tractors), in urban areas (Deribe and Jaleta, 2019).

Most of Ethiopia's land is managed by smallholder farmers (Gelaw & Ababa, 2018), with cereal crops occupying about 86% of this land. Teff, maize, wheat, barley, and sorghum comprise a significant portion of the cultivated area (Belachew et al., 2022). The cereal crop requires the highest energy input for seedbed preparation (Tsige et al., 2020).

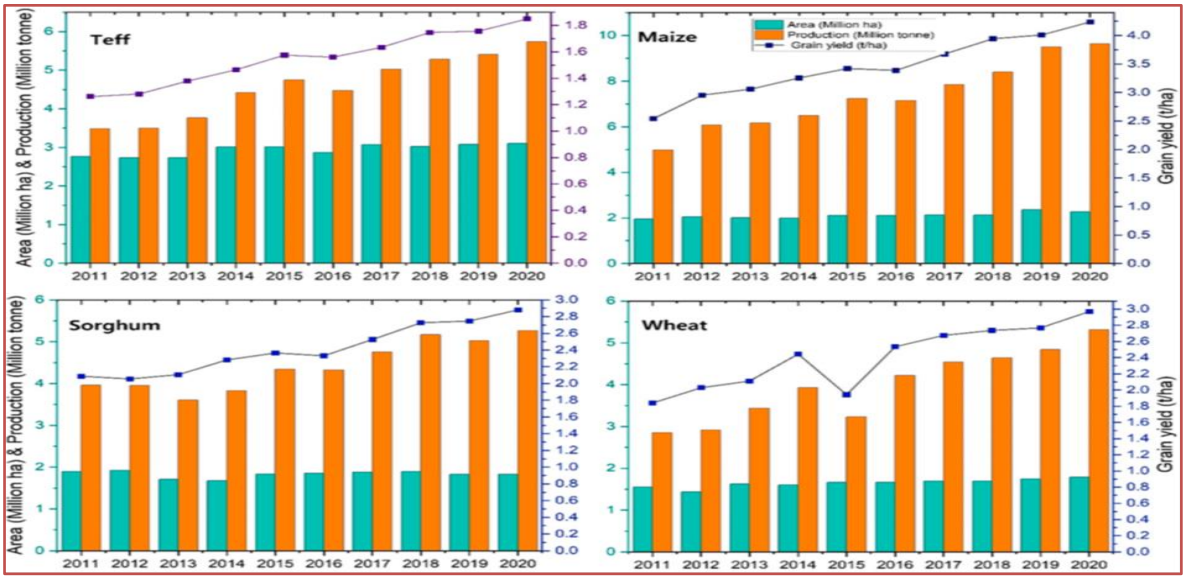

Figure 1.1 Total cultivated land cover by cereal crops in Ethiopia from 2011 to 2020

(Source: Belachew et al., 2022)

Seedbed preparation of cereal crops requires multiple passes of tillage tools. Aune and Bussa (2020) indicated that teff requires an average of four passes for cultivation, whereas maize

and sorghum require three passes. The authors also concur that the expense of using tractors for these crops is greater than the cost of oxen tillage for smallholder farmers.

Similarly, socio-economic and agroecological factors significantly contribute to the dominant use of animal drafts and other small power tillers as power sources for smallholder farmers (D'Annolfo et al., 2017). These tillers are particularly well-suited for farming on hills and uneven terrain because they can plow along curves and easily navigate hillside land, which poses challenges for four-wheel tractors. Using animal and tiller power effectively has considerable promise for boosting food production and promoting sustainable agriculture in Ethiopia.

Previous work has been done on small-scale tillage tools in Ethiopia that emphasize critical gaps that constrain the development and use of efficient and context-specific agricultural equipment. Broadly, they can be grouped into technical, agronomic, and socio-economic dimensions. The studies used generalized designs that rely on Ethiopian unique agroecological zones and smallholder farming practices. For instance, Basore et al. (2024) found that the amount of small-scale tillage in Ethiopia is limited. However, no previous research has highlighted the validated or optimized models to predict the draft force of small-scale tillage tools in Ethiopian soils.

Ethiopian soils are notably heterogeneous on account of their complicated topography (relief varies from -126 m to m 4620 m above sea level), a range of climate (from arid to humid), and geological petrogenesis (volcanic, sedimentary, or metamorphic). Regassa et al.(2023) observed natural factors account for soil differences at both the regional and local levels. Given that context, some of the leading soil types in Ethiopia are examined while also considering their geographic distribution and extent of coverage. Nitisols Characteristics: Fertile, red or reddish-brown soils; drained; developed from volcanic materials; contain different ratios of iron and aluminum oxides; well-drained. Distribution: Prevalent in most of the Western and Eastern Highlands (e.g. Ethiopian Plateau, Jimma, Harar) usually occurs at higher elevations above 1500 m, has volcanic parent materials present, and more precipitation. Extent coverage: 10-15% of the land area, particularly involved in coffee-growing agricultural systems. Vertisols Characteristics: Dark, clay-rich soils, have high shrink-swell potential and are usually viewed as difficult to work for tillage purposes because they expand quite a bit when they absorb water, but they are very fertile when handled correctly. Distribution: Typically found in the Western Lowland areas (e.g. Didessa

watershed, Gambella) and foothills of Western Highlands. Occur in some of the depressions of the Rift Valley System (at lower/elevations of about 500-1,500 m) and commonly are near seasonal flooding. The extent of coverage: 10-12% of the land area is an important component of the cereal and pulse-growing agricultural system.

The gaps need to be addressed by a multidisciplinary approach ranging from engineering, agronomy, socio-economic research, and policy support. In Ethiopian agriculture, there are different soil types, varying climatic conditions, and socio-economic contexts, and detailed models for small-scale tillage tools must be developed. In addition, the tools would need to be both practical and available and affordable, and closer cooperation between researchers, manufacturers, and farmers would be required. The gaps in agricultural productivity and sustainability in Ethiopia can be addressed, and agricultural productivity can be dramatically increased.

Researchers, manufacturers, and farmers need to work together to maintain adequate access and affordability for the tools to be implemented. The effective handling of these gaps will create substantial improvements throughout Ethiopia's agricultural sector since both productivity and sustainability will benefit. The success or failure of small-scale tillage tools usually depends on the amount of draft available.

Identifying the draft force acting on a tillage-tool interaction helps to determine the total power required for small-scale tillage, select and manage suitable hitches, and design strong tillage tools. Correctly predicting this force is crucial for assisting farmers, designers, and tool manufacturers with the optimal operations and tool geometry (Gebregziabher et al., 2006). This calls for improved, under-utilized small-scale tillage tools, owing to the impacts of ineffective and sub-optimum conventional practices in the area and within Ethiopia. These are not coincidences that enhance social, economic, and environmental vulnerabilities that keep people locked in poverty.

The prediction draft force facilitates improved management practices, minimizes power consumption, and prevents soil compaction. Affordable cost and proper application of small-scale power tillers can reduce the time for land preparation (Matched et al., 2022). Properly applied prediction of draft force can create the notable potential for sustainable agriculture using draft animals and walking tractors (Figure 1.2) for small-scale farmers in developing countries (Cunguara et al., 2016; Garré, 2022).

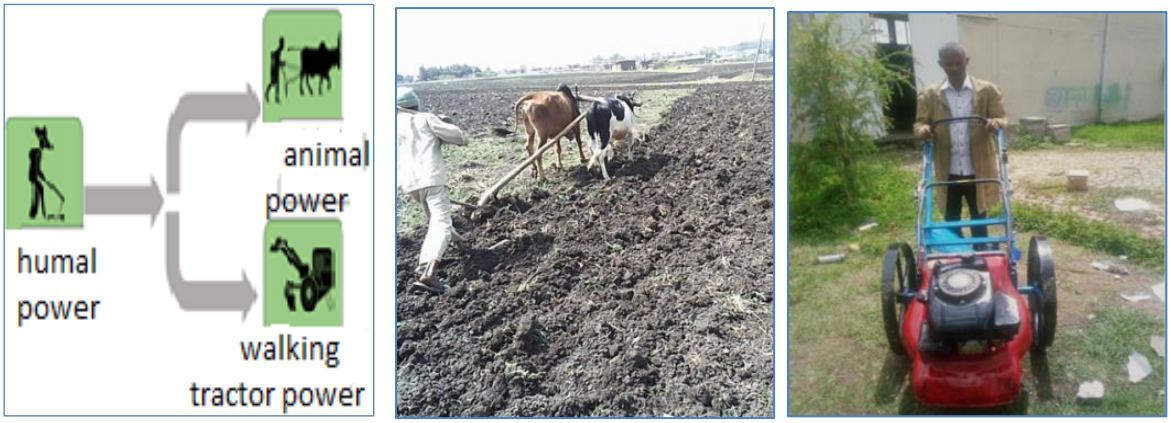

Figure 1.2 Human power and farm mechanization using small-scale tillage tools.

The draft force of the tillage tool affects the soil properties, tool geometry, and operating conditions (Oduma et al., 2018; Liu et al., 2022). Investigating soil-plow interaction measures is essential to measure soil failure arrangements (Ashrafi, 2006).

This research involved theoretical and dimensional analyses of the prediction draft force with data collection in the field area. Dimensional analysis helps to simplify a system and express the relationship between dependent and independent variables (Ogunnigbo et al., 2022). The Buckingham Pi theorem is used to construct a mathematical model for forecasting the draft force during tillage operations by applying dimensional analysis (Buckingham, 1914). The mathematical model for predicting the draft force offers the most accurate assessment of the system and its physical nature. The JMP software identified the optimal dependent and independent variables and simulated their relationship to minimize the draft force.

1.2 Problem Statement

Agricultural productivity in Ethiopia relies heavily on small-scale farming practices, where the efficient use of tillage tools is critical in crop yield and resource management. However, the performance of such tools, especially their draft force demand, could be highly different for different soil types because of differences in soil characteristics such as texture, moisture content, and compaction level (Bae et al., 2023).

Soil displays highly high variability in mechanical properties (e.g., cohesion, adhesion, shear strength) due to variability in seasonal moisture fluctuations, unequal distribution of organic matter, and localized compaction (Ma et al., 2016). The features of small-scale tools, such as the Maresha plow, operate at shallow rake angles and have an exceptional depth-to-width

ratio, giving out a non-uniform soil failure pattern (Mwiti et al., 2023). As confirmed in previous research, relying solely on limited variables can lead to significant uncertainties in draft force predictions (Bae et al., 2023). Despite this variability, there remains a lack of comprehensive mathematical models that accurately predict the draft forces required by small-scale tillage tools under diverse Ethiopian soil conditions.

There are also lacking validated, general models that account for the important soil-tool interacting parameters (e.g., shear strength of soil, depth of the tool, speed, and the rake angle) covering various soil types. This gap prevents the implementation of adaptive and cost-effective tillage technologies used in mosaic areas dominated by small farms.

This research was innovative by studying specifically smallholder farmer needs in Ethiopia with widely used small-scale tools, accounting for the effect of soil texture and operator input forces and employing a complete set of mathematical models and validation methods to predict and optimize the draft force. The outcomes are meant to have real-world applications in Ethiopia's agricultural practices and tool development.

By precisely forecasting the draft force demanded by diverse soil conditions, farmers can prefer their tillage tools more suitable to specific ground. This increases the efficiency of human and animal power use, results in a minimum amount of physical effort for human and animal power, and results in the potential to reduce the time needed to complete the tilling operations. A precise mathematical model allows for the optimal selection and operation of tillage tools, minimizing energy consumption where small-scale tillage tool mechanized equipment is used.

When tillage tools are operated within their designed capacity, accurate draft force predictions are expected, and less mechanical stress is placed on them. This results in a prolonged tool life and reduced frequency of repairs or replacements. In summary, a reliable mathematical model for predicting draft forces development and its application will significantly contribute to Ethiopian agricultural growth by enhancing sustainable farming practices, improving profitability, and reinforcing sustaining farming machinery.

1.3 Objectives of the Research

1.3.1 General Objective

The general objective of this study was to predict the draft forces acting on small-scale tillage power across various soil types using mathematical models.

1.3.2 Specific Objectives

The specific objectives of this research were as follows:

- To determine the soil properties in the study areas.
- To identify the effect of operator operating and rake angle on soil-cutting force.
- To screen and identify the most influential variables significantly influence draft force.
- To determine the impact of soil shear stress and deformation on draft force.
- To predict and validate the draft forces of the scaled model moldboard plow.
- To predict, perfect, and confirm the draft forces of the ard Plow in Ethiopian soil types.

1.4 Expected outcomes of the study

This research will enable smallholder farmers to use different draft animals or walking tractors based on the force required to test specific soil types and conditions. Designers and manufacturers will obtain data for small-scale tillage tools, providing sustainable agriculture that matches prime movers to the required draft force for soil resistance. It helps select and manages suitable hitching designs and determines the adequate strength of tillage tools. Smallholder farmers will have access to information about the required draft forces of tillage tools to till their land.

1.5 Significance of the Study

Ninety percent of Ethiopian farmers are smallholders (Zerssa et al., 2021). They may not have the purchasing capacity for medium- and heavy-duty tractors to till their lands. Most of these farmers use draft animals and sometimes walk tractors for tillage. Draught animals and walking tractors are eco-friendly and satisfy the socio-economic needs of small-scale farmers. Studies on small-scale tools have enabled tillage optimization and increased smallholder farmers' productivity. This study predicted the draft forces of small-scale tillage tools, enabling farmers to select suitable tillage power sources. It provides the data required for small-scale tool design and supports the manufacturing of appropriate tools. The system also provides information for selecting suitable tillage power to match the draft force required to pull the tool.

1.6 Scope and Limitations of the Study

Agricultural mechanization is categorized into animal traction, walking tractors, and medium and heavy tractors. This study focused only on animal traction and walking tractors, used by smallholder farmers (Daum et al., 2023). Researchers have limited themselves to ard plow and scaled moldboard plow tillage tools. Draught animals and walking tractors are eco-friendly and can help identify the draft force needed to pull the tillage tools. This study predicted the draft force of tillage tools operating in silt clay and loam silt soil, which are dominant in the study area.

1.7 Structure of the Dissertation

This dissertation contains six chapters. The structure of the study is as follows: Chapter 1 provides the Introduction, which discusses the background of the study, the problem statements, the objectives, expected outcomes, significance, scope, and structure. Chapter 2 presents a literature review, including a discussion of the soil properties, soil composition, operating conditions, and the design of the small-scale tillage equipment. It also identifies gaps in prior studies. Chapter 3 describes the Materials and Methods used to predict the draft force of small-scale tillage tools, explaining the mathematical models used to calculate the draft force. Chapter 4 includes the Results and Discussion section, presenting findings from field and laboratory tests and theoretical developments. Model validation of the measured and predicted draft forces is also covered. Final chapter concluded the dissertation, summarizing the study and recommendations for future research.

CHAPTER TWO

LITERATURE REVIEW

The prediction of draft force for tillage tools is critical in agricultural engineering, as it directly impacts farming operations' energy consumption and efficiency. This literature review aims to synthesize existing knowledge on predicting draft forces using mathematical models, focusing on small-tillage tools suitable for Ethiopian soil types. Agricultural productivity in Ethiopia can be significantly enhanced by optimizing tillage tools. One key factor in this optimization is understanding and predicting the draft force required by these tools under various soil conditions. Several factors, including soil physical properties, tool geometry, and operational parameters influence the draft force (Ortopan et al., 2024). Earlier techniques for analyzing and predicting small-scale tillage tools, research findings, and gaps identified in the literature review are described.

2.1 Classification of Soil Types and Their Characteristics

The influence of soil properties, soil composition, operating conditions, and the design of small-scale tillage equipment are required to predict the draft force. Earlier techniques for analyzing and predicting small-scale tillage tools, research findings, and gaps identified in the literature review are described.

2.1.1 Soil properties and soil mechanics

Agriculture utilizes tillage equipment to prepare the soil for sowing by establishing the breaking up and tilling of the land. Many different tillage devices have been designed based on the soil type and the desired outcome of the tillage operation. Understanding the features of different soil types is crucial for selecting appropriate tillage tools that achieve optimal results. Understanding soil properties can help determine the pulling forces of tillage implements. This section discusses some basic soil parameters and the physical and mechanical properties that affect the pulling requirements of tillage equipment. This is a helpful guide for selecting appropriate soil parameters to predict the pulling force requirements of small-scale tillage implements.

The physical properties of soil are used to characterize soil and release soil activities like the movement of matter and energy (Reichert et al., 2016). The physical condition of the soil significantly influences the tractive force required by tillage equipment (Loukanov et al.,

2018). This method focuses on soil resistance titration using tillage tools. The soil mechanical property is examined to determine the extent of bulk density and compression in the soil, which supports hydraulic conductivity. According to Imhoff et al. (2016), variability in soil mechanical behavior is related to physical properties such as structure, texture, composition, moisture, organic matter, and bulk density. When the plow touched the soil and stirred it up, shear forces were applied, causing the soil to fail.

2.1.2 Soil Type

Various soil types are classified based on composition, texture, and structure (Nikiforova, 2019). Soil types used for tillage include sandy, clay, and sandy soils. Sandy soil contains large particles with low water content and high nutrient retention capacity (Basso et al., 2013). It is easy to till but requires frequent irrigation and fertilization. Clay soils contain small soil particles that hold water and nutrients well but are easily compacted (Kome et al., 2019). The specialized tillage tool requires prevention of compaction. Silt soil contains fine particles that hold moisture but are easily eroded (Gowers, 1895).

2.1.2.1 Soil texture

USDA identified twelve texture classes. Percentages of soil particles, such as silt, sand, and clay, determined from laboratory tests are used to determine soil structural classification. The content of clay in soil texture affects the soil bulk density, penetration resistance, soil adhesion, and soil cohesion force (Al-Neama et al., 2021). This means the pulling force required for working on different soil textures varied. Soils with high clay contents require a higher tractive force for cultivation in the dry season; tillage can only begin after rains have begun (Temesgen et al., 2008). Likewise, soils with a slightly sandy texture require less draft for tillage (Okoko et al., 2018).

2.1.2.2 Moisture contents

The moisture content in agricultural soils is the dry matter water mass ratio to moisture content. Soil moisture content is an important parameter in tillage because it influences the pulling force requirements of tillage implements. Smolders (2017) reported that the pulling force's magnitude varies with the soil's water content and bulk density. Soil compaction and variations in tool geometry, working conditions, and soil conditions, resulting in soil depth, vary depending on the soil conditions. Soil type affects soil's mechanical behavior and strength (Florence et al., 2023). Different researchers have reported different pulling forces

in textural classes. Therefore, identifying the soil type is important because each area has a unique soil type that affects the pulling force requirements of the tillage equipment. However, further increases in soil moisture content affect plant growth. Liu et al. (2022) measured the pulling requirements of tillage tine under different soil moisture conditions to evaluate soil disturbance parameters.

Figure 2.1 Source of soil texture triangle source:(Barman & Choudhury, 2020)

They found that the tensile force quadratically increased with decreasing moisture content. Naji Al-Dosary et al. (2023) reported that the pulling force of soil can be minimized under soil moisture conditions. Cardei et al. (2020) identified the optimal moisture content for different soil types.

2.1.2.3 Bulk density

Research has shown that as the dry bulk density of the soil increases, so does the draft force required to pull tillage tools through it (Bravo et al., 2016). Bulk density represents the pore spaces within individual soil spaces and compaction. The draft force of the tillage tool increases with increasing bulk density (Kotrocz et al., 2016). An increase in bulk density typically leads to an increase in draft force due to reduced porosity and higher mechanical strength of the soil (Ranjbar et al., 2013).

2.1.2.4 Soil cohesion force

The cohesive soil force is an internal force that holds soil particles together. Shear strength holds soil components together in a soil structure. Soil properties influence cohesion, such as soil moisture content, pore space, and soil texture (Rabot et al., 2018). Akayuli et al. (2013) examined how cohesion increases with increasing clay and soil moisture content.

2.1.2.5 Internal friction angle

The internal friction angle (φ) expresses the friction force between the interactions of soil particles. It occurs through contact with soil particles. Tilling also requires force to break up soil particles by sliding and rolling against each other. Larger soil particles make better contact with the surface than smaller ones. The internal friction angles were larger than those of the smaller ones. The soil resistance to a tillage tool is related to the soil cohesion between soil particles and is expressed by the angle of internal friction (Akayuli et al., 2013). Soils with high moisture content have a smaller contact area; thus, the angle of internal friction is expected to be smaller. Soil texture and moisture content affect soil cohesion and internal friction angle. Sandy soils have larger diameters (2.05 mm) than clay soils (less than 0.002 mm). Therefore, it has a larger contact area and is considered for friction because of its larger internal friction angle. (Jiang et al. (2020) reported that soil moisture content significantly affects soil cohesion, internal friction angle, and shear strength. Additionally, this study investigated whether soil cohesiveness rises and falls in response to rising soil moisture content (Hales & Miniat, 2017).

2.2 Soil Mechanics

Soil tillage (mechanics) refers to movement under an acting soil load. The interaction between soil mechanics and tillage tools is critical for understanding the draft forces required. The process involves separating soil from disturbed to undisturbed using a tool to influence the soil at a certain time. For desired plant development, change unfavorable soil conditions to favorable conditions. Soil collapse predicts pressure exceeding soil shear strength (Mahmood & Abrahim, 2021).

When the cutting blade penetrates the soil and moves forward, the soil is subjected to compressive stress (passive pressures). When the applied force exceeds the soil shear strength, failure occurs. The pressure distribution under a flat cutting blade follows a triangular pattern, with the maximum and lowest pressures at the leading and trailing edges,

respectively. This pressure distribution can cause significant shear stress at the blade-soil interface, leading to soil failure. A separated soil block with a logarithmic spiral shape crossed the undisturbed soil and blade surface. Figure 2.2 illustrates the shape of the separated soil, which was sliced by the blade. This process continues until another block is sheared off with greater knife action.

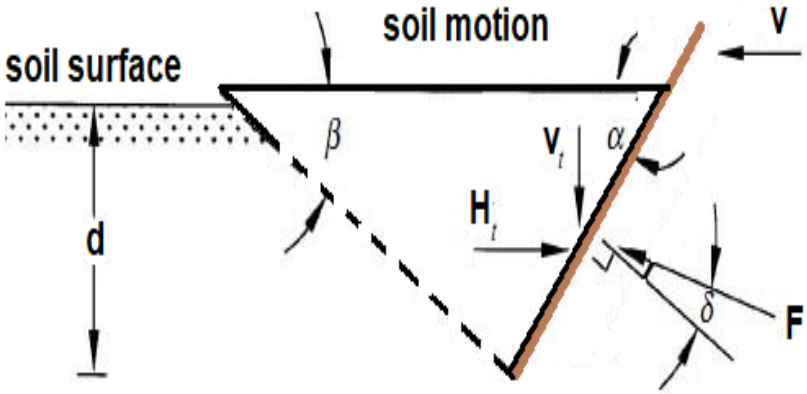

Figure 2.2 Soil block separated from soil surface.

2.2.1 Soil strength

The soil strength factor determines the draft force required for efficient agricultural tools. This measure measures soil ability to resist deformation caused by external forces, such as the weight of agricultural equipment or tillage operations. The factors determining soil strength consist of three elements which are soil moisture, soil type and soil structure. Penetration resistance and shear strength represent the two major methods used for measuring soil strength. Penetration is the resistance to a probe or other object being pushed into it. Shear strength is the soil resistance to deformation caused by forces acting parallel to the soil surface.

Soil resistance (R) estimates soil properties such as penetration resistance, shear strength, and moisture content (Cardei et al., 2019). For example, a common equation for estimating the draft force in sandy soils is:

$$R = K \times P \times d \times \gamma \qquad (2.1)$$

Where k is a constant that depends on the tool configuration, P is the penetration resistance of the soil (N/m^2), d is the penetration depth, m, and γ is the bulk density of the soil (kg/m^3).

In clay soils, the draft force can be estimated using the following equation relating to shear strength:

$$R = \tau \times A \qquad (2.2)$$

Where: τ; is the shear strength of the soil (N/m^2); and A; is the area of contact between the tool and the soil, m^2.

Soils are characterized by strength using the Mohr-Coulomb failure criterion (Labuz & Zang, 2012). Coulomb law states that soil shear resistance can be caused by cohesion and friction (Mckyes E., 1989). Mohr developed a generalized theory based on the Coulomb idea and identified soil cohesion (c) and internal friction as two parameters affected by soil failure (Hormazabal and E, 2018). The extent of cohesion (c) depends directly on the internal friction angle (φ), the relation illustrated in Figure 2.3.

The interaction between external forces (load) exerted on soil causes soil movement and motion. Shear characterizes the occurrence of soil failure along internal soil surfaces. Soil shear strength represents its capability to resist disaster and slide beside any internal plane and is quantified as the internal resistance per unit area. When a failure happens, shear resistance helps achieve shear strength by reducing the shear stress along the failure surface.

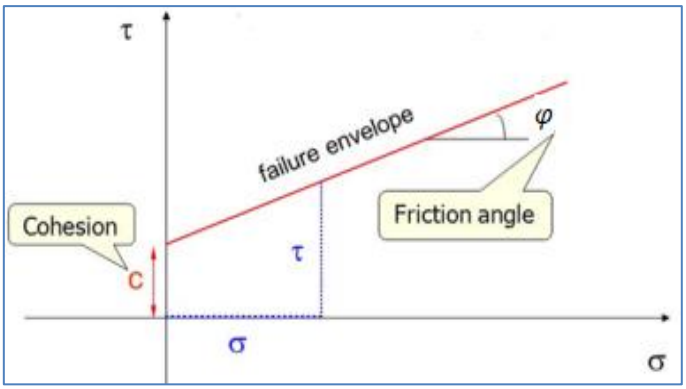

Figure 2.3 Relationship between the internal friction angle and cohesion force

The soil shear strength is found using the following formula.

$$\tau = c + \sigma_n \tan(\varphi) \qquad (2.3)$$

Where: τ; shear stress at the failure surface (N/m^2), φ; internal friction angle (degree); c: soil cohesion (N/m^2), σ_n; normal stress at the failure surface (N/m^2).

The response at soil-tool interfaces shares a related principle:

$$\tau' = c_a + \sigma' \tan(\beta) \qquad (2.4)$$

Where: τ′ is shear stress at the soil-tool interface (N/m^2), c_a is soil-tool adhesion (N/m^2), σ′ is normal stress at the soil-tool interface (N/m^2), β is soil-tool friction angle (degree).

These equations are approximations, and the actual draft forces may vary depending on several factors. Therefore, field tests are recommended for determining the drafts of specific tools and soil conditions.

2.2.2 Soil Mechanics Fundamentals

Soil mechanics provides the theoretical foundation for soil response to external forces, such as those applied by tillage tools. Foremost among these are principles of soil strength, stress distribution, and failure mechanisms that are necessary to simulate soil-tool interaction. As a tillage tool interacts with soil, it imposes stresses that result in soil deformation and failure. Stress distribution depends on the geometry of the tool, depth of operation, and soil properties. The Mohr-Coulomb failure criterion has been extensively used to predict soil failure due to imposed stresses (Das, 2010).

2.3 Tillage Tools

Modern agriculture depends heavily on tillage tools because they create suitable seedbeds and keep crops healthy throughout the growing period. Different soil profiles, climatic conditions, and preferred cultivation techniques determine which tillage instruments should be selected (Baker, 2006). Farmers acquire better insights for system selection by studying how different tillage implements function and operate in agricultural settings.

2.3.1 Tool geometry parameters

The rake angle defines the forward angle between the tool front and the horizontal ground surface. This parameter is related to the tensile force. If the rake angle is slight, the pulling width, plowing length, plow shape, and rake angle are geometrical tillage tools that influence the draft force. Gebregziabher et al. (2016) applied three rake angles (8^0, 15^0, and 24^0) and performed minimum pulling forces for primary, secondary, and tertiary tillage processes. (Guadie et al. (2018) determined the average incline angle during animal movements, especially during cattle movements. Plowing with the tine tool increased the pulling force at a minimum plow angle of 10°; this force decreased as the rake angle of the blade increased to 15^0. Further increasing the blade pitch angles increased the draft force.

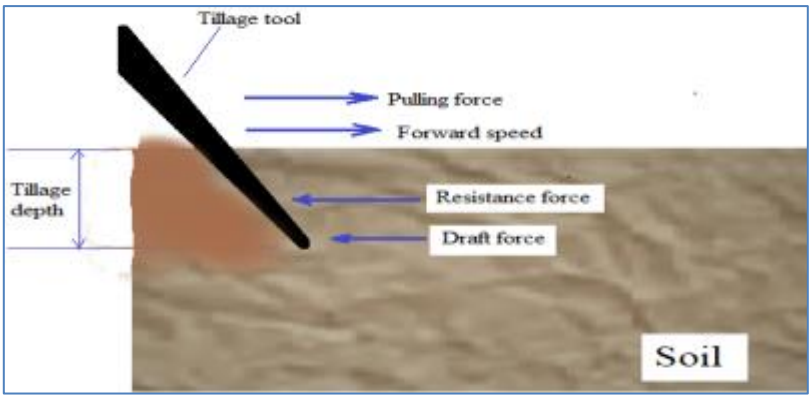

Figure 2.4 Tillage tool interactions with soil

2.3.2 Mouldboard Plow

Moldboards commonly used in plows are described as follows:

Standard Moldboard: A Twisted Moldboard is a variation that improves soil inversion and mixing. It can be useful when soil incorporation is necessary (Reicosky, 2001).

Notched Moldboard: Notched moldboards have serrated edges that can help with cutting.

Use thorny vegetation or compacted soil more efficiently (Pandey, 2006).

Slatted Moldboard: Slatted moldboards have openings or slots that allow for better.

Residue flow and reduce clogging when working in fields containing high levels of crop residue.

Each moldboard has advantages based on the requirements of the farming operation and soil conditions. For smallholder farmers, moldboards are the most suitable choice, and they are adequate for tasks performed by primary tillage (Bello et al., 2023). When selecting a moldboard plow for smallholder farmers, factors such as farm size, soil type, and specific crop are considered (Twomlow et al., 1999). The simplicity and effectiveness of a single-blade moldboard plow make it a practical choice for smaller farming operations.

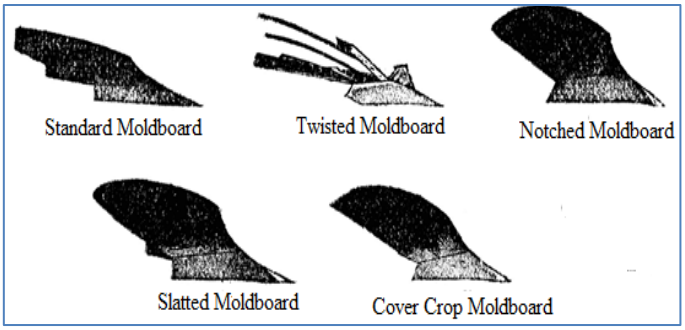

Figure 2.5 Mouldboard Plow types

By opting for a Moldboard Plow with a single blade or moldboard, smallholder farmers can efficiently prepare their fields for planting while benefiting from increased crop yields and improved soil health (R.K. Gupta et al., 2017).

2.4 Operational Conditions

2.4.1 Operational speed

Several researchers have identified different operating speeds for draught. The average working speed of draft animals varies. Gebregziabher et al. (2016); Kyalo & Nairobi (2019) studied the average operating speed of a pair of oxen pulling ard shares of 0.56 m/s in light soils with an average moisture content of 22%. Geza (1969) examined the working speed of the horse with the collar harness and identified a range of 0.75 - 1.07 m/s and a range of 0.4 - 0.5 m/s for the Ethiopian ox pulling speed with the yoke harness. Gebregziabher et al. (2016) determined an average working speed of 0.63 m/s for the ox draft. A Loukanov et al. (2018) studied the working speed of draft animals on red clay soil with a 25% - 32% moisture range.

2.4.2 Working depth.

Soil texture influences soil depth, soil compaction level, and moisture content (Badalíková, 2010; Aune & Bussa, 2020). Working depths of 5-10 cm for the first tillage with an ard plow; during the second tillage, the depth was increased to 20 cm with additional passes. However, plowing can change the length and angle of the plowshare by applying downward pressure on the handle (Aune et al., 2001). Smolders (2017) found that the tillage depth is proportional to the draft force. Thus, soil quarantine results in pure cutting at greater depths, whereas other types of soil failure may occur at shallower depths. Kim et al. (2022) investigated how tillage depth and working speed affect the draft.

2.5 Development of the Mathematical Model

Mathematical modeling plays a crucial role in predicting the performance and behavior of tillage tools in agriculture. Mathematical modeling uses mathematical language to express the manners of a system. Using mathematical models, researchers and engineers can simulate various scenarios, analyze different parameters, and predict outcomes before implementing them in real-world settings (Ejiko et al., 2021). A mathematical model represents a real-life system using mathematical concepts and equations. This model describes, analyzes, and predicts the behavior of the studied system. The steps involved in

developing a mathematical model (Anhalt & Cortez, 2015) typically include the following steps:

Problem Formulation: The first step in developing a mathematical model is to define the problem to be addressed. This involves identifying the system's key variables, parameters, and relationships.

Assumptions made to reduce model complexity while capturing the system. These assumptions help develop the mathematical equations that govern the system's behavior.

Mathematical Equations: Based on the problem formulation and assumptions, a mathematical equation is derived to represent the relationships between different variables in the system. These equations can be differential, algebraic, or other mathematical expressions depending on the system's nature.

The parameters of the mathematical model are estimated from data or experimental observations. Regression analysis and optimization methods serve as parameter estimation techniques to establish these values. After creating a mathematical model, checking accuracy and reliability standards through testing becomes essential. Verification through experimental data comparisons must be executed to demonstrate correct system behavior representation. The method evaluates the outcome sensitivity to changes in input values and initial starting points.

Model reliability testing and base predictive elements recognition are featuring that the evaluation process establishes. Through Model Refinement, we execute an iterative process that keeps our model relevant and accurate during prediction activities and decision-making processes. A systematic process to create mathematical models demands both a deep understanding of system structure and a basic understanding of fundamental mathematical rules. Researchers develop effective tools for complex system prediction by following this systematic process while executing continuous model refinements.

2.6 Mathematical Model for Predicting Draft Force of Tillage Tools

Mathematical models have a greater ability to predict the behavior of tillage tools (Alimardani et al., 2009). The forecasting ability of tillage equipment behavior in agriculture mechanization depends heavily on mathematical modeling. Simulation analysis based on the model evaluates the relationship between tillage tools and soil to offer key insights regarding performance impacts via various elements. It is essential for forecasting how agricultural

tillage instruments will behave and perform (Almaliki, 2018; Drwish, 2020). Using mathematical equations and computational algorithms, researchers can also predict parameters of the draft force, soil disturbance, fuel consumption, and overall efficiency of tillage operations (Almaliki, 2018; Algezi & Almaliki, 2022). Al-Hamed et al. (2014) develop Computer Program using Visual Basic for predicting performance parameters of tillage implements.

Mathematical models are divided into three classes: empirical models (experimental) that produce significant empirical results and have undergone experimental validation. Creating a generalized model based on experimental data is equivalent to empirical modeling. Several studies have predicted the draft forces of tillage tools applied to soil-tool interaction using empirical approaches (Almaliki, 2018; Aune & Bussa, 2020; Makange et al., 2021). Empirical techniques take time because they require data to be collected, and most empirical predictions are not very accurate because inconsistent soil characteristics cause data to be extremely variable (Makange et al., 2020).

An analytical model for studying soil-tool interaction is limited analysis. This method considers limited soil conditions and Mohr-Coulomb requirements for soil strength. An alternative assumption is that soil is a hard, nondeformable body. These assumptions allow the application of analytical techniques to gather data on the forces at play during soil-tool interaction (Mckyes E., 1989; Smolders, 2017).

As a result, several tools have been developed to delegate the delegated pulling force, such as Dimensional analysis (Koolen & Kuipers, 1983), regression technique (Alimardani et al., 2009), and numerical technique (Karmakar & Lal Kushwaha, 2005). Makange et al. (2021) predicted the cutting forces of subsoil using an analytical model and the Distract Element Method. Using the Distract Element Method simulation, the draft force of the moldboard plow can be estimated based on the amount of tillage in cohesive soil (Dizaji et al., 2022).

2.7 Dimensional Analysis to Develop a Mathematical Model

Mathematical modeling using dimensional analysis is a powerful technique that enables scientists and engineers to understand complex systems by examining the relationships among different physical quantities. The foundation of dimensional analysis is that physical rules apply regardless of the units used to measure quantities and deconstruct complicated issues. Dimensional analysis relies on the fundamental principle that physical equations must be dimensionally consistent (Misic et al., 2010). This means that each term in an equation

must have the exact dimensions on both sides. Researchers can derive dimensionless parameters that govern the system's behavior by analyzing the dimensions of various physical quantities involved in a problem.

2.7.1 Dimensional Analysis approach

The dimensional Analysis approach involves applying Buckingham's Pi Theorem (Buckingham, 1914), which helps to understand the complex interactions between various factors affecting tillage operations. Dimensionless parameters contain reduces the number of variables (Mahoney & Yeralan, 2019). The key concepts in this approach are Buckingham's Pi Theorem and dimensionless Parameters. This mathematical method allows the formation of dimensionless groups by eliminating fundamental dimensions from a set of equations involving different variables. Dimensionless Parameters: These are ratios of physical quantities with the exact dimensions that simplify complex problems and predict system behaviors under several conditions.

Estrada-Díaz et al. (2021) created a general mathematical model for forecasting the bulk density of Inconel parts made by selective laser melting using dimensional analysis. (Pratap et al., 2023) created a dimensional analysis-based mathematical framework that measures the surface roughness of microdots using Buckingham's π-theorem. (Pratap et al., 2023) developed a mathematical model based on dimensional analysis that uses Buckingham's π-theorem to quantify microdots' surface roughness.

Complex problems become simpler to tackle through dimensional analysis because it minimizes the required variables. Dimensionless parameters help discover physical scaling laws that occur in scientific phenomena, while dimensional analysis checks mathematical models against physical laws. Combining dimensional analysis with mathematical modeling is beneficial for exploring complex systems in different science areas.

The soil, plow, and working condition parameters of tillage tools are considered in input models (Ranjbar et al., 2013; Jiang et al., 2020; Kim et al., 2022). Tillage research identifies the minimum draft force from input effort by matching the mechanical interaction with soil and the operator force. As a result, several methods have been applied to predicting the draft force, such as dimensional analysis (Koolen & Kuipers, 1983; Moinfar & Shahgholi, 2018), regression technique (Abbaspour-Gilandeh et al., 2018; Sadek et al., 2021), and numerical technique (Karmakar & Lal Kushwaha, 2005).

2.7.2 PI-Buckingham theorem

A fundamental theorem for dimensional analysis is the PI-Buckingham theorem, which states that a dimensional homogeneous equation with specific physical quantities can be transformed into an equivalent equation with a perfect set of independent non-dimensional results (Higgins & Moran, 1968). For a similar approach, the ratio between the model and prototype dimensions was a non-dimensional constant that governed the model's testing conditions and parameters.

Dimensional analysis is essential for evaluating processes at different scales (Hajiahmadi et al., 2019). According to Buckingham's theorem, if a dependent variable is controlled entirely by the values of a group of independent quantities (m), of which the number of basic units (h) in an absolute system is required to measure, then this is a suitable dimensionless variable (Q), which is entirely determined by dimensionless products (Buckingham, 1914). The nun-dimensional dependent and independent variables f (1, 2, 3... n) are expressed in Eq. 2.5.

$$\pi_1 = f\ (\pi_2 . \pi_3 . \pi_4 . \ldots . \pi_{n-k}) \qquad (2.5)$$

The units are assigned dependent and independent variables, which are assigned to the dimensional form. The function is expressed in terms of length (L), time (T), and mass (M). Therefore, three fundamental dimensions (MLT) were applied, and independent variables were identified as repeated and non-repeated variables. It was assumed that the dimensional matrix did not form a dimensionless group (Casaburo et al., 2019). The form repeated variable (A), non-repeated variable (B), unknown values, and unknown values (X) are written in Equation 2.6.

$$A(X) = B \qquad (2.6)$$

Unidentified value (x) is written in the matrix form $\frac{1}{A}AX = \frac{1}{A}B$ to $X = A^{-1}B$. Therefore, it is possible to search for these arbitrary exponents and, hence, the π parameters by requiring that each product group be dimensionless ($\pi_1, \pi_2, \pi_3 \ \ldots\ldots . \pi_n$) methods to reduce dimensional variables to the reduced quantity of dimensionless groups (Buckingham's theory).

2.7.3 Similitude

Similarity theory is a complex phenomenon used to improve comparative prototype model studies, but together with dimensional analysis, it can solve the problem (Smith & Strahan,

2004). The similarity theory is the basis for developing field treatments (Wang et al., 2022). Scale models of share plows specify the tillage characteristics of full-scale share plows; validate the characteristics of share plows expected by theory and fill in gaps in theory. The sizes of medium and heavy tractor implements are too large to be suitable for small agricultural land.

A model that is effective for an actual system can be implemented. Currently, similarity theory is a widely used research problem in model test design (Wang et al., 2022). To transfer the full-scale design's desired geometric and dynamic features to the scaled-down plow, the proposed technique must ensure geometric and dynamic similarity between the full-scale and scaled-down plows. Focusing on the dynamic behavior of arable land in this scaled-down interaction between the plow and soil is critical to achieving an adequate draft.

The similarity theory reduces the number of dimensions that fit at small scales. Creating appropriate similarity situations between the prototype and model is the goal of similarity theory (Sousseau et al., 2021). Scaling rules explain how a prototype structure differs from its model and is easy to follow. Scaling rules explain how a prototype structure can convert experimental findings from tiny, inexpensive, and testable model design data for a prototype (Blomkvist, 2011).

2.8 Draft Force Parameters of the Functional Variables

It is essential to predict the required pulling force of tillage tools to identify unexpected minor components. Such sets are legitimate dependent variables to predict. Mckyes (1989) Selected independent variables as functions to develop a design force model based on the dimensional analysis described in Equation 2.7.

$$F_d = \mathrm{F}\,(\mathrm{D}, \lambda, \mathrm{V}, \mathrm{g}, \theta, \mathrm{w}, \mathrm{C}, \tan\varphi, \mathrm{A}, \tan\mu) \qquad (2.7)$$

Factors affecting soil forces in soil cuts using functional relationships in terms of variables listed in Equation 2.8.

$$F_d = \mathrm{f}\,(\gamma, \varphi, \mathrm{c}, \delta, \mathrm{Ca}, \alpha, \mathrm{d}, \mathrm{q}) \qquad (2.8)$$

Koolen & Kuipers, (1983) developed the draft force necessity for agricultural tools, characterized in the functional form Equation 2.9.

$$F_d = \mathrm{f}\,(\rho, \mathrm{C1}, \mathrm{d}, \mathrm{S}, \mathrm{w}, \alpha, \vartheta) \qquad (2.9)$$

Okoko et al. (2018) used the draught (effect) as a function of the draught characteristics (cause) expressed in Equation 2.10 to predict the draft force of tool implementation.

$$F_d = \mathrm{f}\,(\mathrm{M}, \rho, \mathrm{d}, \mathrm{S}, \mathrm{I_m}) \qquad (2.10)$$

The researcher used annotation variables (parameters) to predict the tillage implementation draft. One researcher used variables, and another researcher did not consider them. These results show no standard independent variables for the dependent variable of the draft force of tillage implements.

The most critical assumptions for such problems are the complexity of soil conditions, geometric shapes of tillage tools, and operating conditions of the tillage process. Therefore, theoretical knowledge and practical measurements are required to predict the pulling force of small tillage implements using mathematical models.

Over the past 50 years, several researchers have proposed theoretical solutions to the problem of implementing draft tillage systems. The parameters considered when estimating the pulling power of plows were the pulling force, speed of plowing, depth, width of the plowing, and soil conditions (Loukanov et al., 2018).

Patel et al. (2020) identified parameters (soil cohesion, soil weight, overload, soil adhesion, and structural shape) to predict the pulling force of a bucket. Pass such as soil bulk density, working depth, internal cohesion, soil-metal coefficient, and soil surface additive pressure affect the pulling force of the tillage tool.

The general function of the depth factors of the tillage equipment depends on parameters such as the working depth, forward speed, width, static component of the bottom shear stress, and bottom metal coefficient of friction. Okoko et al. (2018) used moisture content, working depth, working speed, soil bulk density, and implement mass to predict the pulling force of the tillage implement. Al-Hamed et al. (2014) developed a program using visual software to calculate the pulling force of the tillage tool with input parameters such as soil bulk density, cohesion, internal friction angle, working speed, working depth, and tool-soil friction angle.

2.9 Socio-economic Approach of Smallholder Farmers in Ethiopia

Smallholder farmers in Ethiopia play a critical role in the country's agricultural sector, rain-fed and labour-intensive. Understanding their socio-economic conditions is essential when studying the prediction of draft force for small-scale tillage tools, as these factors influence tool adoption, soil management practices, and overall productivity. This review synthesizes

key socio-economic aspects of Ethiopian smallholder farmers and their relevance to developing and applying mathematical models for predicting draft forces.

2.9.1 Socio-economic characteristics of smallholder farmers

The socio-economic profile of smallholder farmers, including household size, education level, income, and access to resources, significantly affects their ability to adopt improved tillage tools and techniques. For instance, studies have shown that education and access to credit facilities are critical determinants of farmers' willingness to invest in modern farming equipment (Tariku etal., 2025). These factors also influence their ability to manage soil properties effectively, which is crucial for perfecting draft force predictions in different soil types. In the context of coffee production in the Wolaita zone, ordered logistic regression models revealed that education and access to resources were significant predictors of higher productivity among smallholders (Tegegn et al., 2024).

2.9.2 Socio-economic Benefit of small-scale tillage to Smallholder Farmer

Previous research studies investigate whether the use of draft animal power (DAP) increases the economic efficiency of smallholder farms in Kenya, specifically in the Kirinyaga district. The research compares two groups of farmers: those using DAP and those using hand hoes for maize production (Guthiga et al., 2007).

Takele & Selassie (2018) concluded that integrating motorized technology with traditional draught animal technology could be beneficial, especially for private investors and female-headed households. Awareness creation and close follow-up are essential for the successful adoption of mechanization. Improving working animals causes economic confidence and independence, improves social participation, and overcomes poverty (Geiger et al., 2020).

2.10 Draft Force Measurement

Three instruments were used for the draft force measurement of the tillage equipment: the dynamometer, the transducer (load cells), the strain gauge, and the extended orthogonal ring transducer (Gebregziabher et al., 2016). Most researchers have used load cells to measure the pulling force required for tillage in field experiments (Okyere et al., 2019b). Smolders (2017) measured the pulling force generated at the loading cell assembly site by connecting the cell load on the beam to that on both sides of the animal yoke at different depths.

2.11 Experimental Design (DoE)

The design of any task aims to characterize and explain data variability under circumstances considered experimental design (Englis & Frederiks, 2024). An experimental predicted outcome changes initial conditions through independent or predictor variables (Chimunhu et al., 2024).

Choosing appropriate independent, dependent, and control variables, the experimental design entails scheduling experimental deliveries under statistically ideal circumstances (Schweitzer et al., 2023). The experimental design was applied for two purposes: Screening and Optimization (Candioti et al., 2014).

2.11.1 Optimization of the Draft Force

Draft force optimization is essential for increasing productivity, reducing energy use, and boosting overall performance in agricultural equipment like walking tractors and ard plows. The draft force is needed to pull a tool that interacts with the soil through tillage processes (Riaz et al., 2023). Optimizing this force can lead to better soil engagement, reduce power consumption, and increase productivity in farming.

Utilizing the robust optimization features of JMP software is a key objective in conducting a Design of Experiments. The profiler option provides a cross-section of the model, displaying each factor's curve to show its relationship with the response. Several considerations can guide model optimization. One effective method is to use the profiler to adjust all available variables simultaneously to achieve the desired outcome.

To effectively optimize the draft forces, statistical software such as JMP. It is a powerful tool that enables researchers to optimize problems and find optimal solutions efficiently (Jiménez et al., 2022). JMP data can be viewed visually. Given its interactive features, extensive analytical powers, intuitive interface, and adaptability to several data studies, JMP is a promising tool for statistical analysis.

2.11.2 Linear model

Alternative methods, such as linear, interaction, and quadratic methods, were applied to the model. The three simplest model complexities Hocking (2013) expresses are a single linear model (Equation 2.11), an interaction model (Equation 2.12), and a quadratic model (Equation 2.13).

$$y = \beta 0 + \sum_{i=1}^{k} \beta_i x_i + \epsilon \quad (2.11)$$

$$y = \beta 0 + \sum_{i=1}^{k} \beta_i x_i + \sum_{i}^{k} \sum_{j>i}^{k} \beta_{ij} x_i x_j + \epsilon \quad (2.12)$$

$$y = \beta 0 + \sum_{i=1}^{k} \beta_i x_i + \sum_{i}^{k} \sum_{j>i}^{k} \beta_{ij} x_i x_j + \sum_{i=1}^{k} \beta_{ii} x_i^2 + \epsilon \quad (2.13)$$

Where: y; is the Response (draft force), which depends on the k factor, the error term, β_i, and β_{ij} are coefficients and is the level of the i^{th} factor.

Optimizing Tillage Operations: Variable Width Ploughs: Crdei et al. (2021) assessed the optimal parametric combinations in operating regime agricultural aggregates with ploughs variable width. The starting point was from the classic expression of the tillage draft force required for traction. The extremes provided by the working regime and speed were found.

2.12 Validation and verification of models

Assessing prediction uncertainty is critical for validating and predicting as-yet-unmeasured data. This uncertainty often stems from various factors, including incomplete understanding of parameters and model inputs, inconsistencies within the model, inadequate assessments of the computing model, and errors in the solution and coding. Verification is a method for determining whether a demonstration implementation accurately represents the developer's theoretical description of the show and its solution. The validation of mathematical models is an essential prerequisite for practical, real-world applications (Brown, 2005). The relative root-mean-square error is the most used metric for assessing forecast accuracy by scaling each residual against the actual value (Equation 2.14). A minimal difference between actual and predicted values indicates a strong model. The RRMSE value must be less than 1 to fit the model. Otherwise, the model cannot identify suitable solutions (Thorp et al., 2007).

$$RRMSE = \sqrt{\frac{\frac{1}{n}\sum_{i=1}^{n}(y_i - \bar{y}_i)^2}{\sum_{i=1}^{n}(\bar{y}_i)^2}} \quad (2.14)$$

Let y (i) represent the i^{th} measurement, $\bar{y}$ (i) the corresponding prediction, and on the total number of data points.

The normalcy assumption validates the model and the actual amount within the forecasting range. The Z-score is another metric that assesses the expected value's relation to the

meaning of a group, serving as a verification check based on the principle of normality. To verify this, we applied a numerical approach. Descriptive statistics, including skewness and kurtosis, were used to indicate levels of secrecy. Skewness is calculated using the formulas in Equations 2.15 and 2.16.

$$\text{Skewness} = \frac{\sum(x-\tilde{x})^3}{(n-1)*y^3} \quad (2.15)$$

Here, $\tilde{x}$ is the mean, and y is the standard deviation.

$$\text{kurtosis} = \frac{\sum(x-\tilde{x})^4}{(n-1)*y^4} \quad (2.16)$$

At a 99% confidence level, the measured and expected draft forces are normally distributed, with skewness values acceptable between +3 and -3. Kurtosis, measured using SEM ranges from +10 to -10 (Kenny & Editor, 2007).

Regression modeling was used to evaluate potential dimensionless assemblies using the IBM SPSS statistical software version 26. Multivariate analysis of variance assessed the correlation between experimental and predicted draft force values. The validity (goodness of fit) model was evaluated by comparing it with the experimental data, as indicated by the established R^2. The correlation coefficient (R^2) is determined by dividing the regression sum of squares (SSR) by the total sum of squares (SST) using Equation 2.17.

$$R^2 = \frac{SS_R}{\text{SS}_\text{T}} \quad (2.17)$$

2.13 Mathematical Models for Predicting Draft Force of Tillage Tools

The prediction of draft force, which is the force required to pull a tillage tool through the soil, is a crucial aspect of agricultural engineering. Accurate prediction of draft force is essential for optimizing tillage operations, selecting appropriate machinery, and estimating energy requirements. Several mathematical models have been developed to predict draft force, each with its advantages and limitations. These models range from simple empirical equations to complex numerical simulations.

Empirical and Theoretical Models

Cardei et al. 2019, present research on the calculation formulas of the draft force of agricultural machines. While the formulas appear different, the study finds cohesion and coherence embodied in a simple generalization that is easy to use theoretically and experimentally. The formulas are convertible between them, and the two languages used for

their definition (the mechanics of deformable solids and that of the phenomenological description) are only different forms of expression for the same phenomenon.

The most general form of the draft force (F) of tools for soil tillage machinery, according to ASAE (American Society of Agricultural and Biological Engineers) standards, can be expressed as:

$$F = A + Bv + cv^2$$

Where: A represents the static component of the draft force. B and C are coefficients related to soil and tool parameters. v is the tillage speed.

This general equation highlights the dependence of draft force on tillage speed (Cardei, 2019). The parameters A, B, and C are determined empirically and depend on soil type, tool geometry, and working depth.

Sohne's Mathematical Model: Drwish (2020) selected Sohne's mathematical model, simulated it using Visual Basic, and validated it. The results indicated that the model could predict draft for simple tillage tools with an accuracy of 86%, 95%, and 85% for rake angle, tool depth, and tool speed, respectively. This suggests that Sohne's model can be a useful tool for predicting draft force under certain conditions, particularly for simple tillage tools. Farman Ali developed a knowledge-based fuzzy logic model to predict draft, side, and vertical forces, as well as the soil disturbance area caused by a disc tillage tool (Chandio et al., 2020). The model was developed using experimental data collected in a soil-bin environment, with three working speeds and depths. The fuzzy logic model demonstrated a close relationship between measured and predicted data, with draft prediction accuracy responding positively. The results also showed that side forces increased slightly with increasing speed and depth, while the disturbed area was significantly affected by higher depth (Chandio, 2020).

Prediction of Draft Force with ANNs: Artificial neural networks (ANNs) used to predict the draft force of a rigid tine chisel cultivator. The draft force was predicted based on tillage depth, soil moisture content, soil cone index, and forward speed. The results showed that the developed ANNs with two hidden layers outperformed the networks developed with other algorithms (AbbaspourGilandeh, 2020). The average simulation accuracy and the correlation coefficient for the prediction of draft force were 99.83% and 0.9445,

respectively. The linear regression model had a much lower accuracy and correlation coefficient compared to the ANNs.

Kazm developed an artificial neural network (ANN) model with a back propagation learning algorithm to predict specific draft force and fuel consumption requirements of a mouldboard plough in clay loam soil (Arman et al., 2019). The input parameters were tillage depth, forward speed, and operation. The model predicted specific draft force and fuel consumption requirement of the plough. The model predicted values with an error of less than 1% when compared to measured values, indicating that ANN prediction could be considered as an alternative practical tool for predicting implements selected experimental conditions soils.

Kazm Arman investigated the effects of a chisel tine on draft force and disturbed area and estimated them using artificial neural networks (ANN) and multiple linear regression equations (MLR). The results showed that ANN models with depth as input variables performed better, with a coefficient of determination of 0.999 and 0.998 and a root mean square error of 0.010 and 0.016, respectively. The ANN model performed better than the MLR model (Arman, 2021).

Abdulrahman Al-Janobi developed a draft model of a moldboard plow based on two novel variables: soil texture index (STI) and field working index (FWI). Coefficient of determination (R^2) values obtained using the testing dataset were found to be 0.9134 and 0.8602 for draft and energy requirements, respectively. The mean absolute errors between measured and predicted values using artificial neural networks (ANN) were 0.99 kN and 2.39 kWh/ha, respectively. The predictions from the proposed ANN were very satisfactory compared to multiple linear regressions (Al-Janobi et al., 2020)

Discrete Element Method (DEM): An analytical model and Discrete Element Method (DEM) were used to predict sub soiling. Experimental data obtained in a soil bin trolley with force sensors were used for verification. The predicted results from DEM had the best regression (R^2 = 0.984) and NRMSE (1.936), while the AM had the lowest R^2 (0.957) and NRMSE (6.008) (Makange, 2021). A field experiment to evaluate the performance of disc furrow openers in paddy soil and used discrete element modeling to develop a 3D DEM model for notched, toothed, and double disc openers using EDEM software (Al-Dosaryet al., 2020). The simulated and experimental data were compared to determine the applicability of DEM under different working conditions. The relative error was lower for the notched opener compared to the toothed and double disc types. The Finite Element

Method (FEM) was applied to simulate the structure of a rotary tillage soil blade with different bending angle parameters and obtained its average stress and deformation position information. A discrete element (DEM) based simulation was used to build a corresponding model of the particle soil-rotary roll interaction and simulate the dynamic process of soil cutting and the change rules of the contact area, energy, resistance, and soil movement. By using an orthogonal test and response surface method, the kinematic parameters of the roller and key design parameters of a single tiller were optimized (Zhang et al., 2022).

In general, mathematical models play a crucial role in predicting the draft force of tillage tools. These models, ranging from empirical equations to fuzzy logic, ANNs, and DEM simulations, provide valuable insights into the complex interactions between soil, tool, and operating parameters. By accurately predicting draft force, agricultural engineers can optimize tillage operations, select appropriate machinery, and promote sustainable agricultural practices. Continued research and development in this area are essential for improving the efficiency and sustainability of agricultural production systems. It is important to consider not only the accuracy of the models, but also the practicality of their implementation and the potential impact on soil health and the environment (Shaheb, 2021, MacLaren, 2020, and Wittwer, 2021).

2.14 Summary of key findings from the literature review

The findings from the research's conclusions focused on predicting the draft force of small-scale tillage tools using mathematical models across different soil types, which are comprehensively outlined in this literature review. The identified knowledge gaps and potential future research directions offer a roadmap for advancing this critical area of small-scale tillage tools.

Even if several previous studies agree that understanding and accurately predicting the draft force required when using tillage tools can improve efficiency and outcomes in farming practices, the ard plow is a traditional tillage tool used for centuries in agriculture. However, the draft force has not been predicted.

Although several studies have shown that moldboard plows mounted on heavy and medium tractors have been used to till land for centuries, there are no precise dimensions for moldboard plows mounted on small-scale power tillers. Effectively using small-scale tillage tools by smallholders, have great tendency to improve the economy of smallholder’s farmer.

The draft force of a tillage tool depends on how the soil deforms with increasing soil shear strength. Thus, the operating velocity was maintained throughout the field test performance. The extent of the soil's cross-sectional surface influences the moisture content of the soil, which also affects the tillage equipment's draft force requirements and other soil parameters. It also affects soil failure. Therefore, during the field testing, the purpose was to stabilize the water content in the soil as much as possible.

It has been demonstrated that the operating conditions of tillage tools, tool geometry, and soil properties affect the degree of soil failure during soil tillage. Several researchers have selected variables to determine the draft of tillage tools. However, no previous studies have referred to the variables created by pushing the ard plow or controlling the power tiller. There is a notable study gap concerning the impact of soil texture on draft force prediction models for small-scale tillage tools, according to literature evaluations of the prediction of draft forces based on soil texture.

CHAPTER THREE

MATERIALS AND METHODS

This chapter designated the study areas, listed the materials and equipment used to determine the soil properties, identified procedures for field and laboratory experiments, developed experimental research design and field measurements of the ard plow and scaled down moldboard tillage tools.

3.1 Description of the Study Areas

Cheha Woreda lies between latitudes 7.99°–8.25° and 37.59°–38.06°. The mean maximum and minimum temperatures were 27°C and 18°C, respectively. Ewan Keble lies on the lower slope, and its elevation is 1908 m. Ewan's coordinates are N 080 13" 43," E 370 48" 45," and Wordene's coordinates are N 080 09" 37," E 370 46" 33'. Teff is the major crop cultivated in Ewan, and farmers are smallholders with an average area of 1 hectare. Enset and maize are the major crops cultivated in Worden, a smallholding with an average area of 0.25 ha. Data were collected from July 1, 2021, to July 30, 2021, after 10 days of rainfall.

The study was conducted in agricultural fields characterized by silt clay and silt loam soils. These soils were selected based on their prevalence in the region and their significance for smallholder farming. The areas were chosen to represent typical conditions encountered by small-scale farmers, including variations in soil texture, moisture content, and compaction levels.

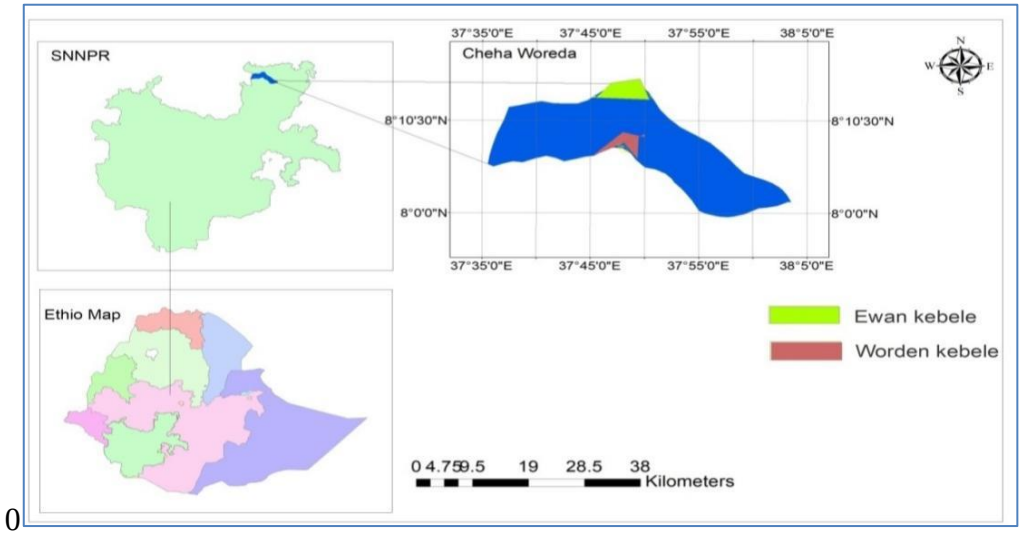

0

Figure 3.1 Map of the study area

3.2 Specifications of Tillage Tools

The study utilized two types of tillage tools: the ard plow (Figure 3.2) and a scaled moldboard plow (Figure 3.3). These tools were selected for their common usage in small-scale farming and their ability to demonstrate varying draft force requirements under different soil conditions.

3.2.1 Ard Plow

The ard plow is a traditional tillage tool widely used by smallholder farmers. It consists of a wooden beam, a metal share, and a leather strap for attachment to the draft animals. The geometry and operating conditions of the ard plow were analyzed to understand their influence on draft force.

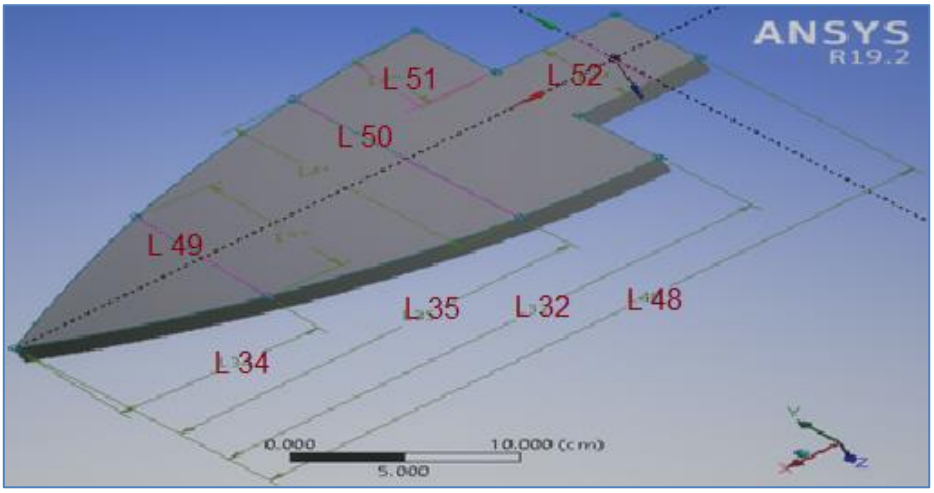

Figure 3.2 ard plow geometry

The specification of the Ard plow is indicated in Table 3.1. To build a model for small-scale tillage tools the basic shape of Ard plows and scaled Moldboard plows.

Table 3.1. Specifications of the Ard Plow

Parts	L32	L34	L35	L48	L49	L50	L51	L52
Length (cm)	23	12	19	42	5	8	1.5	5

3.2.2 Bottom Mouldboard Plow

The bottom moldboard plow prototype made of CK45 with dimensions of 0.86m× 0.48m× 0.42 m was used for the scale-down model. The scaled models were developed based on geometric similitude, ensuring that their dimensions-maintained proportionality with full-

scale plows. This approach allowed for efficient testing and analysis under controlled conditions. The geometry of the full-scale bottom moldboard is listed in Table 3.2, and Table 3.3 describes its material properties.

The moldboard shape was considered as the cylindrical tool used in this study. The full-scale prototype and scaled-down model of the Moldboard plow used in the tillage process are the same. A replica model is a physical representation of a prototype that is geometrically identical in all aspects and uses the same materials.

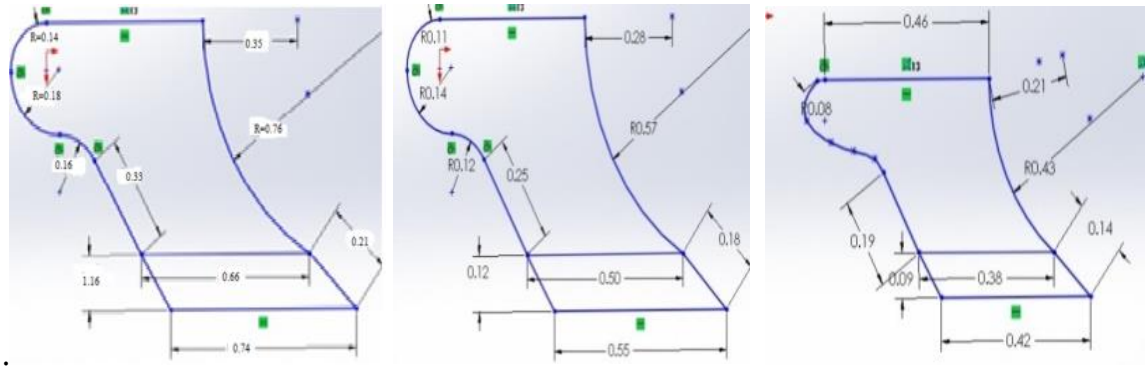

(a) (b) (c)

Figure 3.3 Geometrical structure of the (a) full-scale mouldboard (b) ¾-scale mouldboard (c) ½-scaled mouldboard

Table 3.2. Mechanical properties of CK45

Properties	Unit	Value
Elastic modulus (E)	(GPa)	202
Density, (ρ)	(kg m^3)	7820
Yield Tensile strength (S_y)	(MPa)	580–770
Elongation at fracture	(%)	27.8
Yield stress	(MPa)	393
Ultimate stress	(MPa)	637
Poison ratio (μ)	-	0.29
Yield strength	(MPa)	330–640
Shear modulus	(GPa)	75–80
Ultimate Tensile strength (S_{ut})	(Mpa)	1272

In this research, the objectives were to develop a model of a scaled moldboard plow and predict its draft force that smallholder farmers can use. Two scaled moldboards with 4:3 and

2:1 ratio (Figure 3.3 b and c) taken from the full prototype (Figure 3.3 (a) used in the field area to measure the draft forces.

3.3 Identification of Field Area Soil Textures

Soil samples were collected from the study areas to determine their texture. Hydrometer and sieve analysis were performed to measure the proportions of sand, silt, and clay in each sample. Two kilograms of soil samples were collected from both Keble and submitted to the Ethiopian Planning and Monitoring Works Corporation (EPMWC). Fine soil particles (< 2 mm) separated from larger particles (gravel and stones).

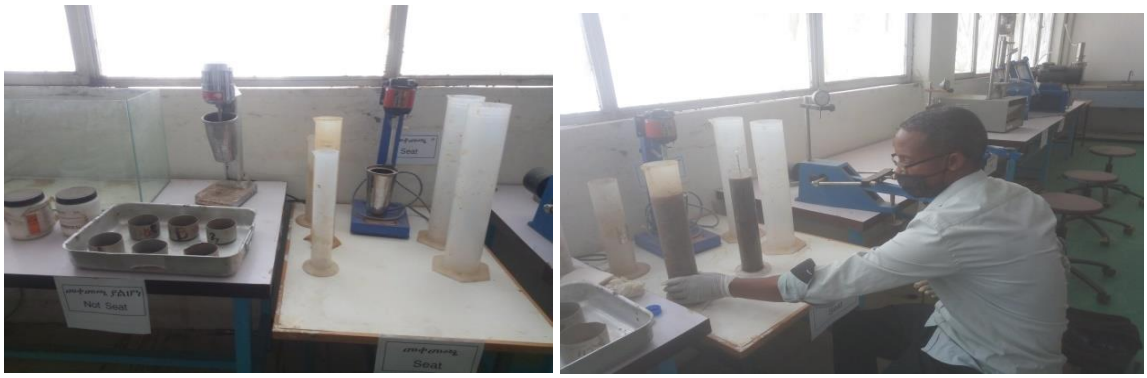

Figure 3.4 Experimental hydrometer readings

The diameter of soil texture is identifying by using hydrometer (Figure 3.4). The soil texture class was used to calculate the percentage of soil particles in the suspension using Equation 3.1. The US Department of Agriculture soil texture triangle used to calculate soil particles.

$$S_{Pa}(\%) = \frac{s \times s_L \pm T_c}{w} \qquad (3.1)$$

Where: S_{pa}; the particles percentage on the suspension, s; the sample measured, s_L; blank sample measured, T_c; temperature correction factor (0.36), and w; the sample weight (g).

3.4 Determination Soil Physical Property

3.4.1 Soil moisture content

After 10 days of rainfall, soil samples were collected from both field areas from July 1, 2021, to July 30 of 2021. The procedure complied with the ASTM standards for assessing soil moisture content in a laboratory. This method represents the percentage of weighted soil water content. To comply with this standard, the soil was dried at high temperatures in an oven. The sample was dried mass-consistently in an oven, and the moisture content was calculated using equation (3.2).

$$\text{M. C} = \frac{WW-DW}{WW} X100 \qquad (3.2)$$

Where: M.C is moisture content, *WW* is Wet Weight and *DW* is dry weight.

Dry samples were collected from the field, placed in containers, and weighed. The soil was ground using a rubber-coated mortar or pestle to a fine powder that could pass through a 2.00-mm sieve. The oven maintained the inner of the dry chamber at a constant temperature of 110.5^0C for 24 h and ensured equilibrium with precision of 0.01 g (Figure 3.5). The samples were removed from the oven, allowed to cool to room temperature, and then weighed once dried.

Figure 3.5 Soil moisture laboratory test equipment.

3.4.2 Soil bulk density

The bulk density test evaluates soil compaction. One method to determine soil bulk density is using a core cutter as per Standard 2720529. For this, we utilized an apparatus for measuring water content, a steel tamper, a pallet knife, a steel ruler, a sample extruder, and a core cutter with an inner diameter and height of 130 mm to collect undisturbed soil samples from the experimental field (Figure 3.6). Expose a small area of the floor to be tested and smooth the surface to about 300 mm².

Attach the dolly to the core drill and use the tamper to press it into the soil. Stop pressing when the stamp is about 15 mm above the soil surface. Remove the soil around the core cutter, as well as the cutter itself, ensuring the bottom protrudes slightly. Carefully trim the top and bottom ends of the core cutter with a straightedge. Weigh the filled core cutter to the nearest milligram, then remove the soil core. Dry the soil samples according to the moisture content drying procedure. Determine the bulk density using Equation 3.3.

Figure 3.6 Soil samples from the field area to evaluate bulk density.

$$\gamma_b = \frac{w_s - w_c}{v_c} \left({}^{g}/_{cm^3}\right) \quad (3.3)$$

Where: γ_b is Bulk density, w_c is Weight of core cutter, v_c is volume of soil, and w_s is Weight of wet soil.

3.5 Determination Soil Mechanical Property

The soil mechanical property measured in this study included the shear strength parameters and soil penetration force (cone index).

3.5.1 Soil shear strength: internal friction angle (φ) and cohesion (C)

A representative soil sample taken from undisturbed and unloaded sites (Figure 3.7 (a) and the sample in the device under the initial stress state are described in triaxial test Figures 3.7 (b), 3.7 (c), and direct shear Figure 3.7 (d).

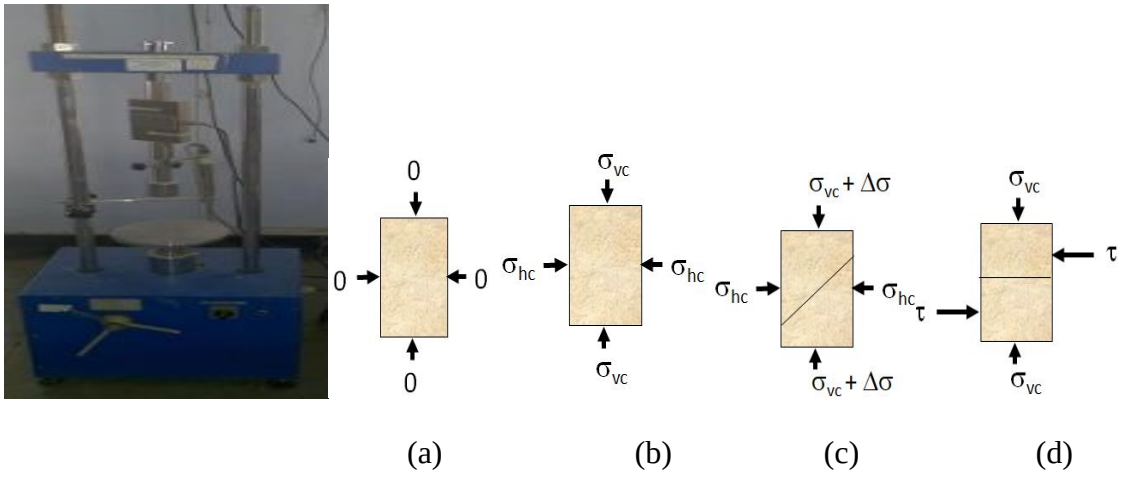

Figure 3.7 Soil specimen apparatus under first and corresponding stress conditions

Laboratory experiments were conducted to determine the mechanical property of the soil. These results were later used to predict the tensile force model, including the cohesion, adhesion, and internal and external friction angles. The soil shear strength was measured using a triaxial test apparatus. This device determined the amount of cohesion resistance and the internal friction angle.

3.5.2 Soil penetration resistance

Soil penetration resistance is a measure of soil strength. Soil penetration resistance measurements using a cone penetrometer enabled the calculation of soil compaction rates. The penetrometer delivered its readings at three different depth points at 10 cm, 15 cm and 20 cm. The resistance force that penetrated the ground was calculated as the force resulting from the scale value divided by the cone base area in Equation. (3.4).

$$P_r = \frac{F}{A} \tag{3.4}$$

Here, P_r is the penetration resistance in N/m, F is the force in N, and A is the area in m.

3.6 Determination of Soil Shear Stress and Deformation

The particle size determines the classification of soil materials into three groups: clay, silt, and sand. These particles exhibit significant variations in their mechanical properties. In this study, the researchers investigated multiple soil particle types, including silt clay soil and silt loam soil, which are abundant in the study area. Table 3.3 lists the mechanical properties of the clay, silt, and sandy soils. The numerical method (FEM) was employed in this research to determine soil shear stress.

Table 3.3. The mechanical properties of soil particles

soil particles	Density (kg/m^3)	Young modulus (MPa)	Poisson ratio	Compressive strength (MPa)
Clay	1580	25	0.4	0.16
Silt	1380	20	0.33	0.05
Sand	1520	25	0.27	0.01

3.7 Predicting the Draft Force Using Dimensional Analysis

Identify Relevant Parameters: Dimensional analysis depends on the determination of significant variables before estimating draft force. An analysis of dimensional units starts by studying how velocity, density, viscosity, size and shape of the tool affect results.

Develop Dimensional Relationships: Once the relevant parameters have been identified, dimensional relationships can be expressed based on these parameters. This involves the draft force as a relation between these parameters in dimension units.

Application of Buckingham's Pi Theory: Buckingham's Pi theorem is a fundamental principle in dimensional analysis. The proposed method reduces the number of variables in

a problem. Applying this theorem, it is possible to derive dimensionless groups (Pi terms) that encapsulate the relationships between the different parameters influencing the draft force.

Empirical Formula: By applying the dimensionless Pi terms derived from the Buckingham–Pi theorem, an empirical equation is formulated to estimate the draft force influenced by various parameters. This formula provides insights into how each parameter affects the draft force and allows for predictive modeling.

Experimental Validation: The created model was assessed by contrasting the predicted draft force values with the actual measured values at specific significance levels (for instance, 0.05). No significant discrepancies were found between the predicted and actual values.

Effectiveness Evaluation: The developed model evaluated by comparing the predicted and measured draft force values at certain significance levels (e.g., 0.05). It shows no significant difference found between the predicted and measured values.

3.8 Modelling Assumptions

In modeling the interaction of tillage tools and soil, several assumptions are made to simplify the analysis without compromising accuracy. These include:

i. The soil is considered a continuum medium with homogenous properties.
ii. Experienced operators and farmers were selected to operate walking tractors and draft animals.
iii. The adjusted forward speed was constant throughout the selected operation.
iv. The geometry of small-scale tillage tools assumed idealized shapes in the mathematical model.

3.9 Modelling Approach

Modeling is a technique used to create models representing a system or process. In tillage systems, modeling approaches are used to model and predict the behaviors of interconnected soil and tools.

3.9.1 Modelling of the ard Plow

The operating distance between the share and beam, which was connected using a leather strip, influences the draft force of the tillage tools by increasing and decreasing the depth. In

this study, both parameters were considered in addition to basic parameters such as moisture content, soil bulk density, soil cohesion and adhesion force, internal friction angle, shear strength of soil, mass of implement, rake angle, forward speed of tillage tools, and depth of tillage tools. Thus, the relationship between dependent (draft force) and independent variables can be generalized as follows (Equation. 3.5).

$$F_d = f\ (d, p, v, g, C, CI, \rho, m_s, \phi, \lambda, M) \quad (3.5)$$

3.9.1.1 Pi-theorem

The Pi Theorem references Buckingham's π Theory and works on the perception of dimensional homogeneity. The proposed method minimizes the dimensional variables to fewer dimensionless groups. A credible group of dependent and independent variables is limited dimensionally because a small subset of variable collections can be a suitable dimension. The fundamental units of the dependent variable (draft force) and independent variables: the distance between the leather stripe (metal loops) and share (p), rake angle of plow ($\propto$), angle of soil internal friction (φ), angle of the applied force by the operator (λ), gravitational acceleration (g), soil cohesion force (C), one index (CI), implement mass (m_s), soil bulk density (ρ) and soil moisture content (M), are shown in Table 3.4.

Table 3.4. Variables defining the draft force.

Variable	Symbol	Dimension
Draft force	F_d	MLT^{-2}
Distance b/n the leather stripe and share	p	L
Internal soil friction angle	φ	Deg.
Depth of the plow	d	L
Operator operating angle	λ	Deg.
The plow rake angle	$\propto$	Deg.
Forward speed	v	LT^{-1}
Soil bulk density	ρ	ML^{-3}
Soil cohesion	C	$ML^{-1}T^{-2}$
Cone index	CI	$ML^{-1}T^{-2}$
Implement mass	m_s	M
soil moisture content	M	Deg.
Acceleration due to gravity	g	LT^{-2}

The dimensionless parameter "k" required to compare variables in a procedure is calculated by subtracting the number of variables concerned "N" and is the number of basic dimensions incorporated with the variables "M" (Asonye et al., 2019; Ogunnigbo et al., 2022). According to Equation 3.1, the number of variables (N) is 13 (thirteen), and the number of basic dimensions (M, L, T) is 3 (three). Hence, K = 13, which yields 10 (ten). Therefore, 10 dimensionless parameters were constructed, representing the following:

$$\pi_1, \pi_2, \pi_3, \pi_4, \pi_5, \pi_6, \pi_7, \pi_8, \pi_9 \text{ and } \pi_{10}$$

It is written as a repeated-variable dimensional matrix: Density (ρ), operating depth (d), and operating speed (v) are selected as repeated variables. The dimensional matrix of the draft force is given in Table 3.5.

Table 3.5. Dimensional matrix

Dimension	P	v	d
M	1	0	0
L	-3	1	1
T	0	-1	0

Unrepeated and dimensionless variable arrangement in the dimensional matrix form (Table 3.6).

Table 3.6. Dimensionless variable

Dimension	F_d	p	g	C	CI	α	φ	λ	M	m_s
M	1	0	0	1	1	0	0	0	0	1
L	1	1	1	-1	-1	0	0	0	0	0
T	-2	0	-2	-2	-2	0	0	0	0	0

Simplicity and dimensionless variables were removed from the dimensional matrix form (Simonyan, 2015), and the results are rearranged in Table 3.7.

Table 3.7. Dimension of unrepeated variables.

Dimension	F_d	p	g	C	CI	m_s
M	1	0	0	1	1	1
L	1	1	1	-1	-1	0
T	-2	0	-2	-2	-2	0

Shifting repeating and unrepeated dimensional variables into dimensionless groups forms an equation that divides the unrepeated dimension by the repeated dimension with the power of unidentified values (Alghazali, 2012). These unidentified values are written in matrix form as $y = a^{-1}b$. Three repeated dimensions and six (6) unrepeated dimensions were rearranged in a dimensional matrix form, as summarized in Equation 3.6.

$$\begin{bmatrix} y_{11}\, y_{12} & y_{13\ldots} \cdot\ y_{18} \\ y_{21}\, y_{22} & y_{23\ldots} y_{28} \\ y_{31} & y_{32}\, y_{33} \cdots y_{38} \end{bmatrix} = \begin{bmatrix} 1 & 0 & 0 \\ 0 & 0 & -1 \\ 3 & 1 & 1 \end{bmatrix} \begin{bmatrix} 1 & 0 & 0 & 1 & 1 & 1 \\ 1 & 1 & 1 & -1 & -1 & 0 \\ -2 & 0 & -2 & -2 & 2 & 0 \end{bmatrix} \quad (3.6)$$

The dimensionless group combined into reduced dimensionless groups by multiplication (Shafii et al., 1996). Table 3.8 presents how to achieve the dimensionless group of the ard plow's draft force.

Table 3.8. A summary of the dimensionless draft force

π_1	π_2	π_3	π_4	π_5	π_6	π_7	π_8	π_9	π_{10}
$\frac{F_d}{\rho v^2 d^2}$	$\frac{p}{d}$	$\frac{gd}{v^2}$	$\frac{C}{\rho v^2}$	$\frac{CI}{\rho v^2}$	$\frac{m_s}{\rho d^3}$	α	φ	λ	M

The dimensionless parameters are combined and developed in Equation 4.7.

$$\pi_{1,2} = f(\pi_{3,4}; \pi_{5,6}; \pi_{7,8}; \pi_{9,10}) \quad (3.7)$$

Hence, the functional form given by Equation 3.8:

$$\frac{F_d}{p\rho v^2 d} = f\left(\frac{gd\rho}{C}, \frac{CId^3}{v^2 m_s}, \frac{\alpha}{\varphi}, \frac{\lambda}{M}\right) \quad (3.8)$$

Further rearranged and expressed in Equation 3.9.

$$F_d = f\left(\frac{pd^2\rho^2 v^2 g}{c}, \frac{pCId^4\rho}{m_s}, \frac{p\rho v^2 d\alpha}{\varphi}, \frac{p\rho v^2 d\lambda}{M}\right) \quad (3.9)$$

3.9.2 Application of Buckingham Pi theorem

The moldboard plow performs three core tasks during the tillage process: soil cutting, turning, and soil inverting (Figure 3.8). A plow is used to cut the soil. Side and horizontal forces are required to turn and reverse the soil (Saunders et al., 2007). The reduced physical structure of the moldboard performed a task like that performed by a heavy moldboard plow.

Figure 3.8 Draft force components of the mouldboard Plow (source: Saunders et al., 2007).

The Pi Theorem is referred to Buckingham's π Theory, which considers the perception of dimensional homogeneity. The method minimizes the number of dimensional variables in fewer dimensionless groups.

For the equation, the credible group of dependent and independent variables is limited dimensionally because a single small subset of variable collections can be suitable in this case. Table 3.9 lists the variables desired to describe the draft force.

Table 3.9. Variables wanted to describe the draft force.

Variable	**Symbol**	**Dimension**
Draft force	F_d	MLT^{-2}
Length of the moldboard	L	L
Depth of the plow share	d	L
width of the plow share	w	L
share the rake angle	∝	Deg.
Soil bulk density	ρ	ML^{-3}
Soil cohesion	C	$ML^{-1}T^{-2}$
Forward speed	V	LT^{-1}
Acceleration	g	LT^{-2}
Radius of curvature	R	L
Friction angle between soil and metal	β	Deg.

The draft force (f_d) created at the moldboard plow during soil tillage is based on the plow share (p_s), soil momentum alteration and friction along the moldboard (p_{mb}), soil potential energy on the moldboard and frictional draught (p_{PE}), side friction force at the share (p_{sfs}), side friction at the moldboard force (p_{sfmb}), and side force at the moldboard side movement (p_{ssoil}) (Saunders et al., 2007). Equations 3.10 – 3.16 explain the moldboard plow's draft force.

$$F_p = f(\rho, C, d, w, v, g, \beta) \quad (3.10)$$

Where: ρ = soil bulk density (N/m³), c = soil cohesion (N/m²), d = depth of the plow point in soil (m), w = width of the plow (m), v = forward velocity (m/s), g = acceleration due to gravity (m/s²), and β = angle of soil to metal friction (degrees)

$$p_s = f(d, \propto, w, \beta) \quad (3.11)$$

Where: d = depth of the plowshare in soil (m), w = width of the plowshare (m), and ∝ = share rake angle (degrees).

$$p_{mb} = f(\rho, g, \beta, d, w) \quad (3.12)$$

$$F_{PE} = f(\rho, d, w) \quad (3.13)$$

$$F_{sfs} = f(\rho, v, c, g, d) \quad (3.14)$$

$$F_{sfmb} = f(\rho, v, g, \beta, d, w) \quad (3.15)$$

$$F_{ssoil} = f(L, d, w, R) \quad (3.16)$$

Where: L= the length of the moldboard (m).

Therefore, the above draft force function can be summarized and expressed in Equation 3.17, and it results in a physical equation with the dimensional homogeneity of the tilling process, which describes the physical relationship between the numerical values F_d and the set of other physical quantities.

$$F_d = f(\rho, v, g, \beta, d, w, c, \propto, L, R) \quad (3.17)$$

The Buckingham Pi theorem represents a physical phenomenon through a dimensional quantity (Q) alongside its influencing dimensional quantities of $f_1, f_2, f_3 \ldots n$. The equation describes the relationship between Q and the dimensional parameters and is expressed in Equation 4.18 (Patel et al., 2020).

$$Q = f\ (f_1, f_2, f_3 \ldots f_n) \quad (3.18)$$

The dependent variable (Q) and independent variables f_n..... expresses in a non-dimensionless term (π) in Equation 3.19.

$$\pi_1 = f(\pi_2 . \pi_3 . \pi_4 \ldots\ldots_{n\ldots.}) \quad (3.19)$$

The dimensions of mass (M), time (T), and length (L) are used to express the units for both independent and dependent variables in a dimensional form. There are two types of variables (repeated and unrepeated) in the functional relation of dimensional analysis. Repeated variables summarized from independent variables and their number of basic dimensions. As a result, the dimensionless group does not include the dimensional matrix of repeated variables (Casaburo et al., 2019).

Linear equations for repeated variables (A) and unrepeated variables (B) with unknown values (X) are written using the following form of Equation 3.20.

$$A(X) = B \tag{3.20}$$

Unidentified values of X are written in the matrix form of: $\frac{1}{A}AX = \frac{1}{A}B$ become$X = A^{-1}B$. It addresses these arbitrary exponents and Pi parameters by mandating that each product group be dimensionless ($\Pi_1, \Pi_2, \Pi_3 \ldots\ldots\ldots \Pi_n$).

It is known that, among the above parameters, the output variable must be measured in units of Newtonian units, and consequently, all relations in the equation vital look in groupings that create these dimensional units of are MLT^{-2}. The search for an arrangement with an unidentified governing equation can assist by reducing the number of parameter groupings. Combination variables generated MLT^{-2}. After isolating the dimensionless variables, the remaining variables can be written as Equation 3.21.

$$[\rho]^{e_1}.[d]^{e_2}.[v]^{e_3}.[F_d]^{e_4}\,[w]^{e_5}.[c]^{e_6}.[L]^{e_7}.[g]^{e_8}.[R]^{e_9} = 0 \tag{3.21}$$

Rearranging the equation and defining the basic dimensions:

$$(M^1L^{-3}T^0)^{e_1}.(M^0L^1T^0)^{e_2}.\ (M^0L^1T^{-1})^{e_3}.(M^1L^1T^{-2})^{e_4}.(M^0L^1T^0)^{e_5}.(M^1L^{-1}T^{-2})^{e_6}.$$

$$(M^0L^1T^0)^{e_7}.(M^0L^1T^{-2})^{e_8}.(M^0L^1T^0)^{e_9} = M^0L^0T^0$$

For the basic dimension M:

$$e_1 + e_4 + e_6 = 0$$

For the basic dimension L:

$$-3e_1 + e_2 + e_3 + e_4 + e_5 - e_6 + e_7 + e_8 + e_9 = 0$$

For fundamental dimension T:

$$-e_3 - 2e_4 - 2e_6 - 2e_8 = 0$$

The dimensional matrix (D) is expressed as: $N_d \times N_v$ with where N_d is the number of dimensions needed to express and N_v is the number of variables in the set of variables (Szirtes & Rozsa, 2007). The dimensional matrix is present in the dimensions ordered by MLT (Equation 3.22). Researchers attempted to locate parameter groups with a certain unit, resulting

$$\begin{array}{c|ccccccccc} & \rho & d & v & F_d & c & L & w & g & R \\ M & 1 & 0 & 0 & 1 & 1 & 0 & 0 & 0 & 0 \\ L & -3 & 1 & 1 & 1 & -1 & 1 & 1 & 1 & 1 \\ T & 0 & 0 & -1 & -2 & -2 & 0 & 0 & -2 & 0 \end{array} = D \tag{3.22}$$

in Equation 3.23, which can be expressed as follows:

$$D \times e = q \tag{3.23}$$

Where: e ($N_V . 1$) is an unknown in a column vector to be solved for, and q ($N_d . 1$) is column vector with given (known) dimensions. The matrix D can be divided into two matrices (Szirtes & Rozsa, 2007) as follows (Equation 3.24):

$$\underbrace{D}_{N_D . N_V} = \left[\left(\underbrace{B_D}_{N_d \cdot (N_v - N_d)} \middle| \underbrace{A_D}_{N_d . N_d} \right)\right] \tag{3.24}$$

For Equation 3.25, the separating matrix force is arranged into a dimensional matrix of two sub-matrices.

$$\underbrace{\overrightarrow{\boldsymbol{B}\ matrix}\left[\begin{bmatrix} 1 & 0 & 0 \\ -3 & 1 & 1 \\ 0 & 0 & -1 \end{bmatrix}\begin{bmatrix} 1 & 0 & 1 & 0 & 0 & 0 \\ 1 & 1 & -1 & 1 & 1 & 1 \\ -2 & 0 & -2 & 0 & -2 & 0 \end{bmatrix}\right]\overleftarrow{\boldsymbol{A}\ matrix}}_{Dimensional\ Matrix} \tag{3.25}$$

The solution form of a matrix with an unknown exponent (Eq. 3.26):

$$\begin{bmatrix} 1 & 0 & 1 & 0 & 0 & 0 \\ 1 & 1 & -1 & 1 & 1 & 1 \\ -2 & 0 & -2 & 0 & -2 & 0 \end{bmatrix}\begin{bmatrix} e_{11}\, e_{12} & e_{13\ldots}. & e_{1n} \\ e_{21}\, e_{22} & e_{23\ldots} & e_{2n} \\ e_{31}\, e_{32} & e_{33}\ldots. & e_{3n} \end{bmatrix} = \begin{bmatrix} 1 & 0 & 0 \\ -3 & 1 & 1 \\ 0 & 0 & -1 \end{bmatrix} \tag{3 .26}$$

Pi Theorem enables the identification of six (6) independent dimensionless variable groups.$N_P = N_v - N_d$, is $(9 - 3)$. $\propto$, and given that they are dimensionless and eliminated from the dimensionless terms' determination for later addition (Simonyan, 2015), while the other parameters are merged to construct the group by appropriately dividing or multiplying. M, L, and T, the other seven unutilized parameters, are rebuilt as dimensionless π groups (Table 3.10).

Table 3.10. Pi parameter dimensionless product groups.

π_1	π_2	π_3	π_4	π_5	π_6	π_7	π_8
$\frac{F_d}{\rho v^2 d^2}$	$\frac{c}{\rho v^2}$	$\frac{w}{d}$	$\frac{L}{d}$	$\frac{gd}{v^2}$	$\frac{R}{d}$	$\propto$	β

The nondimensional term can be further simplified as follows:

$\widetilde{\pi_1}$	$\widetilde{\pi_2}$	$\widetilde{\pi_3}$	$\widetilde{\pi_4}$	$\widetilde{\pi_5}$
$\frac{\pi_1}{\pi_2}$	$\frac{\pi_3}{\pi_4}$	$\frac{\pi_5}{\pi_6}$	$\propto$	β

It expressed:

$\widetilde{\pi_1}$	$\widetilde{\pi_2}$	$\widetilde{\pi_3}$	$\widetilde{\pi_4}$	$\widetilde{\pi_5}$
F_d	$\frac{Cwd^2}{L}$	$\frac{Cd^4 g}{Rv^2}$	$Cd^2 \propto$	$Cd^2\beta$

$$\widetilde{\pi_1} = f\,(\widetilde{\pi_2}, \widetilde{\pi_3}, \widetilde{\pi_4}, \widetilde{\pi_5})$$

$$\widetilde{\pi_1}(F_d) = f(\frac{Cwd^2}{L}, \frac{Cgd^4}{Rv^2}, Cd^2 \propto, Cd^2\beta) \qquad (3.27)$$

In a unified model that is applied in silt clay soil, the contributions of each predictor are weighted based on their significance and influence on the draft force.

3.9.2.1 Similitude theory of the moldboard plow

Required and adequate situations of likeness between the prototype and model are the focus of similarity theory (Sousseau et al., 2021). The full-scale prototype and scaled-down model of the Moldboard plow used in the soil tillage process are the same. A replica model is a physical representation of the prototype that is geometrically equal to the prototype and uses the same materials. $\pi_i^p = \pi_i^m$. Because all groups identified in Table 3.7 satisfied dimensionless rules; the functional relationship was satisfied. A similar situation results in the equivalent of two similar coordination equations, the similitude law, in which pi and mi represent full scale (prototype) and scale-down (model), respectively. The dimensionless product groups should have satisfactory responses and replicas for the prototype and model. The draft force prediction factor (Z) describes the association between the length scale of the moldboard (r) of variables and the developer for a certain soil-plow method (Tekeste et al., 2020). The draft force prediction factor (Z) (Equation 3.28).

$$Z = \frac{P_i}{m_i} = r^x \qquad (3.28)$$

Geometrically similar scaling principles dictate that certain parameters, including soil-soil contact angle, rake angle, soil-metal contact angle, and gravitational acceleration, cannot be scaled down (Neuberger et al., 2007).

$$F_d = kr^m \qquad (3.29)$$

Where: F_d; the prediction draft force (N), k; the coefficient that approximates the draft force from a full-scale moldboard plow (n = 1), and "m" the exponential classical coefficient that approximates the grade of a straight-line relation between the draft force and the length scale, r; the length of the moldboard (L).

The physical relationships between the prototype and model take the moldboard length scale $(r) = \frac{L_m}{L_p}$ is the dimensionless scale of π groups and becomes.

$$\frac{F_{dm}}{\rho_m v^2{}_m d^2{}_m} = \frac{F_{dp}}{\rho_p v^2{}_p d^2{}_p}; \quad F_{dm} = \frac{F_{dp} * \rho_m v^2{}_m d^2{}_m}{\rho_p v^2{}_p d^2{}_p} = F_{dp}(\frac{\rho_m}{\rho_p} + \frac{v^2{}_m}{v^2{}_p} + \frac{d^2{}_m}{d^2{}_p}) = (\pi_1)^m$$

$\frac{c_m}{\rho_m v^2_m} = \frac{c_p}{\rho_p v^2_p}$, $c_m = \frac{c_p * \rho_m v^2_m}{\rho_p v^2_p}$, $c_m = c_p \left(\frac{\rho_m}{\rho_p} + \frac{v^2_m}{v^2_p}\right) = (\pi_2)^m$

$\frac{w_m}{d_m} = \frac{w_p}{d_p}$, $w_m = \frac{d_m w_p}{d_p}$, $w_m = w_p \frac{d_m}{d_p} = (\pi_3)^m$

$\frac{L_m}{d_m} = \frac{L_p}{d_p}$, $L_m = \frac{d_m L_p}{d_p}$, $L_m = L_p \frac{d_m}{d_p} = (\pi_4)^m$

$\frac{g_m d_m}{v^2_m} = \frac{g_p d_p}{v^2_p}$, $g_m = \frac{g_p v^2_m d_p}{d_m v^2_p}$, $g_m = g_p(\frac{v^2_m}{v^2_p} + \frac{d_p}{d_m}) = (\pi_5)^m$

$\frac{R_m}{d_m} = \frac{R_p}{d_p}$, $R_m = \frac{d_m R_p}{d_p}$, $R_m = R_p \frac{d_m}{d_p} = (\pi_6)^m$

The scale factors listed in Table 3.11 describe the scaled bottom moldboard.

Table 3.11. Prototype and model relationships among dependent and independent variables.

Parameters	Scale factor	Scale = 1(prototype)	Scale = ¾	½
Length (L)	R	1	0.75	0.5
Width (w)	R	1	0.75	0.5
Depth (d)	R	1	0.75	0.5
Radius of curvature (R)	R	1	0.75	0.5
Gravity (g)	1	1	1	1
Velocity (v)	1	1	1	1

3.10 Systematic Data Collection and Arrangements

3.10.1 Tillage treatments of ard plow

The plow of the tillage implements was used to determine their pulling needs depending on the working speed and depth. The operation was performed after 10 days of rain. Three blocks (Figure 3.9a), each measuring 30 m wide × 16 m long, (Figure 3.9b) were developed to cover the land in the field area.

The treatments allocated in the 2 x 2 x 3 factorial experiment settled in three repetitions in a random complete block design (RCBD). The RCBD sources were used to collect data in the field area. Divide the experimental area into blocks and randomly assign treatments (different combinations of factors such as various plows or depths of tillage) within each block. This randomization helps ensure uncontrolled variables are evenly distributed across all treatments. Repeat the experiment multiple times to increase the precision of estimates and allow for statistical analysis of the results.

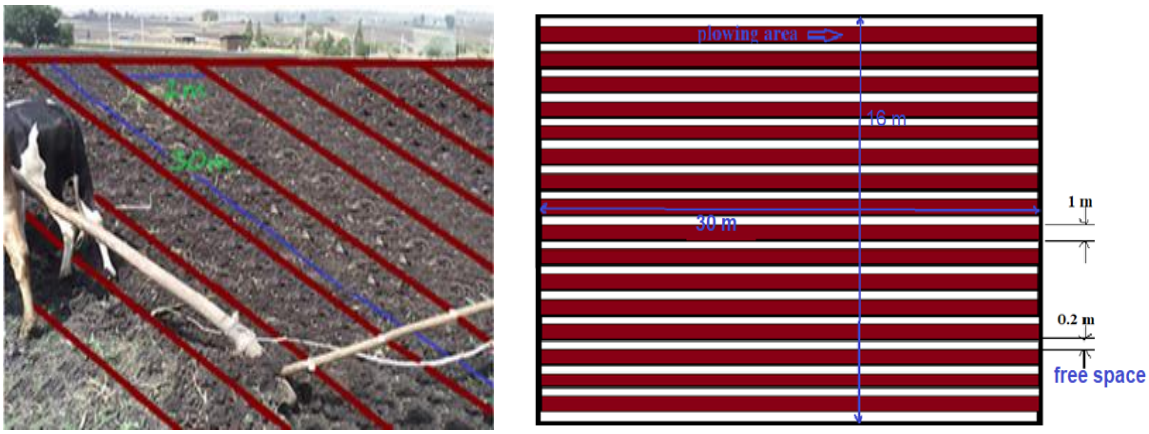

(a) (b)

Figure 3.9 Experimental design of the field area

The angle of the applied force by the operator in field tests: $\lambda_1 = 57^0$, $\lambda_2 = 60^{0,}$ and $\lambda_3 = 63^0$ used as the angle of the applied force by the operator, and the distance between plowshare and the leather strap attachment: P_1=18 cm and p_2 = 22 cm used as the distance between plowshare and the leather strap attachment. Ard plow tillage implements for both silt clay soil (S_1) and silt loam soil (S_2) imposed on the field (Table 3.12).

Table 3.12 A complete block randomized design (2x2x3)

Replication 1

T_1 ($S_1P_1\lambda_1$)	T_2 ($S_1P_1\lambda_2$)	T_3 ($S_1P_1\lambda_3$)	T_4 ($S_2P_1\lambda_1$)
T_7 ($S_1P_2\lambda_1$)	T_8 ($S_1P_2\lambda_2$)	T_5 ($S_2P_1\lambda_2$)	T_6($S_2P_1\lambda_3$)
T_9 ($S_1P_2\lambda_3$)	T_{10} ($S_2P_2\ \lambda_1$)	T_{11} ($S_2P_2\lambda_2$)	T_{12} ($S_2P_2\lambda_3$)

Replication 2

T_4 ($S_2P_1\lambda_1$)	T_3 ($S_1P_1\lambda_3$)	T_1 ($S_1P_1\lambda_1$)	T_2 ($S_1P_1\lambda_2$)
T_6 ($S_2P_1\lambda_3$)	T_5 ($S_2P_1\lambda_2$)	T_7 ($S_1P_2\lambda_1$)	T_8 ($S_1P_2\lambda_2$)
T_{12} ($S_2P_2\lambda_3$)	T_{11} ($S_2P_2\lambda_2$)	T_9 ($S_1P_2\lambda_3$)	T_{10} ($S_2P_2\ \lambda_1$)

Replication 3

T_3 ($S_1P_1\lambda_3$)	T_4 ($S_2P_1\lambda_1$)	T_{12} ($S_2P_2\lambda_3$)	T_6 ($S_2P_1\lambda_3$)
T_5 ($S_2P_1\lambda_2$)	T_7 ($S_1P_2\lambda_1$)	T_2 ($S_1P_1\lambda_2$)	T_{10} ($S_2P_2\ \lambda_1$)
T_{11} ($S_2P_2\lambda_2$)	T_9 ($S_1P_2\lambda_3$)	T_1 ($S_1P_1\lambda_1$)	T_8 ($S_1P_2\lambda_2$)

3.10.2 Experimental Instrumentation

Zebu oxen are the main draft animals weighing 250-300 kg and are used for seedbed preparation (Gebregziabher et al., 2006). The force data were obtained using a hanging circular spring balance connected between the beam and the center of the yoke (Figure 3.10).

Figure 3.10 Draft force of the ard Plow drawn on the animal.

3.10.3 Tillage treatments of walking tractor (scaled mouldboard Plow)

The treatments allocated in a 2 x 3 x 3 factorial experiment settled in a randomized complete block design (RCBD) in three repetitions. Tillage depths taken: D_1 = 10 cm, D_2 = 15 cm, and D_3 = 20 cm, and the working speeds of the power tiller selected: v_1 = 0.75 ms^{-1}, v_2 = 1.00 ms^{-1} and v_3 = 1.50 ms^{-1} with ¾-scaled bottom moldboard tillage implements (M_1) and ½-scaled bottom moldboard tillage implements (M_2) imposed on the field (Table 3.13).

Table 3.13. Design of the block of plots

T_1	T_2	T_3	T_1	T_2	T_3
$M_1v_1D_1$	$M_1v_1D_2$	$M_1v_1D_3$	$M_2v_1D_1$	$M_2v_1D_2$	$M_2v_1D_3$
$M_1v_2D_1$	$M_1v_2D_2$	$M_1v_2D_3$	$M_2v_2D_1$	$M_2v_2D_2$	$M_2v_2D_3$
$M_1v_3D_1$	$M_1v_3D_2$	$M_1v_3D_3$	$M_2v_3D_1$	$M_2v_3D_2$	$M_2v_3D_3$
$M_1v_1D_2$	$M_1v_1D_1$	$M_1v_1D_2$	$M_2v_1D_2$	$M_2v_1D_1$	$M_2v_1D_2$
$M_1v_2D_2$	$M_1v_2D_1$	$M_1v_2D_2$	$M_2v_2D_2$	$M_2v_2D_1$	$M_2v_2D_2$
$M_1v_3D_2$	$M_1v_3D_1$	$M_1v_3D_2$	$M_2v_3D_2$	$M_2v_3D_1$	$M_2v_3D_2$
$M_1v_1D_3$	$M_1v_1D_3$	$M_1v_1D_1$	$M_2v_1D_3$	$M_2v_1D_3$	$M_2v_1D_1$
$M_1v_2D_3$	$M_1v_2D_3$	$M_1v_2D_1$	$M_2v_2D_3$	$M_2v_2D_3$	$M_2v_2D_1$
$M_1v_3D_3$	$M_1v_3D_3$	$M_1v_3D_1$	$M_2v_3D_3$	$M_2v_3D_3$	$M_2v_3D_1$

An 8-hp walking tractor was operated in the field area to measure the draft force of the scaled moldboard plow. The moldboard implements used for the field area were general-purpose bottom moldboards of ¾-scale and ½-scale from full-scale general-purpose bottom moldboards. The pull force (draft force) was measured by a circular spring balance with a load capacity of 100 kg and an accuracy of 500 g per dial inch, mounted between the walking and supplementary tractor.

3.11 Quantitative Data Analysis

3.11.1 Statistical Design

Use randomized complete block designs (RCBD) or factorial designs to analyse the effects of independent variables (soil properties, tool geometry, operational parameters) on draft force.

3.11.2 IBM SPSS statistical software

It used to develop linear regression functions to predict draft force. ANOVA (Analysis of Variance) evaluates whether the model significantly affects the drag force. Validated the model performed by generating R^2, RRMSE, and CRM.

3.11.3 Laboratory and Software Analysis

Conduct laboratory tests to decide Shear Strength Using direct shear or triaxial tests. Cohesion and Angle of Internal Friction: These parameters are critical for modelling soil-tool interaction.

3.11.4 Field Sampling

Soil Texture: Collect soil samples from various depths (e.g., 0–15 cm, 15–30 cm) using soil augers or cores.

Particle size Analyse: The sand, silt, and clay content percentage identification using a hydrometer or sieve analysis.

Soil Moisture Content: Measure moisture levels using gravimetric methods (oven-drying) or portable moisture sensors.

Bulk Density: Core samplers measure soil bulk density at different depths.

Soil Strength: Measure soil penetration resistance using a cone penetrometer to assess compact levels.

3.11.5 Experiment Design Procedures using JMP Software

A full factorial experiment was conducted in this study. The following procedures generate the Design:

1. Open the JMP home window and select the DOE/classical/full-factorial design.

2. Identify the Response(s):

Write the dependent variable (draft force) in place of Y.

Change the response Goal and write Upper and Lower Limits.

3. Identify the Factors:

Click Categorical to determine the number of factors and add a factor.

4. Select Randomize and select default in the run order.

5. Select the Make Table to generate the design.

The model script is saved in the data table, and the design arrangement window is open to modify the design.

6. The model is established and evaluated

Select the Analyze/Fit Model.

Fill out the responses and factors related to the space provided.

Click runs.

7. The prediction profiler presents the model for optimization and desirable values and the simulator for determining the response values.

Select optimization and desirability from the prediction profiler.

To adjust desirability from prediction profilers and select optimization and desirability.

Select the simulator from the prediction profilers.

3.12 Model Development of Shear Stress and Deformation in Soil Textural Class

During soil tillage, the interaction between the soil and the tool disrupts the soil structure, making it a focal point for modeling. Most soils exhibit nonlinear behavior, presenting a three-dimensional solid mechanics problem. ANSYS software was used to create 3D representations of soil structures, characterized by their simplicity and rapid use. Thus, this software is an option for implementing multiple soil models.

The cutting behavior of soil is contingent on soil particle resistance strength. Tillage modifies the soil's surface. The conversion of soil into a slender, elongated configuration presents notable challenges for generating friction between the tool and material, which leads to elevated stress levels. The present study examined the finite element method, which investigates the mechanisms of the contribution of stress among particles by applying appropriate contact to soil under an applied force.

Throughout the soil modeling procedure, a hypothesized soil pressure was generated at the uppermost surface upon which the plowshare encounters the soil for agricultural tillage implements. The tool can be regarded as moving while the domain is established within the soil influence zone. The tillage tool's impact can be used to determine soil disruption and the magnitude of the force.

3.12.1 Model Geometry

An ANSYS Workbench was used to demonstrate the application of the plowshare force to the soil. The plow creates a path in the soil, causing the upper part of the soil to move and the lower part of the soil to appear as a solid object. The test was performed on soil with a volume of 2 m long, 1 m wide, and 1.5 m high (Figure 3.11).

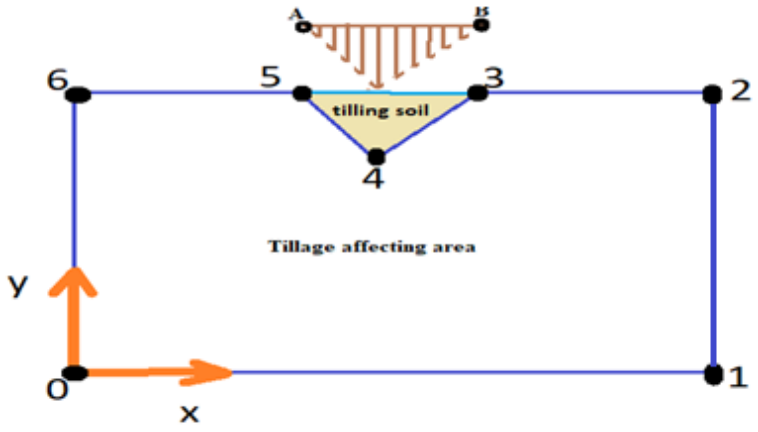

Figure 3.11 Geometry model

The advance of the disturbed soil dimensions outside the upper layer was assumed to have no effect on the shear forces.

3.12.2 Loads and boundary conditions

The movement of the plowshare pushes the soil with an applied horizontal force of 615, 815, 1115, 1315, and 1515 N in the forward direction (Figure 3.12).

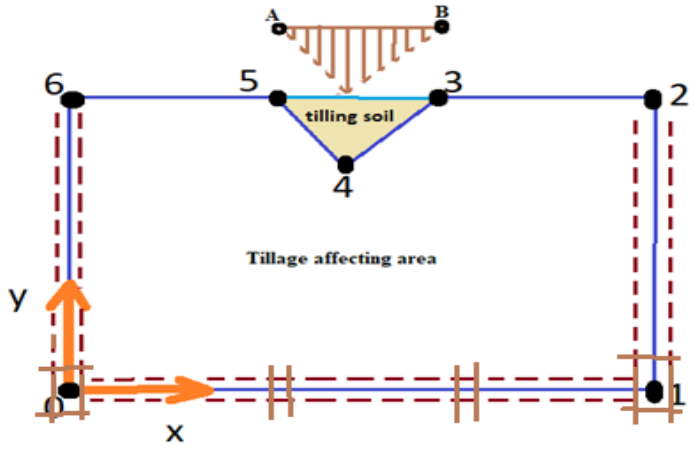

Figure 3.12 Boundary conditions.

3.12.3 Mesh generation

Enhance calculation precision and minimize potential effects on mesh density during analysis. A tetrahedral mesh has the advantage of being able to accurately approximate the surface morphology (Pan et al., 2009). Tetrahedral meshes are commonly used to simulate stress distribution in computational modeling. This method was employed in this investigation. Therefore, control mesh with an element size of 25 mm and a defeater size of 10 mm (Figure 3.13).

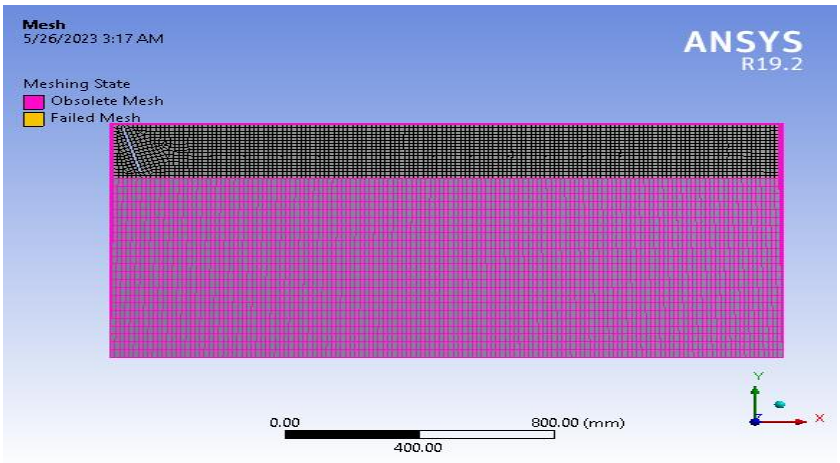

Figure 3.13 Mesh of the model geometry.

CHAPTER FOUR

RESULTS AND DISCUSSION

4.1 Soil properties in the study areas

4.1.1 Textural classes of soil in the Worden field

Sieve analysis and hydraulic tests were performed to study the Worden field area soil particles by measuring their settling speed in water solutions. The testing method used classification protocols to divide particles into clay groups (< 2.0 µm), silt groups (2.0 – 50 µm), and sand groups (50 – 2000 µm respectively). Hydraulic tests, as a supplement to these classifications, relied on the principle that particle settling velocities differed since gravity acted on particles of different sizes at different rates. The outcomes of the hydrometer tests for the Worden field area are summarized in Table 4.1, which provided insights into the distribution of particle sizes within the sample.

Table 4.1. Hydrometer analysis

Elapsed time (min)	Actual hydrometer reading, Ra	Temp (°c)	Effective Depth (cm)	K From Table	Temperature correction factor (Ct)	Modified Hydrometer Reading R=Ra-Cz+Ct	Partial diameter	Percentage Pass (%)	Corrected Percentage pass (%)
0									
2	27.00	20	11.68	0.04	0.04	20.95	0.034	43.05	39.16
5	24.00	20	12.17	0.04	0.04	17.95	0.022	36.69	33.55
15	23.00	20	12.34	0.04	0.04	16.95	0.012	34.63	31.66
30	20.00	20	12.83	0.04	0.04	13.95	0.009	26.67	26.08
60	18.00	20	13.16	0.04	0.04	11.95	0.006	24.56	22.34
250	14.00	20	13.62	0.04	0.04	7.95	0.003	16.35	14.67
1440	12.00	20	14.15	0.04	0.41	6.49	0.001	13.16	11.97

Sieve analysis was applied to define the grain-size spreading of soils with diameters >0.075 mm. Woven wire sieves with square apertures were used for this technique. Table 4.2 lists the U.S. standard sieve records and the corresponding aperture widths.

Table 4.2. Experimental data for Sieve analysis with a disturbed sample size

Sieve size (mm)		Retained 1st sieving Weight	% Rtd.	Percentage (%)
3”	75.000	0.00	0.00	100.00
$2\frac{1}{2}$	63.000	0.00	0.00	100.00
2”	50.000	0.00	0.00	100.00
$1\frac{1}{2}$	37.500	0.00	0.00	100.00
1"	25.000	0.00	0.00	100.00
0.75"	19.000	0.00	0.00	100.00
0.5"	12.500	0.00	0.00	100.00
0.375"	9.500	0.00	0.00	100.00
$N^0 4$	4.750	0.20	0.20	99.80
$N^0 10$	2.000	0.40	0.39	99.41
$N^0 16$	1.180	0.80	0.79	98.62
$N^0 30$	0.600	1.50	1.47	97.15
$N^0 40$	0.425	0.60	0.59	96.56
$N^0 50$	0.300	0.60	0.59	96.97
$N^0 100$	0.150	1.60	1.57	94.40
$N^0 200$	0.075	3.50	3.44	90.96
Pan		92.60	90.96	
Total		102		

Soil analysts classify sediments based on their dimensions since clay defines the smallest units while sand shows the largest structure. The tests showed that the soil sample included 18.69% clay with 72.47% silt and 8.84% sand, thus defining it as a silt loam soil texture (Figure 4.1).

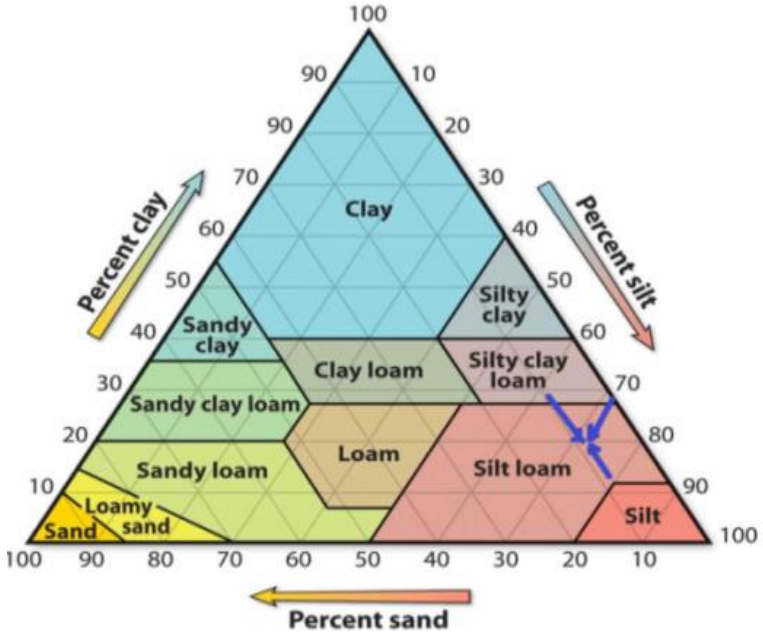

Figure 4.1 Soil textural class of Worden Keble

Tillage force: the high proportion of silt in this soil type suggests that the draft force required for tillage may be moderate compared to soils with higher clay or sand content. Silt loam soils typically offer less resistance than clayey soils, known for their stickiness and increased draft requirements due to higher cohesion (Akayuli et al., 2013).

Conversely, they require less energy than sandy soils, where larger particle sizes can lead to more excellent wear on tillage implements (Malvajerdi, 2023). The presence of 18.69% clay creates soil cohesiveness that will raise the required tillage force, but the silt content contributes to an ideal balance between tractor power needs and field working efficiency. Soil composition analysis contributes to optimizing proper design decisions of tillage tools because it helps achieve improved performance with enhanced energy efficiency.

4.1.2 Textural classes of the Ewan Keble Texture Classification

Table 4.3 presents the findings from the hydrometer test conducted on the soil samples collected from the Ewan Keble field area. The results displayed are essential for making informed decisions regarding the specific characteristics of the Ewan Keble field area.

Table 4.3. Soil data for Hydrometer Analysis

Elapsed Time (min)	Actual hydrometer	Temp (°c)	Effective Depth (cm)	K From Table	Temp, Correction	Reading R=Ra-Cz+Ct	Partial diameter (mm)	Percentage Pass (%)	Corrected Percentage
0									
2	25.00	20	11.68	0.04	0.04	20.95	0.033	43.05	39.16
5	24.00	20	12.27	0.04	0.04	17.95	0.023	36.69	33.55
15	23.00	20	12.22	0.04	0.04	16.95	0.012	34.63	31.66
30	20.00	20	12.63	0.04	0.04	13.96	0.009	26.67	26.08
60	18.00	20	13.25	0.04	0.04	11.96	0.006	24.56	22.34
250	14.00	20	13.52	0.04	0.04	7.97	0.003	16.35	15.69
1440	12.00	20	14.19	0.04	0.41	6.92	0.001	13.16	12.86

Soil particles of Ewan field area (Table 4.4) were determined using sieve analysis.

Table 4.4. Sieve analysis data.

Sieve size (mm)		Retain E weight 1st sieving% Rtd.		Percentage passing (%)
3"	75	0.00	0.00	100.00
$2\frac{1}{2}$	63	0.00	0.00	100.00
2"	50	0.00	0.00	100.00
$1\frac{1}{2}$	37.5	0.00	0.00	100.00
1”	25	0.00	0.00	100.00
0.75“	19	0.00	0.00	100.00
0.5“	2.5	0.00	0.00	100.00
0.375“	9.5	0.00	0.00	100.00
$N^0 4$	4.75	0.00	0.00	100.00
$N^0 10$	2	0.10	0.10	99.90
$N^0 16$	1.18	0.10	0.10	99.81
$N^0 30$	0.6	1.30	1.25	96.58
$N^0 40$	0.25	1.20	1.15	97.41
$N^0 50$	0.3	1.40	1.34	96.06
$N^0 100$	0.15	3.20	3.07	92.99
$N^0 200$	0.075	3.10	2.98	90.01
Pan		93.70	90.01	
Total		104		

The soil in the Ewan Keble is dominant in 45.50% clay, 44.51% silt, and 9.99% sand, which places it in the silt clay class according to the soil texture triangle (Figure 4.2).

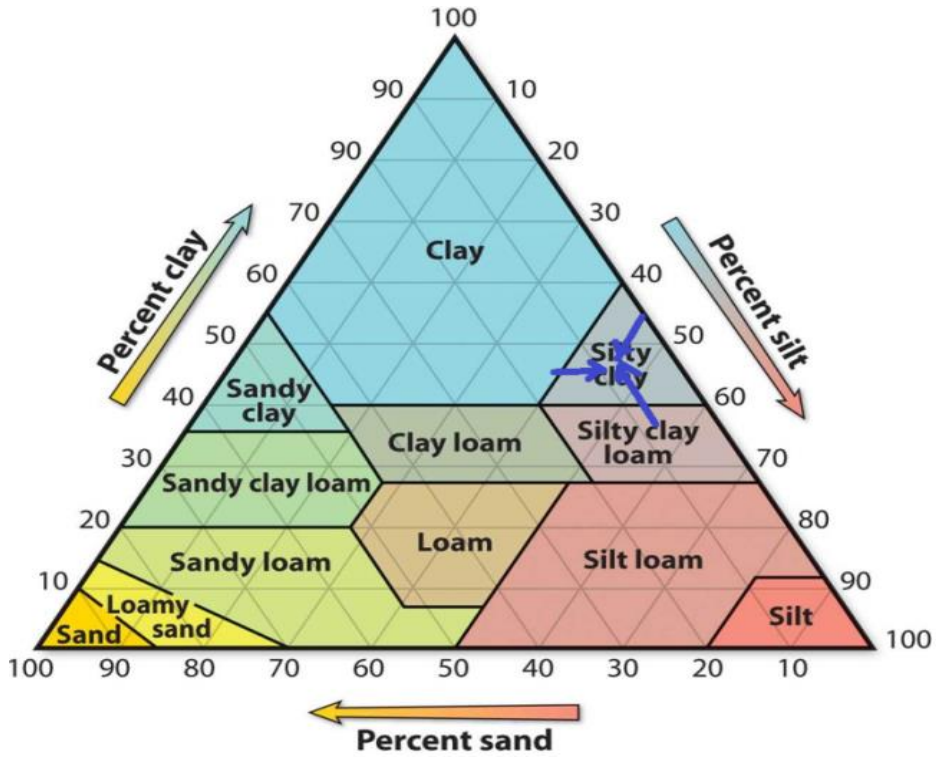

Figure 4.2 Location of the soil texture of Ewan Keble in the soil textural triangle.

As silt clay soil its properties should consist of strong adhesive behavior and plastic characteristics because the soil contains a high percentage of clay particles (Aziz, 2023). Due to their cohesive and adhesive properties silt clay soils need stronger machine force demands than other types of soils. (Okoko et al., 2018). The high clay content contributes to increased soil strength, particularly when the soil moisture content is optimal for tillage, leading to greater resistance against the tillage implement. This means that animal and walking tractors with tillage equipment will need more power to penetrate and turn over the soil effectively. Therefore, understanding the specific composition of the Ewan Keble soil helps in selecting appropriate machinery and optimizing operational parameters to achieve efficient tillage while minimizing wear on equipment and energy consumption.

4.2 Laboratory and Field Test of Soil Properties Results

Researchers assessed Ewan and Worden field soil properties at three levels for both physical characteristics and mechanics through measurements of moisture content and bulk density and shear strength analysis and penetration resistance data.

Table 4.5. Properties of Silt Clay and Silt Loam soil

Soil texture	Depth (cm)	Moisture content (%)	Bulk density (g/cm^3)	Soil cohesion	Soil internal friction (°)	Pen. resistance
Silt	10	29.99	1.13	19.4	26.37	1.64
loam	15	29.95	1.36	19.8	26.51	1.86
	20	29.96	1.45	20.9	26.53	2.00
Average		29.97	1.31	19.9	26.47	1.84
Silt clay	10	28.84	1.21	19.51	27.21	1.79
	15	29.87	1.25	19.71	27.61	1.80
	20	30.18	1.38	20.10	27.84	1.80
Average		29.63	1.28	19.77	27.55	1.80

Average moisture content of silt clay soil, is slightly lower compared to silt loam, but the bulk density also increases with depth, ranging from 1.21 g/cm³ at 10 cm to 1.38 g/cm³ at 20 cm. The penetration resistance for silt clay soil, however, remains constant at around 1.80 kPa across all depths. This stability in penetration resistance could be attributed to the soil's higher clay content, which provides greater cohesion even at varying levels of moisture and bulk density. Despite having a similar moisture content to silt loam, the silt clay soil exhibits slightly higher penetration resistance values, likely due to its inherently greater cohesiveness and plasticity (Usaborisut & Ampanmanee, 2015).

Soil properties, highlighting significant differences in moisture contents, bulk density, and cohesion between the two soil types as presented in Table 4.5. The documents identify significant variations in cohesion and internal friction angle between these two soil types This trend aligns with findings that soil penetration resistance generally increases with higher bulk density (Salman, 2020).

4.3 Effects of Plow Geometry and Screening Variables on the Ard Plow Draft Force

4.3.1 Influence of distance between leather stripe-share (p) and operator operating angle (λ) of ard Plow tillage tools on the draft force

The results of the distance between the leather stripe (metal loops) and the share (p) and angle of the operator force (λ) taken from the field area are presented in Table 4.6.

Table 4.6. Draft force (N) under the distance (p) and angle of the operator force (λ)

T_1 (Av_1D_1)	T_2 (Av_1D_2)	T_3 (Av_1D_3)	T_4 (Av_2D_1)	T_5 (Av_2D_2)	T_6 (Av_2D_3)	T_7 (Av_3D_1)	T_8 (Av_3D_2)	T_9 (Av_3D_3)
442	440	458	436	458	455	440	453	468
457	501	491	501	462	447	501	501	501
494	495	533	509	494	495	495	501	533
530	566	541	530	525	566	578	562	566
539	589	589	581	588	579	579	581	589
603	599	598	603	589	615	605	615	615

For a fixed p value (e.g., P_1), as the operator operating angle increases ($\lambda_1 \rightarrow \lambda_2 \rightarrow \lambda_3$), the draft force also increases: ($P_1\lambda_1$) = 452.57 N → ($P_1\lambda_2$) = 486.28 N → ($P_1\lambda_3$) = 508.57 N.

This trend is consistent for both P_1 and P_2, showing that increasing the operating angle requires a greater draft force. The effect of the distance between the leather stripe and share (p) and the operator operating angle (λ) of ard plow tillage tools on the draft force at specific depths and speeds is shown in Figure 4.3.

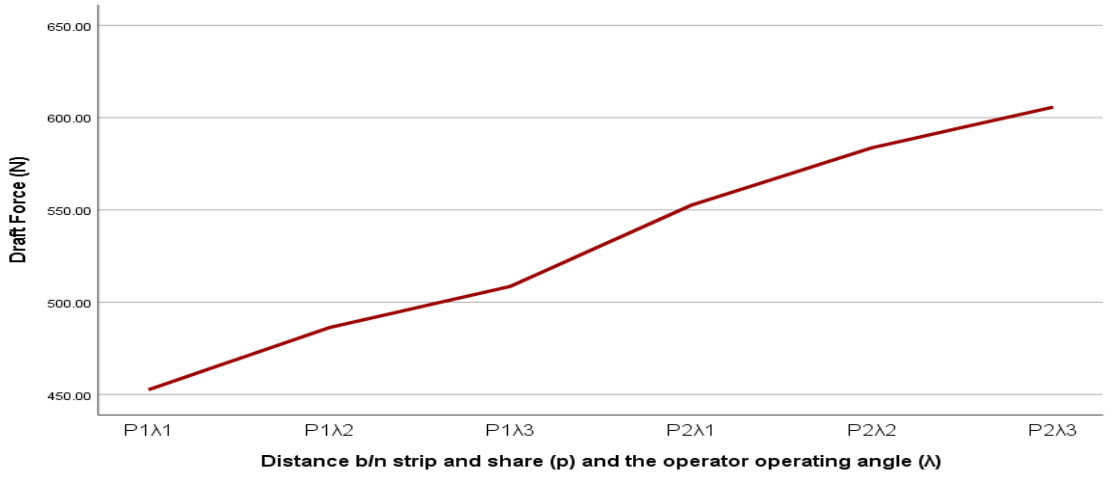

Figure 4.3 Draft force of Distance Stripe and Share, and operator operating angle.

Figure 4.3 shows the relation between the distance stripe and share (p) and the operator operating angle (λ) significantly influence draft force. Increasing either parameter leads to an increase in required draft force, likely due to greater resistance met during operation. As operator operating angle (λ) increases, it caused the equipment to encounter more soil or material, requiring additional effort to maintain movement. Distance Stripe and Share (p) increases correspond to higher draft forces, suggesting that larger distances or shares more

energy to overcome resistance. This could be because a wider or deeper cut into the soil demands more power.

4.3.2 Screened Variable Predictors of Ard Plow Draft Force in Soil Textures.

The draft force model predicted changes in one functional group parameter while keeping the others constant (Equation 3.5). This was done by comparing the measured results of the draft force design with the selected parameters, with three functional parameters held constant.

4.3.2.1 Screening variables for the predictor "A" of ard plows in silt clay soil

Predictor screening for variable "A" was performed using JMP 8, and regression analysis assessed the correlation between measured and predicted values. Figure 4.4 shows the actual predicted plot, effect summary and predicted profiler for Predictor "A." The data points align with a linear fit and include a confidence interval and mean response value. For effects with a P-value under 0.05, the RMSE was 23.66, the P-value was < 0.0001, and R^2 was 0.91.

A. Actual by Predicted Plot

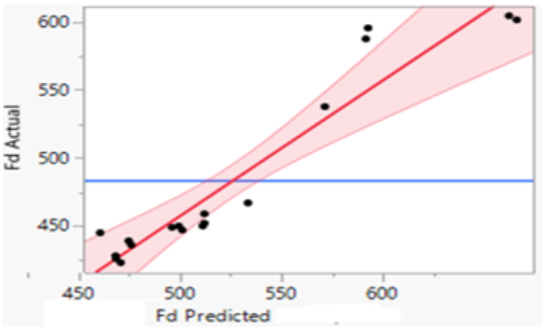

B. Effect summary

Source	Logworth	p-value
ρ	1.565	0.027
v	0.955	0.110
C	0.499	0.317
d	0.047	0.898
p	0.015	0.966
g	.	.

C. Prediction profiler

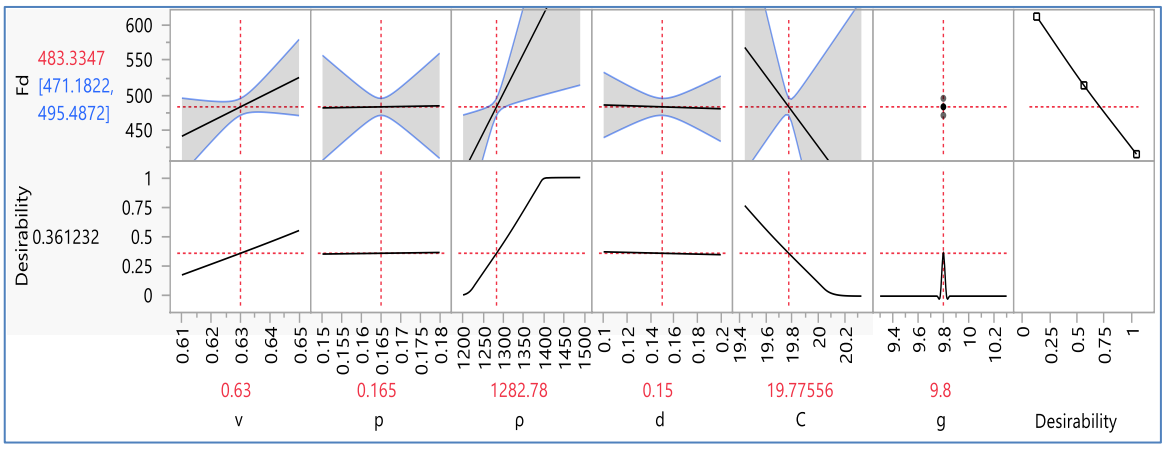

Figure 4.4 Predictor "A" variable screening design of experiments

The actual draft force strongly correlates with the predicted draft force values (Figure 4.4A). The p-value of less than 0.05 (Figure 4.4B), showing a highly significant effect. High R^2 values and low p-values collectively suggest a meaningful relationship. The mean, maximum and minimum draft force were 483.3, 495.4, and 471.1 N, and the slopes of all variable lines were the highest, showing a strong relationship with the response (draft force) (Figure 4.4C). Therefore, the predictor variables 'A' is highly correlated with the response (draft force). But variable "d," "g," and "ρ" excluded from the predictor 'A' because it minimizes the strength of the predictor 'A'.

4.3.2.2 Screened variables for predictor "B" of ard plow in silt clay soil

Figure 4.5 displays the predicted plot, effect summary, and predicted profiler for predictor "B," which has a P-value of <0.0001, an RMSE of 18.3, and an R^2 of 0.92.

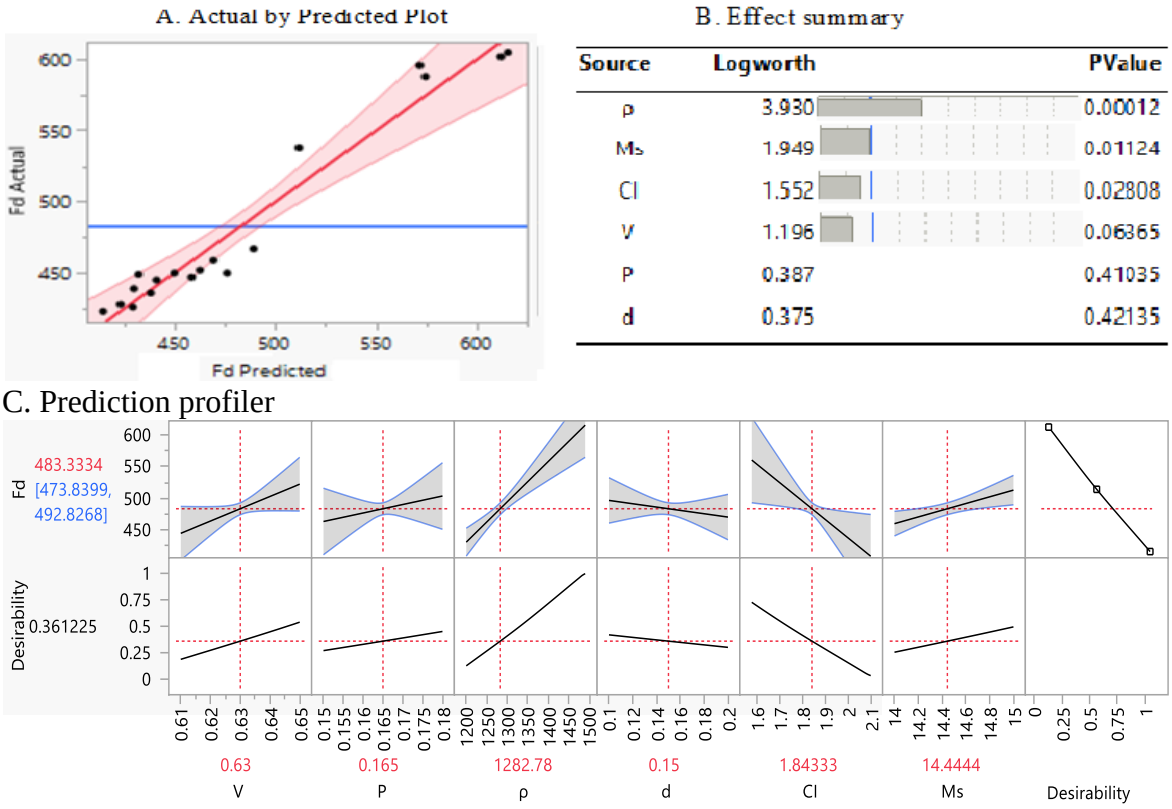

Figure 4.5 Square least square regression model of the predictor "B" screening DoE

The actual draft force strongly correlates with the predicted draft force values (Figure 4.5A). The p-value is less than 0. 05 (Figure 4.5B), showing a highly significant effect. High R^2 values and low p-values collectively suggest a meaningful relationship. The mean, maximum and minimum draft force were 483.3, 492.8, and 473.8 N, and the slopes of all variable lines were the highest, showing a strong relationship with the response (draft force) (Figure 4.5C).

Therefore, the predictor variable 'B' is highly correlated with the response (draft force). But variable “d,” “v” and “p” excluded from the predictor 'B' because it minimizes the strength of the predictor 'B'.

4.3.2.3 Screened variables for the predictor “C” of ard plow in silt clay soil

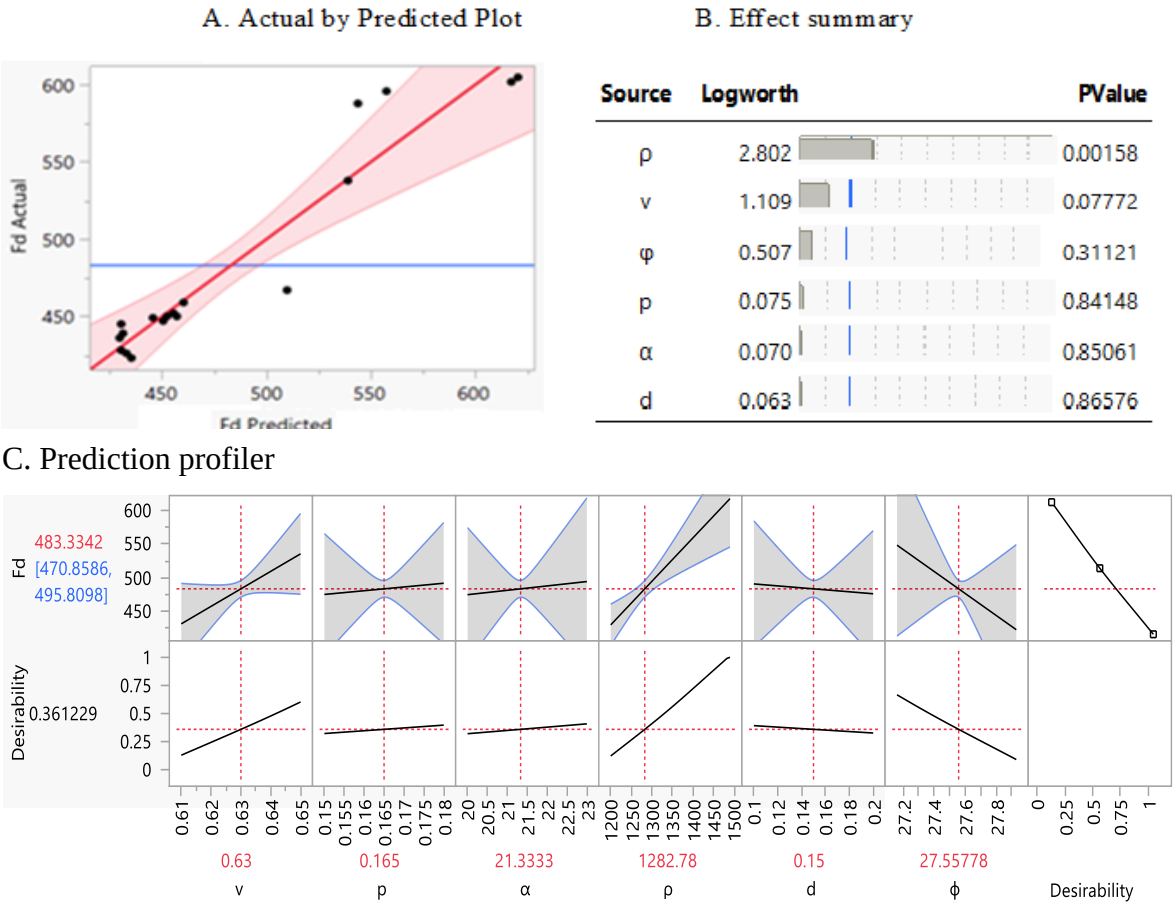

Figure 4.6 Square least regression model of the predictor “C” screening DoE

The actual draft force strongly correlates with the predicted draft force values (Figure 4.6A). The p-value is less than 0. 05 (Figure 4.6B), showing a highly significant effect. High R^2 values and low p-values collectively suggest a meaningful relationship. The mean, maximum and minimum draft force were 483.3, 495.8, and 470.8 N, and the slopes of all variable lines were the highest, showing a strong relationship with the response (draft force) (Figure 4.6C). Therefore, the predictor variables 'C' is highly correlated with the response (draft force). But variable “d,” “α,” and “ρ” excluded from the predictor 'C' because it minimizes the strength of the predictor 'C'.

4.3.2.4 Screened variables for predictor "D" of ard plow in silt clay soil

A. Actual by Predicted Plot

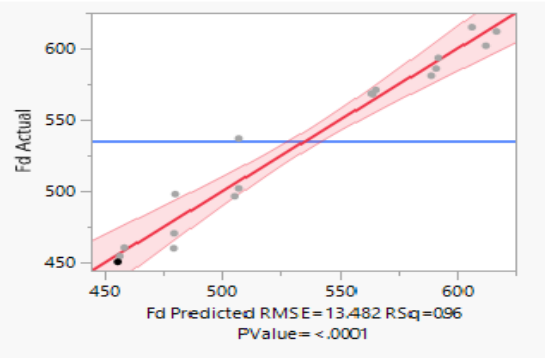

B. Effect summery

Source	Logworth	PValue
P	2.354	0.004
M	0.272	0.534
ρ	0.138	0.728
v	0.098	0.798
d	.	.
λ	.	.

C. Prediction Profiler

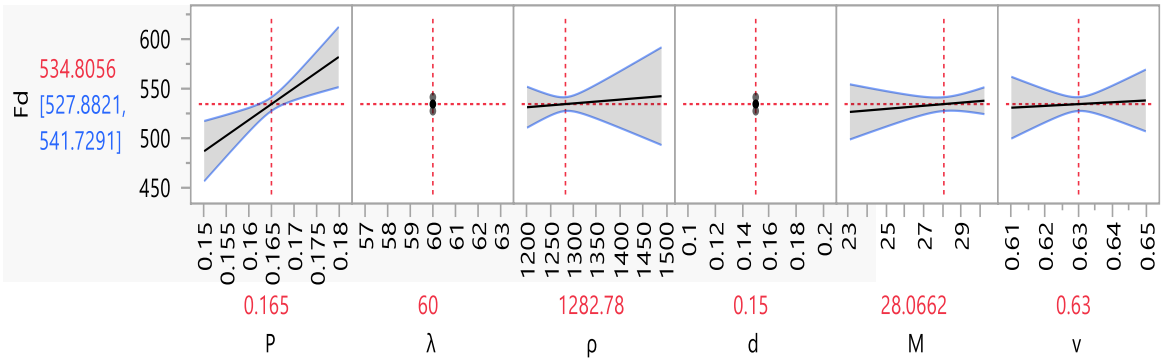

Figure 4.7 Stepwise regressions modelling of the draft force variables screening DoE response.

The actual draft force strongly correlates with the predicted draft force values (Figure 4.7A). The p-value is less than 0. 05 (Figure 4.7B), showing a highly significant effect. High R^2 values and low p-values collectively suggest a meaningful relationship. The mean, maximum and minimum draft force were 483.3, 495.8, and 471.1 N, and the slopes of all variable lines were the highest, showing a strong relationship with the response (draft force) (Figure 4.7C). Therefore, the predictor variables 'D' is highly correlated with the response (draft force). But variable "d," "λ," "v," and "ρ" excluded from the predictor 'D' because it minimizes the strength of the predictor 'D'. In general, the summarized variables of each predictor are presented in Table 4.7.

Table 4.7. Screened variables to predict the draft force of ard Plow in silt clay soil.

Predictor	"A"	"B"	"C"	"D"
Selected variables	P, C and v	CI, ρ, and M_s	ρ, v and φ	P and M

4.3.2.5 Responses of predictors to the ard plow draft force in silt clay soil

The analysis of ANOVA and the effect summary and prediction profiler results of predictors on the actual draft force were performed to evaluate the status of predictors on the measured draft force (Table 4.8).

The results showed the model is highly effective at variability in draft force measurements based on the factors considered. The high F-ratio and low p-value (0.01*) show that the model fits the data well and that the factors included have a statistically significant impact on the outcome.

Table 4.8 ANOVA results for summery and parameter estimates of predictors

Source	DF	Sum of Squares	Mean Square	F Ratio
Model	15	77598.07	5173.21	69.01
Error	2	149.92	74.96	Prob > F
Total	17	77748.00		0.01*

In practical terms, these implied changes in the input variables are likely to result in predictable changes in draft force.

Table 4.9. Effect Summary

Source	Logworth	P-value
predictor B	2.296	0.00506
predictor A	1.809	0.01554
predictor C	1.024	0.09466
predictor D	0.245	0.56877

Reading an effect summary table is crucial for understanding the significance and impact of different variables in a statistical model.

Predictor "A" With a Logworth value of 1.809 and a P-value of 0.01554, this predictor also shows statistical significance at the 0.05 level. The Logworth value of predictor "B" may be less significant, but it effectively contributes to explaining the dependent variable changes.

The Logworth value of 2.296 sets up that this predictor affects the dependent variable significantly because its p-value shows values below 0.05 (0.00506). Changes in predictor "B" prove a strong link to modifications in outcome 6.

The Logworth value from predictor “C” reaches 1.024 while its P-value stands at 0.09466. Another Logworth value was approaches the basic significance threshold although it failed the established requirement of $p < 0.05$. The relationship between predictor “C” and the dependent variable exists at lower strength when compared to predictors “A” and “B”.

The Logworth value from predictor “D” measures 0.245 while its P-value reaches 0.56877. The P-value of 0.56877 shows predictor “D” fails to produce meaningful statistical impact on the dependent variable based on this dataset.

This research shows that the dependent variable is most heavily influenced by both predictors’ "B" and predictor "A" along with the other examined predictors. Statistical values prove a high level of evidence against the null hypothesis because they present low P-values which suggest these variables provide significant contributions to explaining dependent variable variations.

The results from predictor “C” reveal significance but more information would help confirm its impact on the outcome variable. Meanwhile, predictor “D” has little to no effect on the dependent variable based on the current dataset.

4.3.2.6 Screened variables for the predictors of ard plow in silt loam soil

The results of correlation between actual draft force and predicted draft force of predictors (actual drafts by predicted plot), p-value (effect summary), and relationship between draft force and each predictor variable (prediction profiler) are presented in Figures 4.8, 4.9, 4.10, and 4.11, respectively.

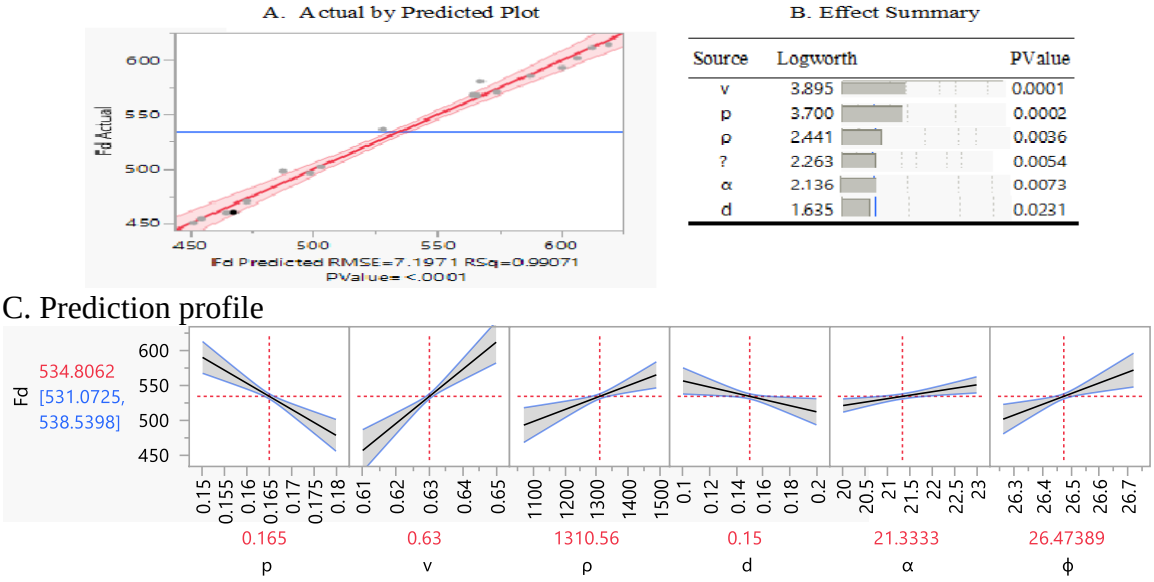

Figure 4.8 Response of the draft force for screening variables of predictor “x”

The optimization process used a stepwise regression model, which is substantial because the actual draft force strongly correlates with the predicted draft force values (as shown in Figure 4.8A). The p-value is less than 0. 05 (Figure 4.8B), showing a highly significant effect. High R^2 values and low p-values collectively suggest a meaningful relationship. The mean, maximum and minimum draft force were 534.8, 538.5, and 531 N, and the slopes of all variable lines were the highest, showing a strong relationship with the response (draft force) (Figure 4.8C). Therefore, the predictor variables 'x' is highly correlated with the response (draft force).

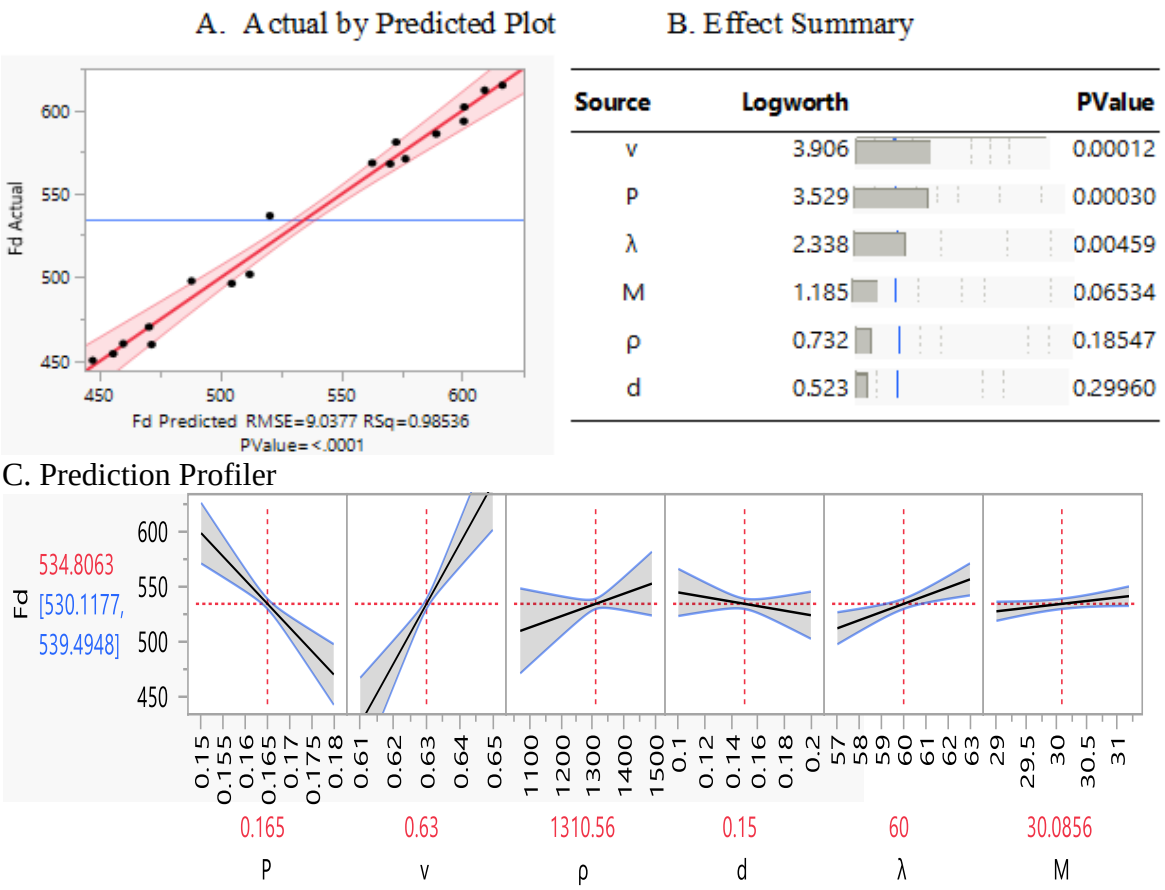

Figure 4.9 Response of the draft force for screening the variables of predictor "y."

The optimization process used a stepwise regression model, which is substantial because the actual draft force strongly correlates with the predicted draft force values (as shown in Figure 4.9A). The p-value is less than 0.05 (Figure 4.9B), showing a highly significant effect. High R^2 values and low p-values collectively suggest a meaningful relationship. The mean, maximum and minimum draft force were 534.8, 539.4, and 530.1 N, and the slopes of all variable lines were the highest, showing a strong relationship with the response (draft force),

except for variable 'd' (Figure 4.9C). But variable excluded from the predictor 'y' because it minimizes the strength of the predictor 'y'.

A. Actual by Predicted Plot

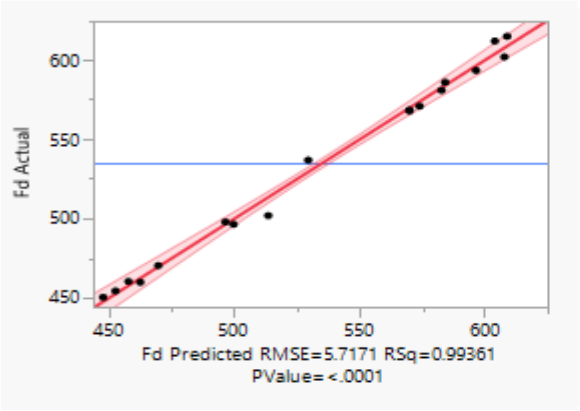

B. Effect Summary

Source	Logworth	p-Value
p	4.150	0.000
Ms	1.193	0.064
Cl	0.723	0.189
d	0.647	0.225
ρ	0.205	0.623

C. Prediction Profiler

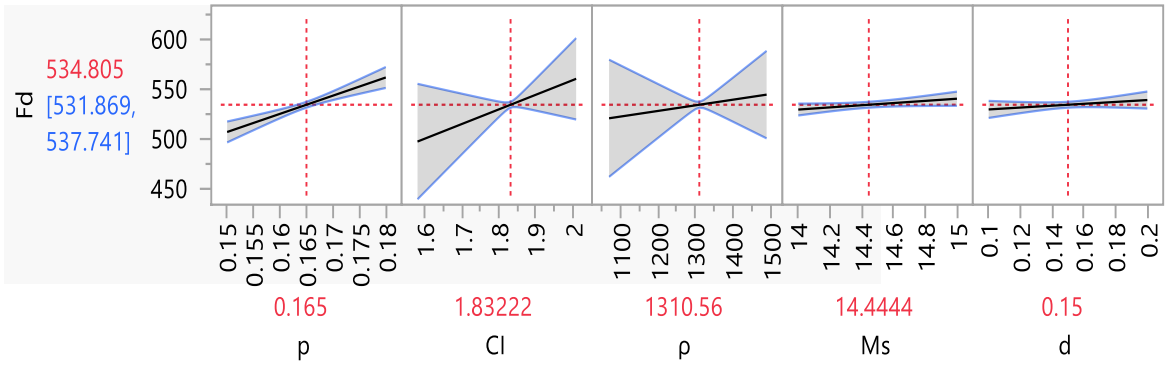

Figure 4.10 Response of the draft force for screening the variables of the predictor "q."

The actual draft force strongly correlates with the predicted draft force values (Figure 4.10A). The p-value is less than 0. 05 (Figure 4.10B), showing a highly significant effect. High R^2 values and low p-values collectively suggest a meaningful relationship. The mean, maximum and minimum draft force were 534.8, 537.7, and 531.8 N, and the slopes of all variable lines were the highest, showing a strong relationship with the response (draft force) (Figure 4.10C). Therefore, the predictor variables 'q' is highly correlated with the response (draft force). But variable "d" and "ρ" excluded from the predictor 'q' because it minimizes the strength of the predictor 'q'.

The actual draft force strongly correlates with the predicted draft force values (Figure 4.11A). The p-value is less than 0. 05 (Figure 4.11B), showing a highly significant effect. High R^2 values and low p-values collectively suggest a meaningful relationship. The mean, maximum and minimum draft force were 534.8, 541.2, and 528.3 N, and the slopes of all

variable lines were the highest, showing a strong relationship with the response (draft force) (Figure 4.11C).

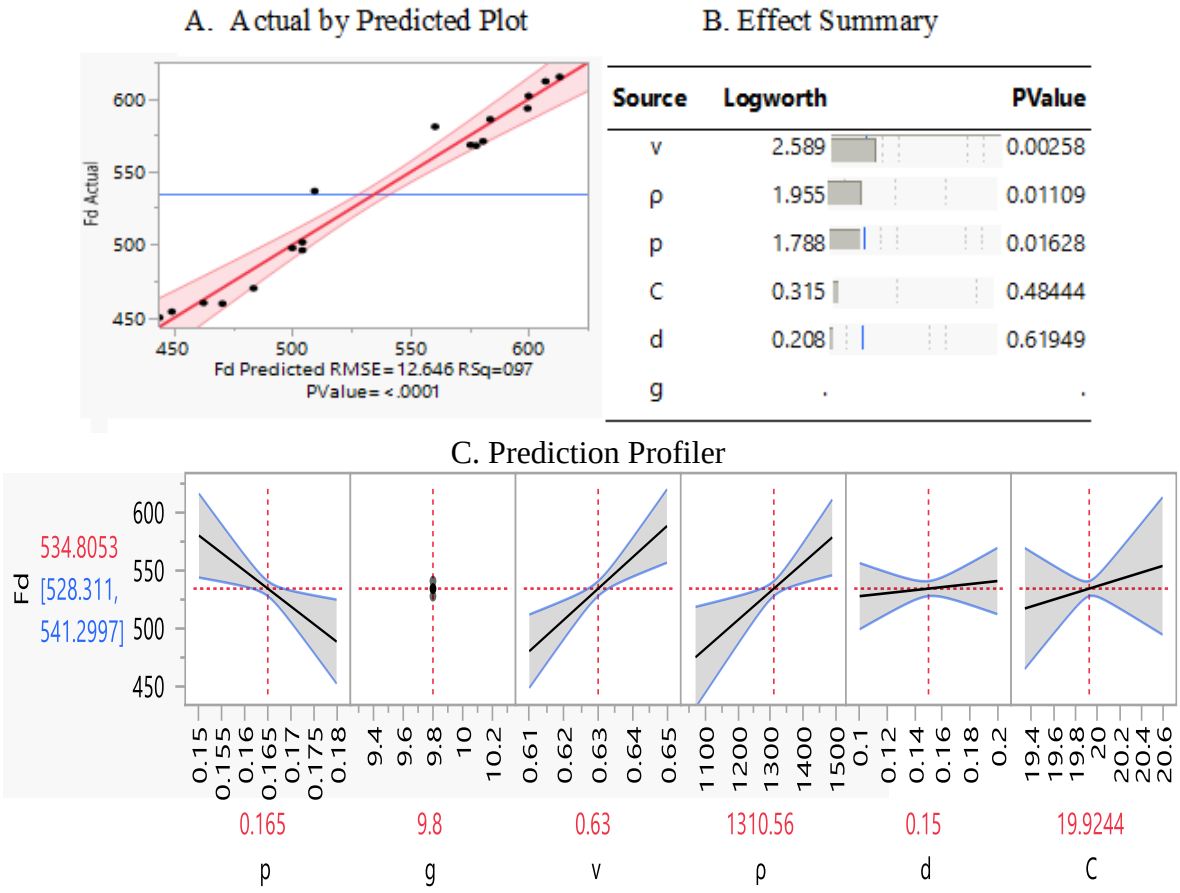

Figure 4.11 Response of the draft force to screening variables of predictor “z.”

Therefore, the predictor variables 'q' is highly correlated with the response (draft force). But variable “d” and “g” excluded from the predictor 'z' because it minimizes the strength of the predictor 'z'.

Overall results showed that predictors "x," "y," "z," and "q" effectively forecast the draft force of an ard plow in silt loam soil. The contributing variables for this prediction are outlined in Table 4.10.

Table 4.10. Predictive variables of summer and Plow screening in silt loam soil

predictor	x	y	Z	Q
Selected variables	P, ρ, d,v, α and φ	P, v, λ,M, ρ	P, ρ, v and C	P, CI and M_s

4.4 Effects of shear stress and soil texture deformation on the Ard draft force

4.4.1 Effects of shear stress on selected draft forces in silt clay and silt loam soil

4.4.1.1 Shear stress of selected draft forces on soil texture (clay, silt and sand)

The shear stress in clay, silt, and sand soils was examined with draft forces of 615, 815, 1115, 1315, and 1515 N, as illustrated in Figures 4.12, Appendix III, and Appendix IV.

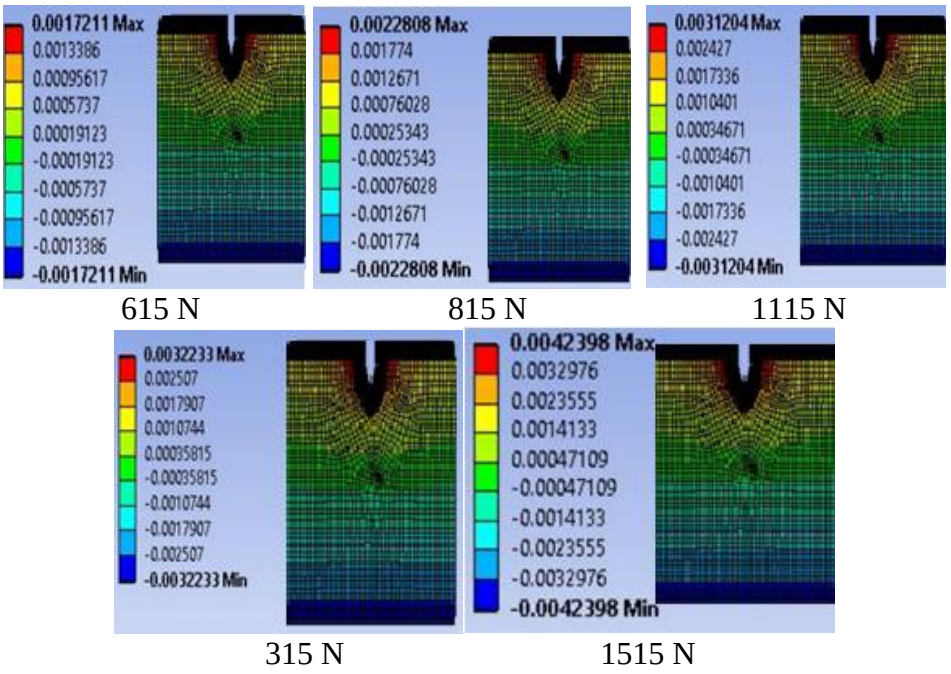

Figure 4.12 Amount of shear stress in clay soil under different force

Shear stress was produced by the force exerted by tillage tools on the contact surface. Figure 4.12, Appendix III, and Appendix IV illustrate the shear direction and total shear stress. The figure shows the largest shear stress values for clay soil: 0.0017211, 0.0022806, 0.0031204, 0.0032233, and 0.0042398 N/m^2 corresponding to tillage application forces of 615, 815, 1115, 1315, and 1515 N, respectively. Appendix III shows largest shear stress values for silt soil: 0.001557, 0.001997, 0.002733, 0.003223, and 0.00371 N/m^2, conforming to loads of 615, 815, 1115, 1315, and 1515 N, respectively. Appendix IV shows largest shear stress values for sand soil: 0.001557, 0.0020633, 0.0028229, 0.0028229, and 0.0038355 N/m^2 corresponding to tillage application forces of 615, 815, 1115, 1315, and 1515 N, respectively.

4.4.1.2 Shear stress in silt clay and silt loam soil

The result of shear stresses with different percentages of individual particles (silt clay and loam silt soil) is shown in Tables 4.11.

The draft force contribution in Silt Clay 1, derives from sand at only 10% but stays lower than the draft force of clay or silt. The draft force contribution from sand stays small in Silt Clay 3, because its sand content measure only at 2%. All tested samples show higher average largest shear stress values as the applied load reaches from 615 N to 1515 N resulting in respective values from 562.55 Pa to 1366.57 Pa. The resistance to deformation of soil rises as the applied load increases.

Table 4.11. Shear stress in silt clay soil

		Particles	Draft force (N)				
			615 N	815 N	1115 N	1315 N	1515 N
silt clay	silt clay 1	Clay (45%)	774.49	1026.36	1229.89	1656.04	1907.91
		Silt (45%)	700.65	898.96	1229.89	1450.35	1671.12
		Sand (10%)	155.7	208.33	282.90	332.92	383.55
	Max. Shear Stress (Pa)		543.61	711.21	914.22	1146.43	1320.86
	silt clay 2	Clay (46%)	791.70	1049.16	1257.22	1692.84	1950.30
		Silt (52%)	809.64	1038.80	1421.21	1675.96	1931.07
		Sand (10%)	186.84	249.99	339.48	399.50	460.26
	Max. Shear Stress (Pa)		596.06	779.31	1005.97	1256.1	1447.21
	silt clay 3	Clay (53%)	912.18	1208.82	1448.54	1950.45	2247.09
		Silt (45%)	700.65	898.96	1229.89	1450.35	1671.12
		Sand (2%)	31.14	41.66	56.58	66.58	76.71
	Stress (Pa)		547.99	716.48	911.67	1155.79	1331.64
Average max. shear stress (Pa)			562.55	735.66	943.95	1186.10	1366.57

The Table examine how draft force and shear stress vary with different soil compositions (clay, silt, and sand percentages) for three types of silt clay samples (silt clay one, silt clay two, and silt clay 3).

The make-up of different soil types shown to markedly influence both draft force operation and largest shear stress levels. Silt Clay 3 shows higher resistance through its bigger draft forces and shear stress values because of its increased clay content. The lower cohesive properties of sand explain why it decreases the values of these measurements when compared to clay and silt.

The results of the table examine how draft force and largest shear stress vary with different soil compositions (clay, silt, and sand percentages) for three types of silt loam soils (silt loam soil 1, silt loam soil 2, and silt loam soil 3).

Table 4.12. Shear stress of loam Silt Soil

		Particle	Draft force				
			615 N	815 N	1115 N	1315 N	1515 N
Silt loam	Silt loam soil 1	Clay (27%)	464.697	615.816	737.937	993.627	1144.746
		Silt (61%)	949.77	1218.59	1667.19	1966.03	2265.29
		Sand (12%)	186.84	249.99	339.48	399.50	460.26
	Max. Shear Stress (Pa)		1601.30	2084.39	2744.60	3359.15	3870.29
	Silt loam soil 2	Clay (12%)	206.53	273.69	327.97	441.61	508.77
		Silt (70%)	1089.90	1398.39	1913.17	2256.1	2599.52
		Sand (18%)	280.26	374.99	509.22	599.25	690.39
	Max. Shear Stress (Pa)		446.82	1576.69	2047.08	2750.36	3296.96
	Silt loam soil 3	Clay (12%)	206.53	273.69	327.97	441.61	508.77
		Silt (50%)	778.5	998.85	1366.55	1611.5	1856.8
		Sand (38%)	280.26	374.99	509.22	599.25	690.39
Max. Shear Stress (Pa)			359.40	1265.29	1647.54	2203.74	2652.36
Average Max. Shear Stress (Pa)			802.50	1642.12	2146.40	2771.08	3273.20

For all three types of silt loam soil, the draft force increases as the applied load increases. This is clear across the range of applied loads (615 N to 1515 N). The highest draft forces are seen in silt loam Soil 1, which has the highest silt content (61%) among the three samples. Despite having lower clay content, Silt Loam Soil 1 exhibits high shear stress values due to its higher silt content (Figure 4.14).

The presence of sand reduces both draft force and largest shear stress compared to clay and silt. In silt loam Soil 3, which has 38% sand, the total draft force is mostly influenced by other components.

All the experimental samples showed elevated largest shear stress throughout the process as the applied load increased from 615 N to 1515 N. As the applied load rises the soil develops stronger resistance to deformation.

The analysis shows that the chemical composition of the examined soil samples decides their impact on draft force measurements and maximum shear resistance levels. Silt Loam Soil 1 unveils higher resistance because it exhibits both increased draft forces and elevated shear stresses. Sand content decreases the observed values because it has less cohesive power than clay or silt.

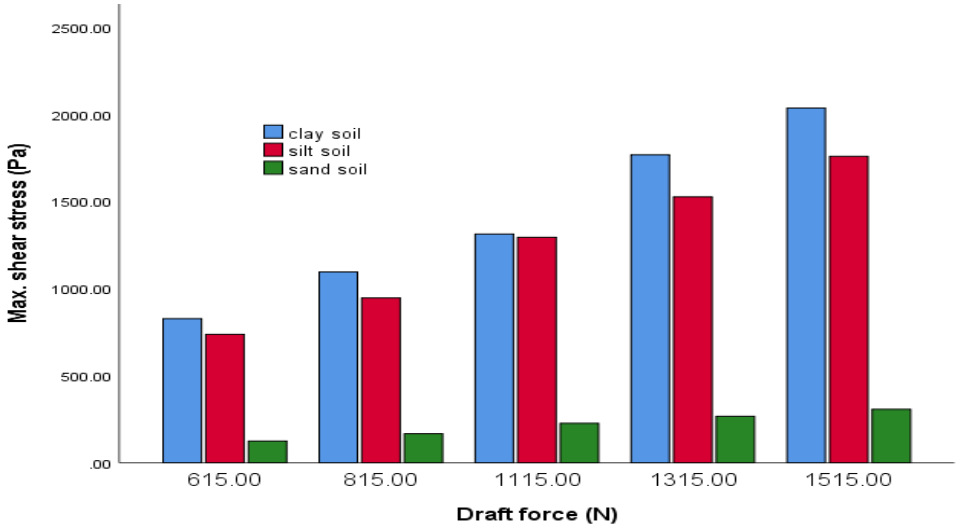

Figure 4.13 Contribution of silt clay soil on relation between draft force and shear stress.

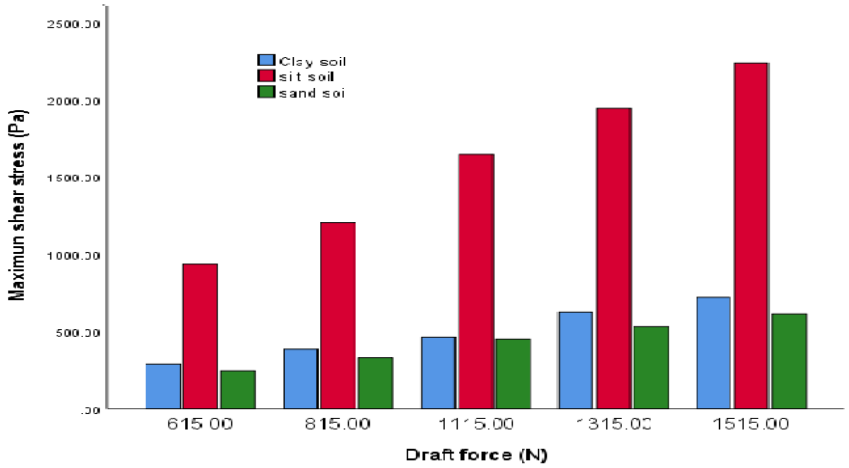

Figure 4.14 Contribution of silt loam on relation between draft force and shear stress.

4.4.2 Deformation in silt clay and silt loam soil

4.4.2.1 Deformation of soil texture on selected draft force

The deformation of clay, silt, and sand soils was studied using draft forces of 615, 815, 1115, 1315, and 1515 N, with results presented in Figures 4.15, APPENDIX V, and APPENDIX VI, corresponding to the applied draft forces.

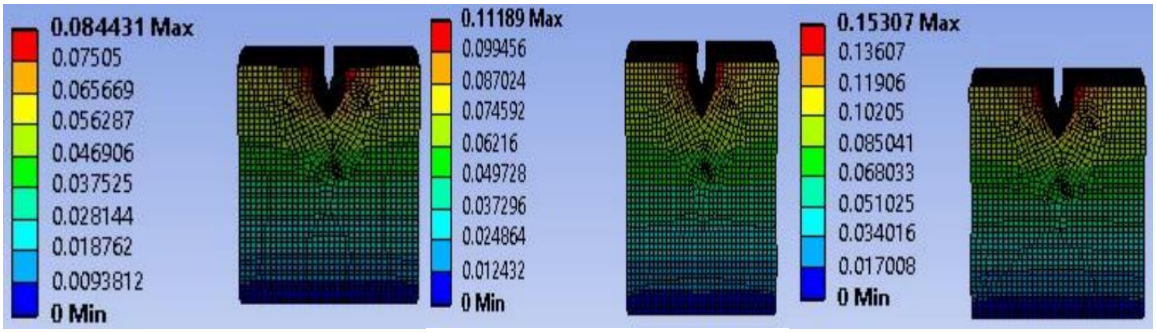

615 N 815 N 1115 N

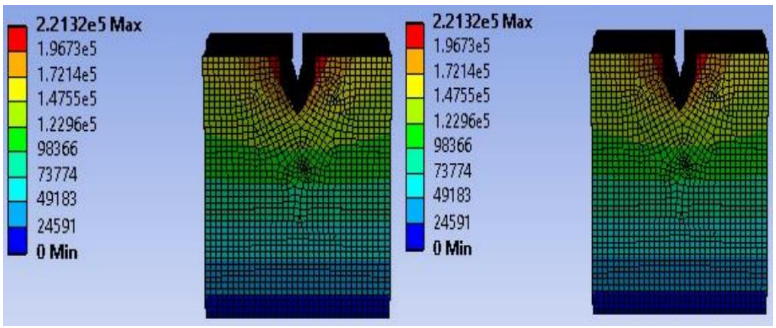

1315 N 1515 N

Figure 4.15 Deformation of clay soil under selected draft forces

4.4.2.2 Deformation on silt clay and silt loam soil

Tables 4.13 present the deformation results for silt loam soil with varying percentages of individual particles.

The results of the Table 4.13 examined silt loam soils (Silt loam one, Silt loam two, and Silt loam 3) influence soil deformation under different applied loads (615 N to 1515 N).

Silt Loam 1 has a higher proportion of silt (61%) compared to clay (27%) and sand (12%). As the load increases, the deformation of silt was more significant. For instance:

Silt Loam 2 has a higher deformation percentage (Figure 4.16).

Table 4.13. Deformation of silt loam soil particles (mm)

	Silt loam 1				Silt loam 2				Silt loam 3			
	Clay (27%)	Silt (61%)	Sand (12%)		Clay (12%)	Silt (70%)	Sand (18%)		Clay (12%)	Silt (50%)	Sand (38%)	
615 N	0.02	0.04	0.009	0.08	0.01	0.05	0.01	0.08	0.01	0.04	0.03	0.08
815 N	0.02	0.08	0.01	0.12	0.013	0.095	0.019	0.12	0.01	0.06	0.04	0.121
1115 N	0.041	0.114	0.017	0.17	0.018	0.13	0.026	0.174	0.01	0.093	0.05	0.166
1315 N	0.048	0.136	0.02	0.20	0.021	0.156	0.031	0.208	0.02	0.111	0.06	0.197
1515 N	0.055	0.136	0.024	0.21	0.024	0.156	0.036	0.216	0.02	0.112	0.07	0.212

The results show that the composition of the soil significantly affects its deformation under varying loads. Conversely, sand content tends to reduce this deformation, likely due to its lower cohesive properties compared to clay and silt.

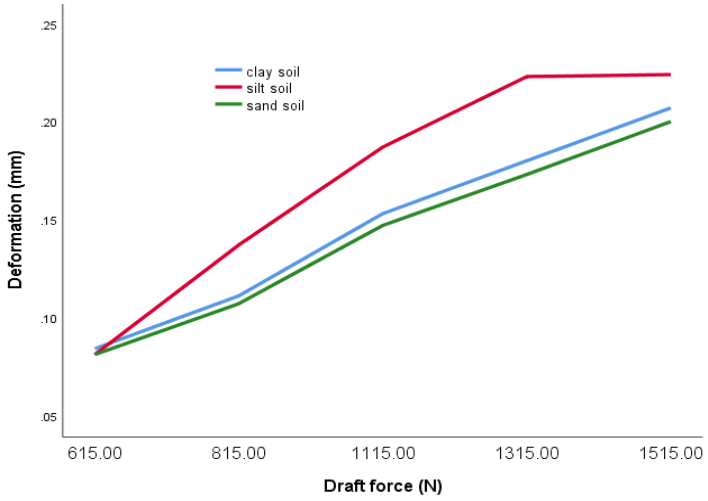

Figure 4.16 Deformation versus draft force

4.4.3 Prediction Draft Force of the Soil Texture

4.4.3.1 Participation of soil particle in silt loam and silt clay soil

Clay, silt, and sand particle contributions to silt loam and silt clay soils are detailed in Equations (4.1) through (4.8).

The function of silt loam soil particles is listed below:

$$y\ (\text{clay}) = 0.06x + 63.5 \quad \text{With } R^2 = 0.973 \tag{4.1}$$

$$y\ (\text{silt}) = 0.06x + 60.9 \quad \text{With } R^2 = 0.969 \tag{4.2}$$

$$y\ (\text{sand}) = 0.06x + 41.7 \quad \text{With } R^2 = 0.983. \tag{4.3}$$

$$y\ (\text{silt loam}) = 0.06x + 56.7 \quad \text{With } R^2 = 0.975 \tag{4.4}$$

The function of silt clay soil particles is listed below:

$$y\ (clay) = 0.73x + 46.8 \qquad with\ R^2 = 0.972 \tag{4.5}$$

$$y\ (silt) = 0.88x + 22.8 \qquad with\ R^2 = 0.999 \tag{4.6}$$

$$y\ (sand) = 4.96x + 5.95 \qquad with\ R^2 = 0.988 \tag{4.7}$$

$$y\ (clay\ silt) = 0.013x + 1.25 \qquad with\ R^2 = 0.984 \tag{4.8}$$

4.4.3.2 Draft force due to soil texture deformation

During the tillage process, disturbed soil moves through tillage tools. Deformation forces cause soil translocation by overcoming the stress inside the soil. The force causes soil translocation or movement under undisturbed conditions. The amount of soil translocated (mass and gravity) exerts a deformation force. The soil texture, moisture content, and depth during tillage can alter soil deformation. The deformation function of the draft force is expressed as follows:

$$F_{df} = f(m, g) \tag{4.9}$$

Where F_{df} is the draft force due to deformation (N), m is the mass of the translocation soil, and g is the gravity due to the weight of the translocation soil (m/s^2).

4.3.3.3 Draft force due to soil texture shear stress

The resistance forces of the soil (shear stress) affect the draft force and expresses:

$$\tau = \frac{F_{ds}}{A} \tag{4.10}$$

Where F_{ds} (N) is the draft force due to shear stress, τ (N/m^2) is the shear stress of soil, and A (m^2) is the area of the tillage tool that contacts the translocation of soil.

$$F_{ds} = f\ (\tau\ , A).$$

Hence, the draft force is the submission of force due to soil deformation, and the soil stress written in Equation 4.11.

4.4.3.4 Draft force under soil texture shear stress and deformation

$$F_d = F_{df} + F_{ds} \tag{4.11}$$

The relationship between the draft force (F_d) and the dimensional parameters: m, g, τ,d, and A is shown by Equation 4.12 with one dependent variable (F_d) and four (5) independent variables.

$$F_d = f(m, g, \tau, d, A) \tag{4.12}$$

The number of dimensionless products (Equation. 4.13) is nine (9). The value was obtained by subtracting the total number of variables (5) from three (3) primary dimensions.

$$\pi_1 = f(\pi_2, \pi_3, \pi_4, \pi_5, and\ \pi_6) \tag{4.13}$$

Dimensioning parameters are represented as repeating variables in Table 4.14 and the other non-dimensional quantities. Textures are expressed as percentages and are dimensionless variables. The dimensionless parameters were temporarily removed for simplicity; however, once the process completed reused it (Simonyan, 2015).

Table 4.14. Repeat and non-repeat variables of parameters

Dimension	repeating variables			nonrepeating variables		
	M	g	d	F_d	τ	A
M	1	1	0	1	1	0
L	0	0	1	1	-1	2
T	0	-2	0	-2	-2	0

The non-dimensional product of the equation

$$\pi_1 = f\ [F_d][\mathrm{d}]^a[\mathrm{m}]^b[\mathrm{g}]^c$$

$$M^0L^0T^0 = [M^1L^1T^{-2}][M^1L^0T^0]^a[M^1L^0T^{-2}]^b\ [M^0L^1T^0]^c$$

$$M: 0 = a + b+1$$

$$L: 0 = c + 1$$

$$T: 0 = -2b - 2$$

$$\pi_1 = f\ [F_d][\mathrm{d}]^0[\mathrm{m}]^{-1}[\mathrm{g}]^{-1} \text{ Or } \pi_1 = \frac{F_d}{mg}$$

$$\pi_2 = f\ [\tau][\mathrm{d}]^a[\mathrm{m}]^b[\mathrm{g}]^c$$

$$\mathrm{M^0L^0T^0} = [\mathrm{M^1L^{-1}T^{-2}}][\mathrm{M^1L^0T^0}]^a[\mathrm{M^1L^0T^{-2}}]^b\ [\mathrm{M^0L^1T^0}]^c$$

$$\mathrm{M}: 0 = \mathrm{a} + \mathrm{b}{+}1$$

$$\mathrm{L}: 0 = \mathrm{c} - 1$$

$$\mathrm{T}: 0 = -2\mathrm{b} - 2$$

$$\pi_2 = f\ [\sigma][\mathrm{d}]^0[\mathrm{m}]^{-1}[\mathrm{g}]^1 \text{ Or } \pi_2 = \frac{\tau g}{m}$$

$$\pi_3 = f\ [\mathrm{A}][\mathrm{d}]^a[\mathrm{m}]^b[\mathrm{g}]^c$$

$$\mathrm{M^0L^0T^0} = [\mathrm{M^0L^2T^0}][\mathrm{M^1L^0T^0}]^a[\mathrm{M^1L^0T^{-2}}]^b\ [\mathrm{M^0L^1T^0}]^c$$

$$\mathrm{M}: 0 = \mathrm{a} + \mathrm{b}$$

$$\mathrm{L}: 0 = \mathrm{c} + 2$$

$$\mathrm{T}: 0 = -2\mathrm{b}$$

$$\pi_3 = f\ [\mathrm{A}][\mathrm{d}]^0[\mathrm{m}]^0[\mathrm{g}]^{-2} \text{ Or } \pi_3 = \frac{\mathrm{A}}{\mathrm{g}^2}$$

Dimensionless parameters for $\pi_1 = \frac{F_d}{mg}$, $\pi_2 = \frac{\tau g}{m}$ and $\pi_3 = \frac{\mathrm{A}}{\mathrm{g}^2}$

$$\pi_1 = f(\pi_2, \pi_3)$$

$$\frac{F_d}{mg} = f\left(\frac{\tau g}{m}, \frac{\mathrm{A}}{\mathrm{g}^2}\right)$$

$$\frac{F_d}{mg} = f\left(\frac{\tau g}{m} x \frac{g^2}{A}\right)$$

$$F_d = f\left(\frac{\tau g}{m} x \frac{g^2}{A}\right) x\ mg$$

$$F_d = f\left(\frac{\tau g^4}{A}\right) \qquad (4.14)$$

4.4.3.5 Predicting Draft Force of Soil Texture

The determinants of the coefficients for *f*1are as follows: the predicted draft force for *f*1, given by the equation 11.67*x*+46.8, has an R^2 = 0.972. The sum of the equations for *f*1 is presented in Equations 4.15.

$$F_d = F_1\left(\frac{\tau g^4}{A}\right) + K$$

$$F_d = -11.67x - 46.8$$

The predicted equation becomes,

$$F_d = -11.67\left(\frac{\tau g^4}{A}\right) - 46.8 \qquad (4.15)$$

Predicted draft force of soil texture (Table 4.15).

Table 4.15. Predicted draft force of soil texture.

Measured draft force (N)	Predicted draft force (f_1)
615	51.63
815	68.42
1115	81.99
1315	110.40
1515	127.19

The predicted draft forces of Equation 4.16 are valid (Figure 4.17) and used for prediction of the draft force in soil texture.

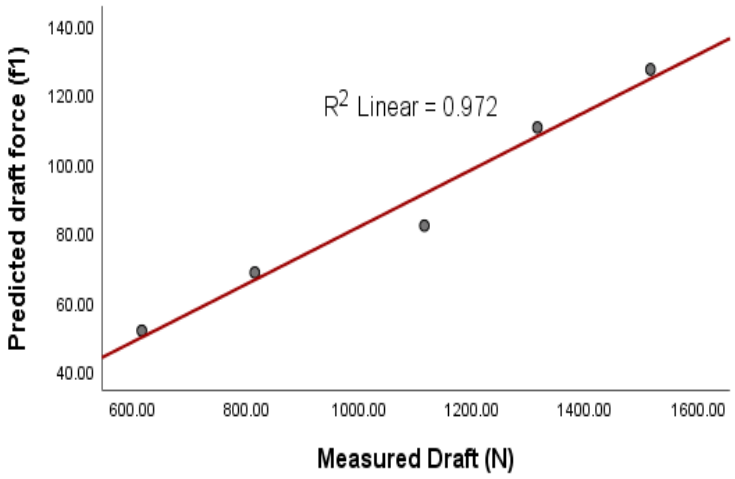

Figure 4.17 Measured and predicted values (f1) of the draft force in soil texture.

4.5 Prediction and Validation of Draft Forces of Scaled Model Moldboard Plow

From Equation 3.20, the following pi terms are decided:

$\overline{\pi_2} = \frac{C\mathrm{w}d^2}{\mathrm{L}}, \overline{\pi_3} = \frac{Cgd^4}{Rv^2}, \overline{\pi_4} = Cd^2 \propto$, and $\overline{\pi_5} = Cd^2\beta$.

According to the basic principles of geometrically similar scaling, several parameters such as acceleration due to gravity, point rake angle, and friction angle cannot be scaled (Neuberger et al., 2007). Therefore, the scale factor in this study was decided based on the physical pi groups found in Equation 3.22. The prototype and model of Moldboard were made from similar materials, and the displacement of the model was less than that of the prototype. The moldboard plow used for the power tiller was scaled down from a standard moldboard, and its dimensions are listed in Table 3.6. The operating parameters of the full-scale moldboard plow are listed in Table 4.16.

Table 4.16. Operating parameters of the full-scale Mouldboard Plow

Operating Parameters	Levels		
	1st level	2nd level	3rd level
Forward speed (m/s)	0.75	0.75	0.75
Soil cutting depth (cm)	10	15	20
Rake angle (degree)	45	45	45

The soil cohesion (kN/m^2) and acceleration due to gravity in the silt clay and silt loam soils are given in Table 4.17.

Table 4.17. Values of soil cohesion and gravitational acceleration of silt clay and silt loam

Parameter	Soil texture	Amount
Soil cohesion (kN/m^2)	Silt clay	19.77
	Silt loam	19.90
Gravity (m/s^2)	Silt clay	9.8
	Silt loam	9.8

4.5.1 Experimental draft force data for ¾-scaled and ½-scaled bottom mouldboards in silt clay and silt loam soil.

The field results obtained during plowing on ¾-scaled and ½-scaled moldboard plow in silt clay soil is listed in Table 4.19.

Table 4.19 results show that parameters ¾-scaled share width (w), ¾-scaled depth, ¾-scaled length of the share Plow, and ½-scaled length of the share Plow) exhibit systematic changes over the course of the experiment, while others (¾-scaled mouldboard, ½-scaled mouldboard radius remain relatively constant. The slight variations in the ¾-scaled mouldboard radius and ½-scaled mouldboard radius reflect measurement uncertainty or natural fluctuations in the system evaluated.

The results suggest that parameters (π_2, π_3, π_4, and π_5) show systematic changes over the time of the experiment, showing consistent reductions.

The ½-scaled mouldboard, however, shows non-linear behaviour, which might reflect measurement uncertainty, natural fluctuations, or changes in experimental conditions.

Table 4.18 Measured parameters using ¾-scaled (A) and ½-scaled (B) mouldboard Plow in silt clay soil.

W		d		L		C		R	
A	B	A	B	A	B	A	B	A	B
0.36	0.24	0.33	0.22	0.64	0.43	19.77	19.77	0.02	0.01
0.36	0.24	0.33	0.22	0.64	0.43	19.77	19.77	0.02	0.01
0.35	0.24	0.32	0.21	0.63	0.42	19.77	19.77	0.02	0.01
0.35	0.24	0.32	0.21	0.63	0.42	19.77	19.77	0.02	0.01
0.34	0.24	0.31	0.2	0.62	0.41	19.77	19.77	0.02	0.01
0.34	0.24	0.31	0.2	0.62	0.41	19.77	19.77	0.02	0.01

Table 4.19. Selected pi groups for draft force for scaled ¾-scaled and ½-scaled mouldboard Plow in silt clay soil.

Predictors of ½-scaled moldboard				Predictors of ¾-scaled moldboard				3/4-scaled Measured F_d scaled (N)	½-scaled Measured F_d scaled (N)
π_2	π_3	π_4	π_5	π_2	π_3	π_4	π_5		
145.7	2889.4	1.6	2.7	47.9	45.3	0.7	1.2	1659	1544
145.7	2889.4	1.6	2.7	47.9	45.3	0.7	1.2	1671	1539
137.3	2713	1.5	2.6	44.9	37.6	0.6	1.1	1687	1577
137.3	2713	1.5	2.6	44.9	37.6	0.6	1.1	1694	1575
129.1	254	1.4	2.4	41.9	31	0.6	1.0	1789	1683
129.1	254	1.4	2.4	47.9	31	0.6	1.0	1782	1688

4.5.2 Prediction draft force of ½-scaled and ¾-scaled mouldboard Prows in silt clay soil.

4.5.2.1 Prediction draft force of ½-scaled d moldboard plows in silt clay soil

Statistical significance and interpretation of the coefficients in the regression model observed in the table is interpreted the unstandardized coefficient for the predictor $\widetilde{\pi_2}$ is -7.245, indicating an inverse relationship between π_2 and the dependent variable. For every one-unit increase in$\widetilde{\pi_2}$, the dependent variable decreases by approximately 7.245, assuming all other variables are held constant.

Table 4.20. Coefficients of the measured draft force using a ½-scale mouldboard Plow in silt clay soil ($\widetilde{\pi_2}$)

Model		Unstan. Coef. B	Unstan. Coef. Std. Error	Stan. Coef. Beta	t	Sig.
1	(Constant)	2709.323	177.937		15.226	.000
	$\widetilde{\pi_2}$	-7.245	1.293	-.942	-5.602	.005

The precision measurement for this coefficient stands at 1.293. When π_2 standard deviation and dependent variable standard deviation are set to 1 with mean at 0 the standardized coefficient value becomes -0.942. The Beta value of -0.942 indicates a substantial negative correlation. The t-value is -5.602, and the significance level (Sig.) is 0.005. Since the significance level is less than the conventional threshold of 0.05, we can conclude that π_2 has a statistically significant effect on the dependent variable. Both the intercept and the predictor π_2 show statistical significance, as indicated by their respective p-values (Sig.). The low p-value for $\widetilde{\pi_2}$ (0.005) confirms that changes in $\widetilde{\pi_2}$ is strongly associated with variations in the dependent variable. The standardized coefficient (-0.942) highlights the strength of the relationship between π_2 and the dependent variable. This large absolute value suggests that $\widetilde{\pi_2}$ is a dominant factor influencing the outcome. The negative coefficient (-7.245) implies that as $\widetilde{\pi_2}$ increases, the dependent variable decreases. Depending on the context of the study, this could indicate, for example, that higher values of $\widetilde{\pi_2}$ lead to reduced performance, lower costs, or decreased output, depending on the dependent variable. Analysis of the table indicates π_2 explains many dimensions of dependent variable variance since it shows a solid t-value together with a minute p-value. A more investigation must take place to find the total explanatory capability of this model.

The results showed that $\widetilde{\pi_2}$ significantly influences the dependent variable, with a strong negative relationship. These findings informed predictions related to the dependent variable.

The linear regression equation of $\widetilde{\pi_2}$ is $F_d = -7.24\widetilde{\pi_2} + 2709.32$

Table 4.21. Coefficients of the measured draft force using a ½-scale Mouldboard Plow in silt clay soil ($\widetilde{\pi_3}$)

Model		Unstan. Coeff. B	Unstan. Coeff. Std. Error	Stan.Coef Beta	T	Sig.
1	(Constant)	2659.243	170.712		15.577	.000
	$\widetilde{\pi_3}$	-.348	.063	-.941	-5.546	.005

Table 4.22. Response of a ½-scale Mouldboard Plow

A. Summary of Fit

R^2	0.99
R^2 Adj	0.99
Root Mean Sq. Error	3
Mean of Response	1601
Observations (or Sum)	6

B. Analysis of Variance

Source	DF	Sum of Squares	Mean Square	F Ratio
Model	2	22611.000	11305.5	1256.167
Error	3	27.000	9.0	Prob > F
Total	5	22638.0		<.0001*

C. Scaled Estimates

Term	Estimate	Std Error	t Ratio	Prob>|t|
Intercept	1601	1.224745	1307.21	<.0001*
predictor 1	-6909.175	457.3135	-15.11	0.0006*
predictor 2	6837.1749	457.2948	14.95	0.0006*
predictor 3	0	0	0.00	1.0000
predictor 4	0	0	0.00	1.0000

The results indicated the model using predictors achieves an excellent fit. The low RMSE value confirms the model's precision, making it a reliable tool for prediction within the tested range. The researchers used the JMP 8 software Equation estimators to develop the mathematical equations for ½-scaled Moldboard in silt clay soil.

$$F_d = 21\left(\frac{C\mathrm{w}d^2}{\mathrm{L}}\right) + \frac{Cgd^4}{Rv^2} + 210 \qquad (4.18)$$

4.5.2.2 Prediction draft force of ¾-scaled d moldboard plows in silt clay soil

The small mean square error (MSE = 9.0) implies that the model's predictions are precise, with minimal deviation between predicted and observed values. Given the high F ratio and low p-value, the predictors included in the model appear to be highly effective at explaining the dependent variable. The research data shows that Predictor 1 and Predictor 2 create significant changes in the dependent variable yet Predictor 1 results in a strong negative effect while Predictor 2 results in a strong positive effect. The analysis shows that Predictors

3 and 4 bring little value to the established model so they should be subject to further evaluation or elimination.

Table 4.23. Coefficients of the measured draft force using a ¾-scaled mouldboard Plow in silt clay soil ($\widetilde{\boldsymbol{\pi_2}}$)

Model		Unstan. Coef. Beta	Unstan. Coef. Std. Error	Stan. Coef. Beta	t	Sig.
1	(Constant)	2118.6	571.0		3.7	0.02
	$\widetilde{\pi_2}$	-11.2	12.4	-0.4	-.9	0.41

The intercept is statistically significant (Sig. = 0.02), suggesting that even when all predictors are zero, the dependent variable is likely to take on a value close to 2118.6. $\widetilde{\pi_2}$ Did not show statistical significance (Sig. = 0.41). This implies that changes in $\widetilde{\pi_2}$ are not strongly associated with variations in the dependent variable based on the current dataset. Based on the results, $\widetilde{\pi_2}$ does not appear to contribute meaningfully to explaining the variability in the dependent variable. Depending on the context, this could indicate that the predictor is irrelevant.

The linear regression equation of $\widetilde{\pi_2}$ is $F_d = -11.262\widetilde{\pi_2} + 2118.695$

Table 4.24. Coefficients of the measured draft force using a ¾-scaled mouldboard Plow in silt clay soil ($\widetilde{\boldsymbol{\pi_3}}$).

Model		Unstan. Coef. Beta	Unstan. Coef. Std. Error	Stan. Coef. Beta	t	Sig.
1	(Constant)	1976	571.0		3.7	0.02
	$\widetilde{\pi_3}$	-9.86	12.4	-0.4	-.9	0.41

The t-value is -0.9, and the significance level (Sig.) is 0.41. Since the significance level is greater than the conventional threshold of 0.05, we cannot conclude that Predictor 1 has a statistically significant effect on the dependent variable.

Significance the significance level is less than the conventional threshold of 0.05, the predictor has a statistically significant effect on the dependent variable. Both the intercept and the predictor show statistical significance, as indicated by their respective p-values. The low p-value for the predictor (0.000) confirms that changes in the predictor are strongly associated with variations in the dependent variable.

The linear regression equation of $\widetilde{\pi_3}$ is $F_d = -9.86\widetilde{\pi_3} + 1976$

Table 4.25. Coefficients of the measured draft force using a ¾-scaled mouldboard Plow in silt clay soil ($\widetilde{\boldsymbol{\pi_4}}$).

Model		Unstan. Coef. Beta	Std. Error	Stan. Coef. Beta		
1	(Const)	359053	97.106		24.293	0.000
	$\widetilde{\pi_4}$	-1120.27	143.067	-.969	-7.830	0.0

The standardized coefficient (-0.969) highlights the strength of the relationship between predictor and the dependent variable. This large absolute value suggests that the predictor is a dominant factor influencing the outcome. The negative coefficient (-1120.27) implies that as the predictor increases, the dependent variable decreases. While the table does not provide explicit metrics like R^2, the high t-value and low p-value for the predictor suggest that the predictor explains a substantial part of the variance in the dependent variable. However, further analysis would be needed to evaluate the overall explanatory power of the model.

The results indicate that the predictor significantly influences the dependent variable, with a very strong negative relationship.

The linear regression equation of $\widetilde{\pi_4}$ is $F_d = -1120.2\widetilde{\pi_3} - 359053$

Table 4.26. Coefficients of the measured draft force using a ¾-scale mouldboard plow in silt clay soil ($\widetilde{\boldsymbol{\pi_5}}$).

Model		Unstan.Coef. Beta	Std. Error	Stan. Coef, Beta	t	Sig.
1	(Constant)	2340.636	112.357		20.832	.000
	$\widetilde{\pi_5}$	-654.545	99.118	-.957	-6.604	.003

The results indicate that the predictor significantly influences the dependent variable, with a very strong negative relationship. The model appears to fit the data well based on the statistics provided, but additional diagnostics (e.g., R^2, residual analysis) would be necessary to fully evaluate its adequacy.

The linear regression equation of $\widetilde{\pi_5}$ is $F_d = -654.545\widetilde{\pi_5} + 2340.63$

The total draft force created in ¾ scaled moldboard plow in silt clay is the submission of all functional variables (Equation 4.21):

$$F_d = -11.26\widetilde{\pi_2} - 9.86\,\widetilde{\pi_3} + 1120.27\widetilde{\pi_4} - 654.54\widetilde{\pi_5} + 8794$$

$$F_d = Cd^2(-11.26\frac{w}{\mathrm{L}} - 9.86\frac{gd^2}{Rv^2} + 1120.27 \propto -654.54\beta) + 8794 \qquad (5.21)$$

4.5.3 Prediction draft force of ½-scaled and ¾-scaled mouldboard Plow in silt loam soil.

4.5.3.1 Draft force of ¾-scaled moldboard plows in silt loam soil

The mathematical equations were developed based on the coefficients of ¾-scaled moldboard plow and the coefficients for ½-scaled bottom moldboard plow, which are listed in Tables 4.27, 4.20, and 4.29.

Table 4.27. Coefficients of the measured draft force using a ¾-scale mouldboard Plow in silt loam soil ($\widetilde{\pi_2}$)

Model		Unstan Coef.		Stan. Coef.		
		B	Std. Error	Beta	t	Sig.
1	(Constant)	1692.33	3.96		427.01	.000
	$\widetilde{\pi_2}$	-.36	.029	-.98	-12.57	.000

The calculation shows a t-value of -12.57 together with a Sig. value of 0.000. The predictor variable shows statistical significance toward the dependent variable because our significance value remains under the well-known threshold of 0.05.

The statistical significance of the model values, including both intercept and predictor, appears through their Sig. values. The predictor keeps a small p-value at 0.000 because it shows substantial relationships between its modification and changes in the dependent variable.

A strong relationship exists between the independent variable and dependent variable as represented by the standardized coefficient (Beta = -0.98). The large value reveals that the predictor plays a leading role in deciding the outcome.

An increase in the predictor leads to a corresponding decrease in the dependent variable according to the negative coefficient value (-0.36). The results demonstrate that higher predictor values negatively affect the dependent variable according to the study's specific variables.

The low P value and high T value in the table indicate that the predictor variable accounts for a major part of dependent variable variance. The model needs additional investigation to determine its total explanatory strength.

The linear regression equation of $\widetilde{\pi_2}$ is F_d =-361$\widetilde{\pi_2}$ +1692.33

Table 4.28. Coefficients of the measured draft force using a ¾-scale mouldboard Plow in silt loam soil ($\widetilde{\boldsymbol{\pi_3}}$)

Model		Unstan Coef. B	Unstan Coef. Std. Error	Stan. Coef. Beta	t	Sig.
1	(Constant)	1692.33	3.96		427.01	.00
	$\widetilde{\pi_3}$	0.01	.029	-.98	-12.57	.00

The results indicate that the predictor significantly influences the dependent variable, with a very strong negative relationship. The linear regression equation of $\widetilde{\pi_3}$ is F_d =-361$\widetilde{\pi_2}$ +1692.33

Table 4.29. Coefficients of the measured draft force using a ¾-scaled Mouldboard Plow in silt loam soil ($\widetilde{\boldsymbol{\pi_4}}$)

Model		Unstan. Coef. B	Unstan. Coef. Std. Error	Stan. Coef. Beta	t	Sig.
1	(Constant)	1672.08	2.875		8.579	.000
	$\widetilde{\pi_4}$	-43.22	4.195	-982	-10.30	.001

The model appears to fit the data well based on the statistics provided, but additional diagnostics (e.g., R^2, residual analysis) would be necessary to fully evaluate its adequacy. The results indicate that the predictor significantly influences the dependent variable, with a very strong negative relationship. The model appears to fit the data well based on the statistics provided, but additional diagnostics (e.g., R^2, residual analysis) would be necessary to fully evaluate its adequacy.

The linear regression equation of $\widetilde{\pi_4}$ is F_d =-361$\widetilde{\pi_2}$ +1692.33

Similarly, $\widetilde{\pi_5}$ is F_d = -25.682$\widetilde{\pi_5}$ + 1671.827

The total draft force created in ¾-scaled moldboard plow in silt loam soil is the submission of all the functional variables in Equation 4.19:

$$361\widetilde{\pi_2} - 0.01\,\widetilde{\pi_3} - 43.226\widetilde{\pi_4} - 25.682\widetilde{\pi_5} + 8794 = F_d$$

$$F_d = Cd^2(361\,(\frac{w}{L}) - 0.01\,(\frac{gd^2}{Rv^2}) - 43.226 \propto -25.682\,() + 8794 \qquad (4.19)$$

4.5.3.2 Draft force of ½-scaled moldboard plows in silt loam soil

Table 4.30. Coefficients of the measured draft force using a ½-scaled Mouldboard Plow in silt loam soil ($\widetilde{\pi_2}$)

Model		Unstan. Coef. B	Std. Error	Stan Coef. Beta	t	Sig.
1	(Constant)	2042.281	47.341		43.140	.000
	$\widetilde{\pi_2}$	-6.116	1.038	-.947	-5.894	.004

The results indicate that the predictor significantly influences the dependent variable, with a very strong negative relationship. The model appears to fit the data well based on the statistics provided, but additional diagnostics (e.g., R^2) would be necessary to fully evaluate its adequacy.

Linear regression equation of $\widetilde{\pi_2}$ is F_d = -6116 $\widetilde{\pi_2}$ + 2042.28

While the table does not provide explicit metrics like R^2, the high t-value and low p-value for the predictor suggest that the predictor explains a substantial portion of the variance in the dependent variable.

Linear regression equation of $\widetilde{\pi_3}$ is F_d = -7.75 $\widetilde{\pi_3}$ +2105

Table 4.31. Coefficients of the measured draft force using a ½-scaled mouldboard Plow in silt loam soil ($\widetilde{\pi_3}$)

Model		Unstan. Coef B	Std. Error	Stan. Coef. Beta	T	Sig.
1	(Constant)	2105.08	79.44		26.49	.000
	$\widetilde{\pi_3}$	-7.76	1.80	-.90	-4.30	.013

However, further analysis would be required to evaluate the overall explanatory power of the model.

Table 4.32. Coefficients of the measured draft force using a ½-scaled Mouldboard Plow in silt loam soil ($\widetilde{\pi_5}$)

Model	Uns and coef. B	StdErr	Sta. Cof. Beta	T	Sig.
(Constant)	2063.670	51.374		40.170	0.00
$(\widetilde{\pi_5})$	11.494	19.10	-.946	-5.847	0.00

The results indicate that the predictor significantly influences the dependent variable, with a very strong negative relationship. The model appears to fit the data well based on the statistics provided, but additional diagnostics (e.g., R^2), residual analysis) would be necessary to fully evaluate its adequacy.

The linear regression equation of $\widetilde{\pi_5}$ is F_d = -367.16 $\widetilde{\pi_5}$ + 2678.09

Mathematical Equation for ½-scaled bottom moldboard plow in silt loam soil is expressed in Equation 4.20.

$$0.16F_d = \widetilde{\pi_2} + 1.27\widetilde{\pi_3} - 30.48\widetilde{\pi_4} - 18.5\,\widetilde{\pi_5} - 1353.8$$

$$0.16\mathrm{F_d} = \mathrm{Cd}^2\left(\frac{\mathrm{w}}{\mathrm{L}} + 1.27\left(\frac{\mathrm{gd}^2}{\mathrm{Rv}^2}\right) - 30.48 \propto -18.5\,\beta\right) - 1353.8 \qquad (4.20)$$

4.5.4 Statistical evaluation of ¾-scaled and ½-scaled draft force mouldboard in clay silt and silt-loam soil using ANOVA.

4.5.4.1 Statistical evaluation of ¾-scaled and ½-scaled draft force moldboards in clay silt soil.

Drafts force of ¾-scale moldboard ANOVA results are shown in Table 4.33. An increase in $\breve{\pi}_2$ and $\breve{\pi}_3$ causes a corresponding rise in the draft force in ¾-scaled moldboard plows. Comparably, the F statistic provides comparable data, $\breve{\pi}_2$ and $\breve{\pi}_3$ is more significant (Allison, 1999). Tables show the results of the ANOVA, indicating whether the means of $\breve{\pi}_2$ and $\breve{\pi}_3$ statistically significantly differ on a ¾-scale moldboard plow. There was a statistically significant difference between the mean amount of $\breve{\pi}_2$ and $\breve{\pi}_3$ which determine the draft

force in silt clay soil. The significance value of the measured draft force using the ¾-scaled moldboard predictor was 0.001, which is below 0.05 (Midi et al., 2010).

Table 4.33. ANOVA Table for the ¾-scaled mouldboard Plow

Model		Sum of Squares	df	Mean Square	F	Sig.
	Regression	16130.33	2	8065.16	199.96	.001[b]
	Residual	121.00	3	40.33		
	Total	16251.33	5			

a. Dependent Variable: Measured draft force using ¾ scaled moldboard

b. Predictors: (Constant), $\widetilde{\pi_2}$, $\widetilde{\pi_3}$

Table 4.33 shown there is significant variance in the mean value of $\widetilde{\pi_2}$ and $\widetilde{\pi_3}$ which determines the draft force of scaled ½-scaled moldboard in silt clay soil. Coefficient of determination (R^2) examines the prediction capacity of the model. Higher R^2 indicates that the model is the best fit for prediction. The R^2 values in Tables 4.34 and 4.35 indicate that 99.6% for scaled moldboard plow and 99.9% for ½-scaled Moldboard plow of the variation in the outcome predicted the outcome.

Table 4.34. ANOVA Table for ½ -scaled Mouldboard Plow.

Model		Sum of Squares	Df	Mean Square	F	Sig.
1	Regression	22611.00	2	11305.50	1256.16	.000[b]
	Residual	27.00	3	9.00		
	Total	22638.00	5			

Table 4.35. Values of coefficients of a determinant for ¾-scaled Mouldboard Plow

Model	R	R^2	Adjusted R^2	Std. Error in Estimate
1	.996[a]	.993	.988	6.35085

a. Predictors: (Constant), $\widetilde{\pi_2}$, $\widetilde{\pi_3}$

Table 4.36. Values of coefficients of determinant for ½-scaled Mouldboard Plow.

Model	R	R^2	Adjusted R^2	Std. Error in Estimate
1	.999[a]	.999	.998	3.00000

a. Predictors: (Constant), $\widetilde{\pi_2}$, $\widetilde{\pi_3}$

Therefore, the statistical data output shows that the parameters selected to predict the draft force of the scaled moldboard plow can have the strength to predict the draft force for both ¾-scaled and ½-scaled moldboard plows. Thus, dimensionless groups $\widetilde{\pi_2}$ and $\widetilde{\pi_3}$ are for predicting the response.

4.4.4.2 Statistical evaluation of ¾-scaled and ½-scaled daft force mouldboard in silt loam soil.

ANOVA results for the draft force ¾-scale moldboard responses to the tillage process are shown in Table 4.39. The result indicated increased in $\breve{\pi}_2$ and $\breve{\pi}_3$ cause a rise in the draft force in both ¾-scaled moldboard plows. Comparably, the Statistic data provide comparable data, $\breve{\pi}_2$ and $\breve{\pi}_3$ is significant. Tables show the results of the ANOVA, indicating whether the means of $\breve{\pi}_2$ and $\breve{\pi}_3$ differ in a statistically significant way on a ¾-scale moldboard plow. This shows that there is significant difference among the mean value of $\breve{\pi}_2$ and $\breve{\pi}_3$ which determine the draft force in silt loam soil. The significance value of the measured draft force using a ¾-scaled moldboard predictor was 0.004, which is below 0.05.

Table 4.37. ANOVA Table for ¾-scaled mouldboard Plow in silt loam.

Model		Sum of Squares	df	Mean Square	F	Sig.
1	Regression	1403.90	1	1403.90	34.36	.004[b]
	Residual	163.43	4	40.85		
	Total	1567.33	5			

a. Dependent Variable: Measured draft force using a ¾-scale moldboard.

b. Predictors: (Constant), $\widetilde{\pi_2}$, $\widetilde{\pi_3}$

Table 4.38 displays a statistically significant difference in the mean amount of $\breve{\pi}_2$ and $\breve{\pi}_3$ which determine the draft force of scaled ½-scaled moldboard in silt clay soil. The significance value of the measured draft force using the ½-scale moldboard predictor was 0.004, which is below 0.05.

The determination coefficient (R^2) examines the prediction capacity of the model. Higher R^2 shows that the model is a best fit for the data, R^2 value in Table 4.39 and 4.40 shows that 89.6% for scaled moldboard plow and 97.5% for ½-scaled moldboard plow of the variation in the outcome predicted the outcome.

Table 4.38. ANOVA Table for ½-scaled mouldboard Plows.

Model		Sum of Squares	df	Mean Square	F	Sig.
1	Regression	32.023	2	16.012	59.164	.004[b]
	Residual	.812	3	.271		
	Total	32.835	5			

a. Dependent Variable: The measured draft force using ½-scale moldboard

b. Predictors: (Constant), $\widetilde{\pi_2}$, $\widetilde{\pi_3}$

Table 4.39. Values of coefficients of determinant for ¾-scale mouldboard Plow.

Model	R	R^2	Adjusted R^2	Std. Estimate
1	.946[a]	.896	.870	6.39

a. Predictors: (Constant), $\widetilde{\pi_2}$, $\widetilde{\pi_3}$

Table 4.40. Values of the coefficients of the determinant for ½-scaled mouldboard Plow Model.

Model	R	R^2	Adjusted R^2 value	Std. Error in Estimate
1	.988[a]	.975	.959	.52

a. Predictors: (Constant), $\widetilde{\pi_2}$, $\widetilde{\pi_3}$

Therefore, the statistical data output shows that the parameters selected to predict the draft force of the scaled moldboard plow can have the strength to predict the draft force for both ¾-scaled and ½-scaled moldboard plows. Thus, the dimensionless groups $\widetilde{\pi_2}$, and $\widetilde{\pi_3}$ is suitable for predicting the response.

4.6 Prediction and Validation of Draft Forces of Ard Plow in Silt Clay and Silt Loam

4.6.1 Prediction of Draft Forces of Ard Plow in Silt Clay

4.6.1.1 Dimensionless ard plow parameters in silt clay soil

The experimental value of the ard plow draft in the Worden field area required different amendments to the independent variable. The type of soil found in the studied field area was silt clay. The equation was separated into groups of parameters using letters A, B, C, and D (Alghazali, 2012).

$$F_d = f(A, B, C, D) \quad (4.21)$$

Where: $A = \frac{\rho^2 V^2}{C}$, $B = \frac{CI\rho}{m_s}$, $C = \frac{\rho v^2}{\varphi}$ and $D = \frac{p}{M}$

It is also possible to analyze function (A) by assuming that functions (B), (C), (D) are constant and vice versa.

Hence,

Function (A):

$$F_d = f(A) \quad (4.22)$$

$$F_d = f\left(\frac{\rho^2 V^2}{C}\right) \quad (4.23)$$

Equation 4.4 gives the mathematical equation produced by the parameters of function (A).

$$\text{Measured } F_d = 0.043\ A + 43.95 \quad (4.24)$$

Function B

$$F_d = f(B) \quad (4.25)$$

$$F_d = f\left(\frac{CI\rho}{m_s}\right) \quad (4.26)$$

Equation 4.7 represents the prediction equation using experimental data.

$$F_d \text{ measured} = 2.349B + 94.971 \quad (4.27)$$

Function C

$$F_d = f(C) \quad (4.28)$$

$$F_d = f\left(\frac{\rho v^2}{\varphi}\right) \quad (4.29)$$

$$F_d\ measured = 31.942C - 309.23 \quad (4.30)$$

Function (D)

$$F_d = f(D) \quad (4.31)$$

$$F_d = f\left(\frac{p}{M}\right) \quad (4.32)$$

The mathematical equation is expressed as Equation 4.33.

$$F_d \text{ measured} = 57.73D - 36.7 \quad (4.33)$$

After substituting the experimental values for the derived equations, the predictor values of the functions (A, B, C and D) are listed in Table 5.44.

Table 5.41. Prediction of the draft forces of functions (A, B, C, and D)

Predictor value "A"	Predictor value "B"	Predictor value "C"	Predictor value "D"	Measured value "F_d"
4134.44	135.43	16.42	8.55	436
4128.07	138.00	16.44	8.55	426
4192.85	140.88	16.54	8.55	439
4251.54	144.66	16.67	9.00	423
4249.36	142.04	16.65	9.00	428
4242.85	142.33	16.65	9.00	445
4600.13	142.68	17.76	9.45	450
4590.75	147.60	17.73	9.45	447
4586.07	154.98	17.72	9.45	449
5652.06	171.43	17.93	10.26	450
5822.58	174.17	18.18	10.26	452
5980.21	178.76	18.43	10.26	459
6343.60	180.60	19.61	10.80	467
6732.98	187.15	20.24	10.80	538
6933.52	178.20	20.51	10.80	588
7201.87	184.92	20.91	11.34	596
8218.05	206.21	22.40	11.34	602
8304.90	208.60	22.53	11.34	605

4.6.1.2 Prediction of the draft force Ard plow equation in silt clay soil

The equations are effective for arranging summation or subtraction and are given by:

Y = AX + M. Each of the above-derived equations was further combined and developed into equations bounded by A, B, C, and D.

$$F_d = 0.043\mathrm{A} + 2.349\mathrm{B} + 31.413\mathrm{C} + 57.73\mathrm{D} + 203 \quad (4.34)$$

Or,

$$F_d = 0.043\mathrm{A} - 2.349\mathrm{B} + 31.413\mathrm{C} + 57.73\mathrm{D} - 285 \quad (4.35)$$

Substituting the grouped parameters that were highly correlated with the draft force, we obtained the following:

$$0.043(\frac{\rho^2 V^2}{C}) + 2.349(\frac{\mathrm{CI}\rho}{m_s}) + 31.413(\frac{\rho v^2}{\varphi}) + 57.73(\frac{p}{M}) = -203F_d \qquad (4.36)$$

Or,

$$0.043(\frac{\rho^2 V^2}{C}) + 2.349(\frac{\mathrm{CI}\rho}{m_s}) + 31.413\frac{\rho v^2}{\varphi}) + 57.73\,(\frac{p}{M}) = 285F_d \qquad (4.37)$$

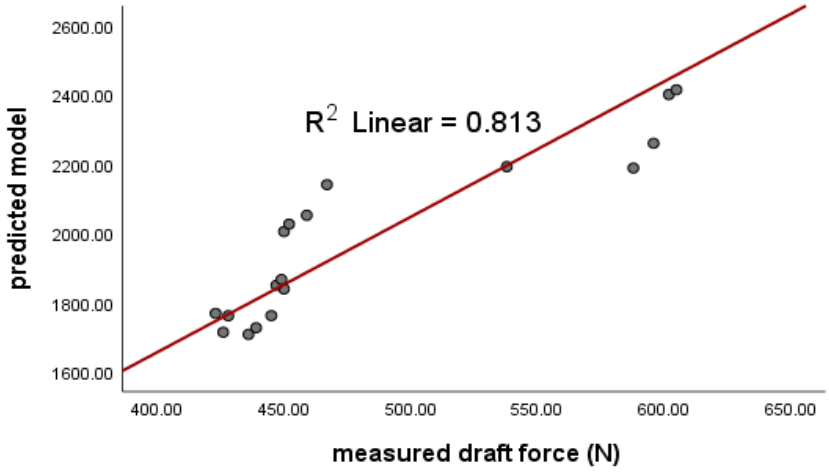

Figure 4.18 Relationship between measured and predicted draft forces (summation)

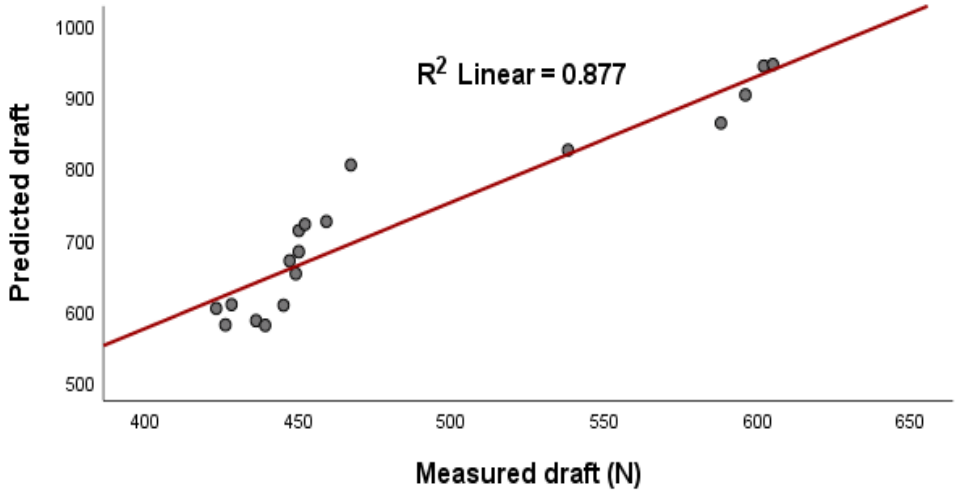

Figure 4.19 Relationship between measured and predicted draft forces (subtraction)

Equation develops a formula for calculating the ad plow draft force generated during tillage. The results revealed that both equations are sufficient to estimate the draft force of the ard plow. Equation 4.17 is a powerful equation used to estimate the draft force of an ard plow in silt clay soil.

4.6.2 Draft Forces of Ard Plow in Silt Loam soil.

4.6.2.1 Dimensionless ard plow parameters in silt loam soil

In the Ewan field area, the experimental value of the ard plow draft necessitated various modifications to the independent variable. In the field under study, silt loam soil was the predominant kind. The equation used the letters x, y, z, and q to divide the parameters into groups.

$F_d =$ f $(x, y, \mathrm{z}, \mathrm{q})$, Where: $x = \frac{p\rho v^2 d^2 \alpha}{\varphi}$; $y = \frac{p\rho v^2 \lambda}{M}$; $z = \frac{p\rho^2 V^2}{C}$ and $q = \frac{\mathrm{pCI}}{m_s}$

Predicted value expected draft forces of the group parameters:

$F_d =$ f$(x) =$ f$\left(\frac{p\rho v^2 d^2 \alpha}{\varphi}\right)$, $F_d =$ f$(y) =$ f$\left(\frac{p\rho v^2 \lambda}{M}\right)$, $F_d =$ f$(\mathrm{z}) =$ f$\left(\frac{p\rho^2 V^2}{C}\right)$, $F(q) =$ f$\left(\frac{\mathrm{CI}p}{m_s}\right)$.

The equations constructed for each grouped parameter x, y, z, q. expressed: F_d measured $A = 6.98x + 274$; F_d measured$B = 74.75y - 3.0$; F_d measured $C = 31.86z + 2.4$; and F_d measured $D = 0.16q + 4.30$.

Table 4.42. Numerical values of x, y, z, and q

Predicted draft x	Predicted draft y	Predicted draft z	Predicted draft q	Measured draft (N)
393.1	407.4	767.4	430.3	450.5
393.1	407.5	767.4	430.3	454.5
393.2	407.5	767.6	430.3	460.5
393.2	407.6	767.9	430.5	470.5
393.2	407.5	767.6	430.4	460.0
393.2	407.5	768.1	430.4	498.0
393.2	407.5	768.6	430.7	496.5
393.2	407.6	769.0	430.6	502.0
393.2	407.8	769.3	430.6	537.0
393.3	409.0	770.9	430.4	568.5
393.3	409.0	770.9	430.4	568.0
393.3	409.0	771.0	430.4	571.0
393.3	409.1	771.7	430.6	581.0
393.3	409.1	771.7	430.6	586.0
393.3	408.8	771.7	430.6	593.5
393.3	408.8	771.9	430.8	602.0
393.3	409.0	772.0	430.8	612.0
393.4	409.1	772.1	430.8	615.0

4.6.2.2 Prediction of the draft force Ard plow equation in silt loam soil

The obtained consequences expose a significant outcome for functions x, y, z, and q in the presence of the draft force. Equations bounded by x, y, z, and q were created by combining the above equations.

$$6.98\left(\frac{p\rho v^2 d^2 \alpha}{\varphi}\right) + 74.75\left(\frac{p\rho v^2 \lambda}{M}\right) + 31.86\left(\frac{p\rho^2 V^2}{C}\right) + 0.16\left(\frac{\mathrm{CI}p}{m_s}\right) = 277.7.$$

The parameters were entered as options-1 and -2 to produce the predicted draft force data, which were plotted against the value of the measured draft results. The coefficients of determination for Figures 4.22 and 4.23 are 0.906 and 0.893, respectively.

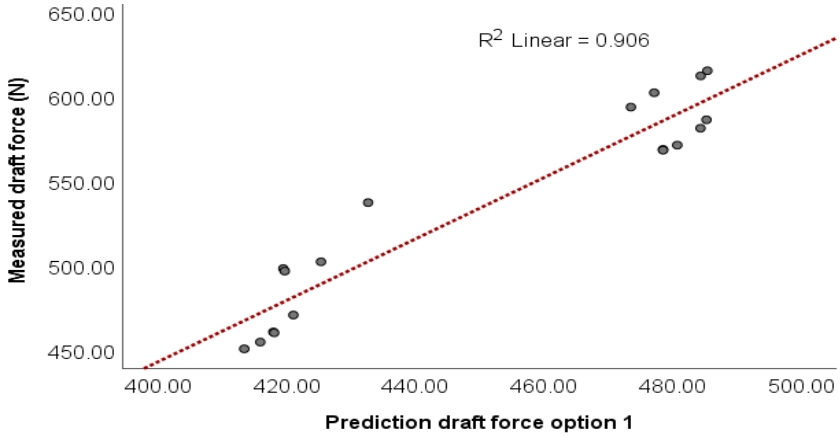

Figure 4.20 Relationship between the measured and predicted draft forces for the summation parameters.

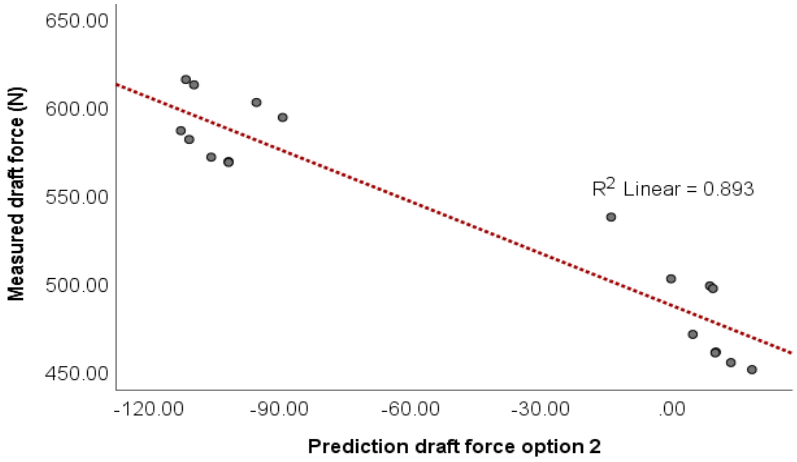

Figure 4.21 Relationship between the measured and predicted draft forces for the subtraction parameters (choice-2)

Data found in the model that projected the draft force for the tillage tool was made to stand up to scrutiny related to output data measured in an actual field area and assessed in the laboratory.

The difference between the measured and predicted values in both equations is minimal; however, option 2 has lower coefficients of determination than option 1. Consequently, option 1 demonstrates superior coefficients of determination and serves as a mathematical model to predict the draft of an ard plow on silt loam soil.

The data revealed a strong correlation between the anticipated and measured draft forces (R^2 = 0.906), with no significant differences observed. The analytical results indicate that the error is within acceptable limits, suggesting that the equation is suitable for determining the ard plow's minimum draft force. This will help reduce farmers' power losses, guide them in selecting the appropriate prime power, and provide valuable input for ard plow designers.

4.6.3 Validation of the Draft Forces of Ard Plow in Silt Clay and Silt Loam Soil

A mathematical model needs validation for practical use (Brown, 2005). This model summarizes the measured and predicted draft forces of an ard plow in silt clay and silt-loam soils (Tables 4.43 and 4.44 For both soil types, the results showed that predictors from groups A, B, C, and D correlated with the experimental draft force values.

Table 4.43 Predictor vs. experiment draft force Model summary in Silt Clay

Model	R	R Square	Estimate	Durbin-Watson	
1	.99[a]	0.996	.99	18.29	1.96

a. Predictors

Table 4.44 Model summary of predictors vs. experimental draft force Values for Silt Loam Soil.

Model	R	R Square	Adjusted R Square	Std. Error in Estimate	Durbin-Watson
1	.973[a]	.948	.944	14.17616	1.122

The coefficient of friction (R = 0.97) indicated a strong correlation between the predictors (independent variables) and the response variable (dependent variable). Durbin-Watson value of 1.122 is slightly less than 2, indicating some evidence of positive autocorrelation in the residuals. The standard error of the estimate (14.17616) suggests that the model provides

reasonably accurate predictions, though the precision depends on the scale of the dependent variable.

The scatterplot graphs are shown in Figures 4.22 and 4.23 for silt clay soil and silt loam soil.

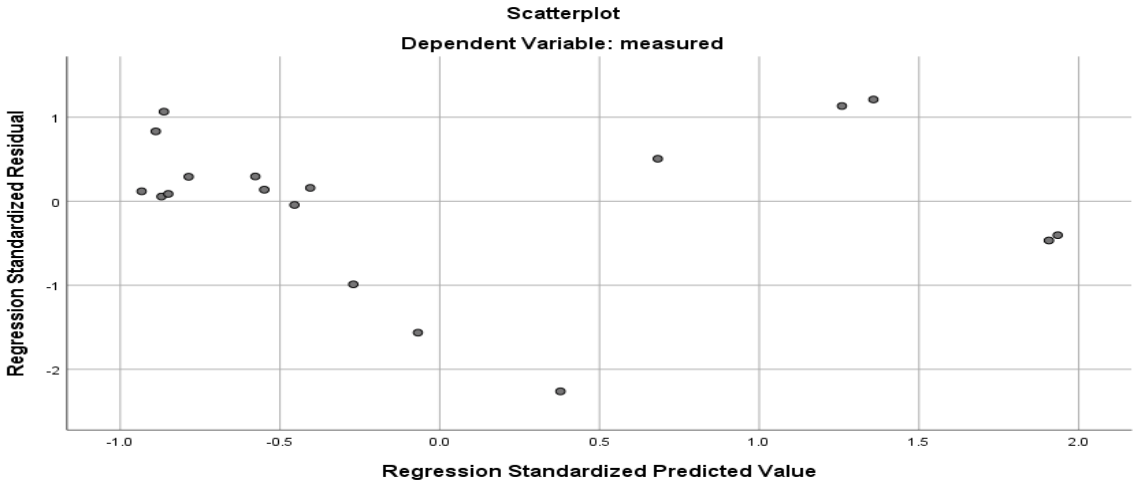

Figure 4.22 Scatterplot regressions standardized predicted Values and predicted functional values of silt clay soil.

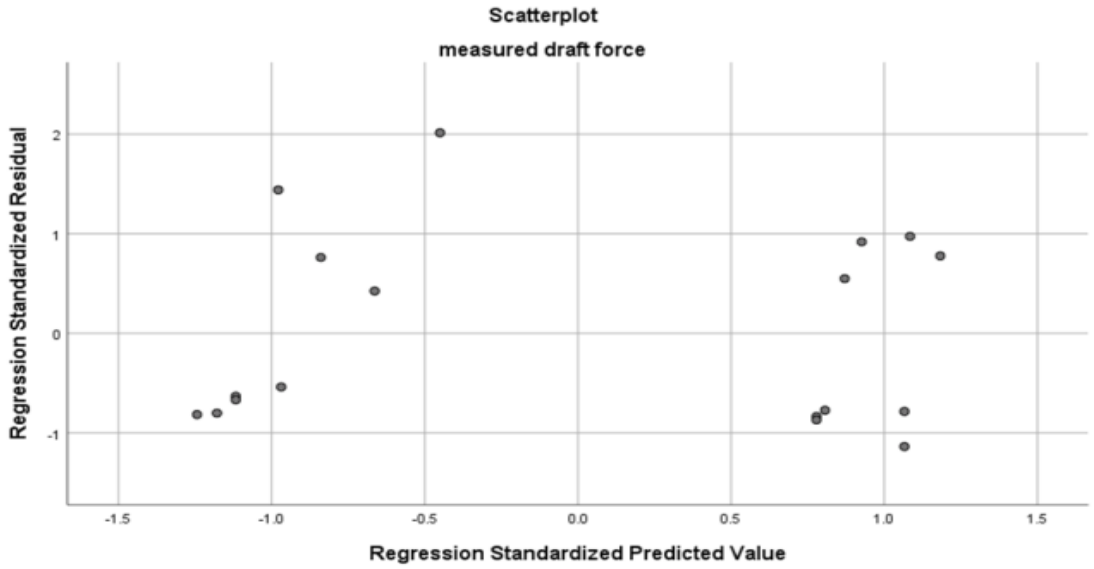

Figure 4.23 Scatterplot regressions standardized the predicted values and predicted functional values of silt loam soil.

To certify the model, validate the actual system across the prediction range while checking the normality assumption. Verification was conducted using the Z-score, which assesses how a value compares to the mean based on standard deviation. Accepted ranges for the Durbin–Watson statistic is 0–4 (Turner, 2020). In silt clay, and silt loam soil, Durbin-Watson values

ranged from 1.96 to 1.12. If scatterplot residuals are evenly distributed, 95% should fall between 2 and 2 (Friendly & Denis, 2005). To satisfy the normality assumption at $\alpha = 0.05$, both skewness and kurtosis must be between −1.96 and +1.96 (Nebiolo, 1958). The predicted values indicate higher concentrations, suggesting that CRM is less than zero (Slezingr & Purcz, 2013).

Skewness and kurtosis results are shown in Table 4.45 for silt clay soil provides statistical measures for both predicted draft force and measured draft force, focusing on skewness and kurtosis. These metrics describe the shape of the data distributions, which can help assess whether the predicted and measured values align with a normal distribution or exhibit deviations. The standard error (SE) of 1.038 provides an estimate of the variability in the kurtosis statistic. Since the kurtosis value (-0.571) is less than twice the SE ($2 \times 1.038 = 2.076$), it suggests that the kurtosis is not statistically significant. Therefore, the deviation from a normal distribution in terms of kurtosis is negligible.

Table 4.45. Descriptive statistics of the measured draft force in silt clay soil.

	N	Skewness		Kurtosis	
	Statistic	Statistic	Std. Error	Statistic	Std. Error
Measured draft force	18	1.107	.536	-.571	1.038
Valid N (list-wise)	18				

Overall, the two distributions appear similar in shape, suggesting that the prediction model is aligned with the actual measurements.

The RMSE and CRM values of silt clay soil calculated using SPSS software and listed in Table 4.46.

Table 4.46. Errors in Options 1 and 2 for silt clay soil

Pointer	Error Value for Option 1	Error Value for option 2
RMSE	0.093	0.246
CRM	0.842	-0.091

According to the results given in Table 4.47, for silt clay, lower RMSE indicates better model performance. Option 1 has a significantly lower RMSE (0.093) than Option 2 (0.246). This suggests that Option 1 provides more accurate predictions with more minor errors related to the actual values.

CRM value close to +1 indicates a strong positive correlation, while a value close to -1 indicates a strong negative correlation. Values near 0 suggest no correlation. Option 1 shows

a strong positive correlation (CRM = 0.842), indicating that the predicted values are closely aligned with the actual values consistently. Option 2 has a CRM of -0.091, which is close to 0. This suggests that there is almost no correlation between the predicted and actual values for Option 2, meaning its predictions are not meaningful or reliable.

Option 1 outperforms Option 2 in both metrics: It has a much lower RMSE, indicating more minor prediction errors. It exhibits a strong positive correlation (CRM = 0.842), showing that the predictions align highly with the actual values.

Option 2 performs poorly: Its higher RMSE (0.246) indicates more significant prediction errors. The near-zero CRM (-0.091) suggests that the predictions made by Option 2 do not correlate well with the actual values, making it unreliable.

4.7 Development of Mathematical model Using Visual Basic Programming Language

Mathematical model to predict draft force of ard Plow (By Pycharm IDE for Python programming language).

```
Import math
def calculate_f_A(rho, v, C):
    """Calculate predictor parameter f(A)"""
    return 0.043 * ((rho * v**2) / C) + 43.95
def calculate_f_B(CI, rho, Ms):
    """Calculate predictor parameter f(B)"""
    return 2.3498 * ((CI * rho) / Ms) + 94.97
def calculate_f_C(rho, v, phi):
    """Calculate predictor parameter f(C)"""
    return 31.91 * ((rho * v**2) / phi) - 309.23
def calculate_f_D(P, M):
    """Calculate predictor parameter f(D)"""
    return 0.043 * (P / M) - 36.7
def calculate_f_sht(Fd, m, L, w):
    """Calculate predictor parameter f(sht)"""
    # Assuming cos230 is in degrees, convert to radians
    return (2 * Fd * m * math.cos(math.radians(230))) / (L * w)
def calculate_f_G(Cw, d, L):
    """Calculate predictor parameter f(G)"""
    return (Cw * d**2) / L
def calculate_draft_force():
    """Calculate total draft force based on user inputs"""
    print("Enter the following parameters:")
      # Input parameters
    rho = float(input("Enter density (ρ): "))
    v = float(input("Enter velocity (v): "))
    C = float(input("Enter C parameter: "))
    CI = float(input("Enter CI parameter: "))
```

```
    Ms = float(input("Enter Ms parameter: "))
    phi = float(input("Enter φ parameter: "))
    P = float(input("Enter P parameter: "))
    M = float(input("Enter M parameter: "))
    Fd = float(input("Enter Fd parameter for f(sht): "))
    m = float(input("Enter m parameter: "))
    L = float(input("Enter L parameter: "))
    w = float(input("Enter w parameter: "))
    Cw = float(input("Enter Cw parameter: "))
    d = float(input("Enter d parameter: "))
    # Calculate individual components
    f_A = calculate_f_A(rho, v, C)
    f_B = calculate_f_B(CI, rho, Ms)
    f_C = calculate_f_C(rho, v, phi)
    f_D = calculate_f_D(P, M)
    f_sht = calculate_f_sht(Fd, m, L, w)
    f_G = calculate_f_G(Cw, d, L)
    # Calculate total draft force
    total_force = f_A + f_B + f_C + f_D + f_sht + f_G
    # Print results
    print("\nIndividual Components:")
    print(f"f(A) = {f_A:.2f}")
    print(f"f(B) = {f_B:.2f}")
    print(f"f(C) = {f_C:.2f}")
    print(f"f(D) = {f_D:.2f}")
    print(f"f(sht) = {f_sht:.2f}")
    print(f"f(G) = {f_G:.2f}")
    print(f"\nTotal Draft Force (Fd) = {total_force:.2f}")
    return total_force
def main():
    print("Draft Force Calculator")
    print("======================")
      try:
        result = calculate_draft_force()
    except ValueError:
        print("Error: Please enter valid numerical values")
    except ZeroDivisionError:
        print("Error: Division by zero occurred. Please check your input values")
if __name__ == "__main__":
    main()
```

5. CONCLUSIONS AND RECOMMENDATIONS

5.1 Conclusions

This study investigated the prediction and optimization of draft forces for small-scale tillage tools across different soil types. Key findings include soil properties, tool geometry, and operational parameters that influence draft force.

Textural Classification: Worden Field (Silt Loam Soil): Contains 18.69% clay, 72.47% silt, and 8.84% sand, classifying it as silt loam. This soil type exhibits moderate resistance due to its balanced composition. Ewan Keble Field (Silt Clay Soil): Contains 45.50% clay, 44.51% silt, and 9.99% sand, classifying it as silt clay. This soil type shows high cohesiveness and plasticity, requiring greater draft forces for tillage. It demonstrates higher shear stress values under applied loads than silt loam soil. This indicates that silt clay soil resists deformation more significantly, requiring more force to overcome internal stresses.

Physical and Mechanical Properties: Key properties analyzed include moisture content, bulk density, soil cohesion, internal friction angle, and penetration resistance. For silt loam soil, bulk density increases with depth (from 1.13 g/cm³ at 10 cm to 1.45 g/cm³ at 20 cm), while penetration resistance rises correspondingly (from 1.64 kPa at 10 cm to 2.00 kPa at 20 cm). For silt clay soil, bulk density also increases with depth (from 1.21 g/cm³ at 10 cm to 1.38 g/cm³ at 20 cm), but penetration resistance remains relatively constant (~1.80 kPa) due to higher clay content.

Effects of Tool Geometry on Draft Force: it examines how the geometry of tillage tools affects draft force, focusing on the distance between the leather stripe and share (p) and the operator operating angle (λ). Increasing p or λ leads to higher draft forces due to increased soil resistance. The lowest draft force occurs when both p and λ a minimized: $P_1\lambda_1$ = 452.57N. The highest draft force occurs when both p and λ are maximized: $P_2\lambda_3$ =605.71N. Optimizing these parameters reduces energy consumption and improves tool efficiency during tillage. In optimizing draft force, silt clay soil consistency requires higher draft forces to achieve the desired tillage effect.

Predictors Screening for Ard Plow Draft Force: Screening variables were identified to determine their influence on draft force in both soil types. Four predictors (A, B, C, D) were evaluated in Silt Clay Soil. Predictor A: Selected variables (ρ, C, v); R^2 = 0.91, Predictor B:

Selected variables (CI, Ms); R^2 = 0.92, Predictor C: Selected variables (v, ϕ); R^2 = 0.896; marginally significant, and Predictor D: Not statistically significant (p>0.05); excluded from the model. Silt Loam Soil also evaluated four predictors (x, y, z, and q). Predictor x: Selected variables (P, ρ, d, v, α, ϕ); R^2 = 0.973, Predictor y: Selected variables (P, v, λ, M, ρ); R^2 =0.969, Predictor z: Selected variables (ρ, v, C); R^2 =0.983, and Predictor q: Selected variables (P, CI, Ms); R^2 = 0.975.ANOVA results show that predictors A and B are the most influential for silt clay soil, with low p-values (<0.05). For silt loam soil, all predictors (x, y, z, and q) show strong correlations with draft force, except for some excluded variables like d and ρ.

Shear Stress and Deformation Effects on Draft Force: Maximum shear stress values increased with clay content and applied load. For Silt clay soil, it is from 0.001 N/m² at 615 N to 0.004 N/m² at 1515 N, and from 0.001N/m² at 615 N to 0.003 N/m² at 1515 N for Silt loam soil. Soil deformation increased with increased loads, particularly in soils with higher clay. The deformation of sand is reduced compared to clay and silt due to lower cohesive properties.

Prediction Models for Draft Force (ard plow): Mathematical equations were developed based on experimental data and regression analysis to predict draft forces.

Ard Plow in Silt Clay Soil: Combination of the effect of all significant predictors (A, B, C, D), the final draft force equation for silt clay soil is:

$$0.043\left(\frac{\rho^2 V^2}{C}\right) + 2.349\left(\frac{\mathrm{CI}\rho}{m_s}\right) + 31.413\left(\frac{\rho v^2}{\varphi}\right) + 57.73\left(\frac{p}{M}\right) = 285F_d$$

Combination of the effect of all significant predictors due to shear stress, deformation, and soil texture, the final draft force equation is:

$$F_d = -11.67\left(\frac{\tau g^4}{A}\right) - 46.8$$

In a unified model applied in silt clay soil, the contributions of each predictor are weighted based on their significance and influence on the draft force.

The general form of the unified draft force model of silt clay soil is:

$$F_d = 0.043\left(\frac{\rho^2 V^2}{C}\right) + 2.349\left(\frac{\mathrm{CI}\rho}{m_s}\right) + 31.413\left(\frac{\rho v^2}{\varphi}\right) + 57.73\left(\frac{p}{M}\right) - 11.67\left(\frac{\tau g^4}{A}\right) - 331.8$$

Combination of the effect of all significant predictors (x, y, q, z), the final draft force equation for silt loam soil is:

$$6.98\left(\frac{p\rho v^2 d^2 \alpha}{\varphi}\right) + 74.75\left(\frac{p\rho v^2 \lambda}{M}\right) + 31.86\left(\frac{p\rho^2 V^2}{C}\right) + 0.16\left(\frac{\mathrm{CI}p}{m_s}\right) = 277.7F_d$$

Combination of the effect of all significant predictors, the final draft force equation is:

$$F_d = -11.67\left(\frac{\tau g^4}{A}\right) - 46.8$$

The general form of the unified draft force model of silt loam soil is:

$$F_d = 6.98\left(\frac{p\rho v^2 d^2 \alpha}{\varphi}\right) + 74.75\left(\frac{p\rho v^2 \lambda}{M}\right) + 31.86\left(\frac{p\rho^2 V^2}{C}\right) + 0.16\left(\frac{\mathrm{CI}p}{m_s}\right) - 11.67\left(\frac{\tau g^4}{A}\right) - 264.8$$

Prediction Models for Draft Force (Scaled Moldboard Plows): Mathematical equations were developed based on experimental data and regression analysis to predict draft forces.

The general form of the unified draft force model of ¾-scaled bottom moldboard plows is expressed as follows:

$$F_d = -2.64\left(\frac{C\mathrm{w}d^2}{\mathrm{L}}\right) + \frac{Cgd^4}{Rv^2} - 11.67\left(\frac{\tau g^4}{A}\right) - 209.3$$

The general form of the unified draft force model of ½-scaled bottom moldboard plows is expressed as follows:

$$F_d = -2.66\left(\frac{C\mathrm{w}d^2}{\mathrm{L}}\right) + \frac{Cgd^4}{Rv^2} - 11.67\left(\frac{\tau g^4}{A}\right) - 213.3$$

Validation of Predictive Models: RRMSE (Relative Root Mean Square Error): Lower RRMSE indicates better model performance. Option 1 has an RRMSE of 0.093 for silt clay soil, significantly outperforming Option 2 (RRMSE = 0.246). For silt loam soil, the model achieves R^2 = 0.906, confirming strong predictive power. CRM (Correlation Ratio): CRM close to +1 indicates a strong positive correlation. Option 1 shows CRM = 0.842 for silt clay soil, while Option 2 is unreliable (CRM = -0.091). For silt loam soil, the model demonstrates an excellent correlation (R^2 = 0.906).

Optimization of Draft Force: Optimization techniques were employed to minimize draft force under varying conditions. Maximizing desirability score (0.99) identifies optimal

parameter settings of Silt Clay Soil. Maximizing desirability score (0.99) identifies optimal parameter settings of Silt Loam Soil.

This dissertation explores the prediction and optimization of draft forces for small-scale tillage tools, specifically focusing on ard plow and scaled moldboard plow in silt clay and silt loam soils. The study integrates soil properties, tool geometry, and operational parameters to develop robust mathematical models that enhance energy efficiency and tool performance during tillage operations.

Understanding the specific composition of soil helps optimize the design and operation of tillage tools, reducing energy consumption and improving efficiency. Optimizing p and λ minimizes draft force, enhancing tool efficiency and reducing power losses. Predicts A and B for the draft force of ard plow are most influential for silt clay soil, while x, y, z, and q effectively forecast draft force for silt loam soil. Both shear stress and deformation significantly affect draft force, with higher clay or silt content increasing resistance during tillage. Developed mathematical models exhibited high accuracy and reliability, with R^2 values exceeding 0.90 in most cases, making them valuable tools for predicting draft forces. The models are well-validated, with option 1 consistently outperforming Option 2 regarding accuracy and reliability. Optimization significantly reduces draft force, ensuring efficient tillage operations and minimal wear on equipment. This research contributes to sustainable agricultural practices by offering data-driven solutions for optimizing tillage operations.

Differences in moisture content, bulk density, cohesion, internal friction angle, and penetration resistance influence draft force requirements between silt clay and silt loam soils. Parameters p and λ strongly affect draft force, with higher values leading to more excellent resistance. Models: Developed equations achieve high predictive accuracy, validated through statistical metrics like R^2, RMSE, and CRM. Maximizing desirability scores (0.99) identifies optimal parameter settings for minimizing draft force.

This dissertation successfully develops and validates mathematical models for predicting draft forces in small-scale tillage tools, contributing to improved energy efficiency and tool performance. By addressing key variables and their interactions, the study offers actionable insights for stakeholders in agriculture and engineering. Further research could explore additional soil types and refine the models to address minor limitations observed in residual analysis and non-normality assumptions.

5.2 Future Research

1. The mathematical model developed the draft force for small-scale tillage tools, particularly the plow and moldboard. Further research on additional small-scale tillage tools is needed.

2. This study focused on oxen-drawn tillage tools, highlighting the need for research on other animal-drawn tools.

3. The field's soil primarily consisted of silt loam, and clay, which informed the mathematical model for predicting draft force. Additional research on other soil textures is required.

4. Data from soil bins improves the accuracy of controlling the operating conditions of tillage tools.

5. Stakeholders (governors, businessmen, can support to manufacture small scale tillage tools to smallholder farmers.

6. Policy makers support the finding by making it easily accusable by small-holder farmers.

7. Further study is needed to predict draft force related to Agronomist discipline.

8. Farmers should practice selecting appropriate power to till their land.

REFERENCE

A Loukanov, I., Uziak, J., & Michálek, J. (2018). Draught requirements of enamel coated animal drawn mouldboard plough. Research in Agricultural Engineering, 51(No. 2), 56–62. https://doi.org/10.17221/4903-rae

AbbaspourGilandeh, Y., Fazeli, M., Roshanianfard, A., Hernndez-Hernndez, M., Gallardo-Bernal, I., & Hernndez-Hernndez, J. L. (2020). Prediction of draft force of a chisel cultivator using artificial neural networks and its comparison with regression model. Agronomy. https://doi.org/10.3390/agronomy10040451

Abbaspour-Gilandeh, Y., Hasankhani-Ghavam, F., Shahgoli, G., Shrabian, V. R., & Abbaspour -Gilandeh, M. (2018). Investigation of the Effect of Soil Moisture Content, Contact Surface Material and Soil Texture on Soil Friction and Soil Adhesion Coefficients. Acta Technologica Agriculturae, 21(2), 44–50. https://doi.Org/10. 24 78/ ata-2018-0009

Ahmed, M. M. (2004). University of Khartoum Evaluation of Some Standards for Tillage Implement's Draft Requirements in Soba Area, Khartoum State, Sudan. University of Khartoum Compartive Study between calculated & measured conditions parameters under field. May 2009.

Akayuli, C., Ofosu, B., Nyako, S. O., & Opuni, K. O. (2013). The Influence of Observed Clay Content on Shear Strength and Compressibility of Residual Sandy Soils. International Journal of Engineering Research and Applications, 3(4), 2538–2542.

Al-Dosary, N. M. N., Al-Hamed, S. A., & Aboukarima, A. M. (2020). Application of adaptive neuro-fuzzy inference system to predict draft and energy requirements of a disk plow. Chinese Society of Agricultural Engineering. https://doi.org/10.25165/ j.Ij abe.20201302.4077

Al-Hamed, S., Wahby, M., Aboukarima, A., & Ahmed, K. (2014). Development of a Computer Program Using Visual Basic for Predicting Performance Parameters of Tillage Implements. Misr Journal of Agricultural Engineering, 31(3), 1157–1190. https://doi.org/10.21608/mjae.2014.99147

Algezi, A., & Almaliki, S. (2022). Prediction of Fuel Consumption Criteria of Tractor using Neural Networks and Mathematical Models. Ann. For. Res, 65(1), 8902–8922. https://www.e-afr.org

Alghazali, N. O. S. (2012). A new method of dimensional analysis (Fluid mechanics

applications). Jordan Journal of Civil Engineering, 6(3), 361–372.

Alimardani, R., Abbaspour-Gilandeh, Y., Khalilian, A., Keyhani, A., & Sadati, S. H. (2009). Prediction of draft force and energy of subsoiling operation using ANN model. Journal of Food, Agriculture and Environment, 7(3–4), 537–542.

Allison, P. D. (1999). Multiple Regression Multiple Multiple Regression. Practical Business Statistics, 1–81. https://linkinghub.elsevier. Com/retrieve/pii/ B9780 124250 20 00122

Almaliki, S. (2018). Simulation of draft force for three types of plows using response surface method under various field conditions. Iraqi Journal of Agricultural Sciences, 49(6), 1123–1124. https://doi.org/10.36103/ijas.v49i6.151

Anhalt, C. O., & Cortez, R. (2015). Mathematical Modeling: A Structured Process. The Mathematics Teacher, 108(6), 446–452. https://doi.org/ 10.5951/ math teacher. 108. 6.0446

arman, K., Marakolu, T., Taner, A., & tl, E. (2021). Prediction of draft force and disturbed soil area of a chisel tine in soil bin conditions using draft force and its comparison with regression model. None. https://doi.org/10.15316/sjafs.2020.229

Arman, K., tl, E., & Taner, A. (2019). Artificial neural network model for predicting specific draft force and fuel consumption requirement of a mouldboard plough. None. https:// doi.org/10.15316/sjafs.2019.183

Ashrafi, S. R. (2006). Modelling Energy Requirements by a Narrow Tillage Tool. Department of Agricultural and Bioresource Engineering, Degree of (July), 190.

Asonye, G. U., Asoegwu, S. N., Maduako, J. N., & Madubuike, C. N. (2019). a Mathematical Model for Predicting the Cutting Energy of Cocoyam (Colocasia Esculenta). 15(1), 174–189.

Aune, J. B., & Bussa, M. T. (2020). The ox ploughing system in Ethiopia: can it be sustained? December. https://doi.org/10.5367/000000001101293779

Aune, J. B., Bussa, M. T., Asfaw, F. G., & Ayele, A. A. (2001). The ox ploughing system in Ethiopia: Can it be sustained? Outlook on Agriculture, 30(4), 275–280. https:// doi. org/10.5367/000000001101293779

Aziz, M. (2023). Mechanical properties of a high plasticity clay mixed with sand and low-plastic silt. Materials Today: Proceedings, August. https://doi.org/10.1016/j.mat pr. 2023.08.012

Badalíková, B. (2010). Influence of Soil Tillage on Soil Compaction. January 2010, 19–30. https://doi.org/10.1007/978-3-642-03681-1_2

Bae, B. M., Kim, Y. S., Kim, W. S., Kim, Y. J., Lee, S. D., & Kim, T. J. (2023). The Development of a Draft Force Prediction Model for Agricultural Tractors Based on the Discrete Element Method in Loam and Clay Loam. Agriculture (Switzerland), 13(12). https://doi.org/10.3390/agriculture13122205

Baker, C. J. (2006). No-tillage drill and planter design-large-scale machines. No-Tillage Seeding in Conservation Agriculture: Second Edition, 185–203. https:// doi. org/ 10. 1079/9781845931162.0185

Barman, U., & Choudhury, R. D. (2020). Soil texture classification using multi class support vector machine. Information Processing in Agriculture, 7(2), 318–332. https:// doi. org/ 10.1016/j.inpa.2019.08.001

Basso, A. S., Miguez, F. E., Laird, D. A., Horton, R., & Westgate, M. (2013). Assessing potential of biochar for increasing water-holding capacity of sandy soils. GCB Bioenergy, 5(2), 132–143. https://doi.org/10.1111/gcbb.12026

Belachew, K. Y., Maina, N. H., Dersseh, W. M., Zeleke, B., & Stoddard, F. L. (2022). Yield Gaps of Major Cereal and Grain Legume Crops in Ethiopia: A Review. Agronomy, 12(10). https://doi.org/10.3390/agronomy12102528

Bello, R. S., Onu, B. O., & Ozor, T. A. (2023). Development of a Ride-On 2-Bottom Mouldboard Plough for Primary Tillage. Trends in Applied Sciences Research, 18(1), 191–200. https://doi.org/10.3923/tasr.2023.191.200

Blomkvist, J. (2011). Conceptualising Prototypes in Service Design (Issue 101).

Bravo, E. L., Suárez, M. H., Cueto, O. G., Coronel, C. I., & Ramon, H. (2016). Effect of Moisture and Soil Compaction on Tillage Operations. Revista Ciencias Técnicas Agropecuarias, March. http://www.redalyc. Org/articulo.oa?id =9324 26 98006

Brown, D. P. (2005). Artificial Intelligence for Creation of Rapid , Low-Cost Models and Simulations Technology and Engineering Dept .

Buckingham, E. (1914). On physically similar systems; Illustrations of the use of dimensional equations. Physical Review, 4(4), 345–376. https://doi.org/10.1103/ Phys Rev.4.345.

Candioti, L. V., De Zan, M. M., Cámara, M. S., & Goicoechea, H. C. (2014). Experimental design and multiple response optimization. Using the desirability function in analytical methods development. Talanta, 124, 123-138.

Cardei, P., Muraru, S. L., Sfiru, R., & Muraru, V. (2019). General structure of tillage draft force. Consequences in experimental and applicative research. INMATEH -

Agricultural Engineering, 59(3), 253–262. https://doi.org/10.35633/INMATEH-59-28

Cardei, P., Sfiru, R., Muraru, S., & Condruz, P. (2020). Soil moisture influences the soil tillage operations. E3S Web of Conferences, 180. https://doi.org/10.1051/e3 scnf/20 20 18003002

Casaburo, A., Petrone, G., Franco, F., & De Rosa, S. (2019). A Review of Similitude Methods for Structural Engineering. Applied Mechanics Reviews, 71(3). https://doi. org/10.1115/1.4043787

Chandio, F. A., Li, Y., Xu, L., Ma, Z., Ahmad, F., Cng, M., & Lakhiar, I. A. (2020). Predicting 3d forces of disc tool and soil disturbance area using fuzzy logic model under sensor-based soil-bin. Chinese Society of Agricultural Engineering. https://doi.org/10. 25165/j.ijabe.20201304.5115

Chimunhu, P., Shirani, R., Erkan, F., Mohammad, T., & Ali, W. (2024). Development of Novel Hybrid Intelligent Predictive Models for Dilution Prediction in Underground Sub - level Mining. Mining, Metallurgy & Exploration, 0123456789. https://doi.org/ 10.1007/s42461-024-01029-8

Crdei, P., Nuescu, C., Matache, M., & Cristea, O. (2021). Optimum working conditions for variable width ploughs. None. https://doi.org/10.35633/inmateh-65-26

Cunguara, B., Mather, D., Walker, T., Mouzinho, B., Massingue, J., & Uaiene, R. (2016). Exploiting the potential for expanding cropped area using animal traction in the smallholder sector in Mozambique. 15(April), 1–46.

Das, B. M. (2010). Principles of Geotechnical Engineering. Cengage Learning.

D'Annolfo, R., Gemmill-Herren, B., Graeub, B., & Garibaldi, L. A. (2017). A review of social and economic performance of agroecology. International Journal of Agricultural Sustainability, 15(6), 632–644. https://doi.org/ 10.1080/14735903. 2017. 1398123

Daum, T., Seidel, A., Awoke, B. G., & Birner, R. (2023). Animal traction, two-wheel tractors, or four-wheel tractors? A best-fit approach to guide farm mechanization in Africa. Experimental Agriculture, 59, e12. Doi: 10.1017/S0014479723000091

Deribe, Y., & Jaleta, M. (2019). Review of National Policies Influencing the Expansion of Agricultural Mechanization in Ethiopia. December 2019.

Dizaji, H. Z., Khorasani, M. E., Nategh, N. A., Sheikhdavoodi, M., & Andekaiezadeh, K. (2022). Specific draft modeling for combined and simple tillage implements. 24(4), 41–56.

Drwish, L. (2020). Modeling the Effect of Soil-Tool Interaction on Draft Force Using Visual

Basic. Annals of Agricultural Science, Moshtohor, 58(2), 223–232. https://doi.org/ 10. 21608/ assjm. 2020.112746

Ejiko, S. O., Ejiko, S. O., & Filani, A. O. (2021). Mathematical Modeling: A Useful Tool for Engineering Research and Practice. International Journal of Mathematics Trends and Technology, 67(9), 50–64. https://doi.org/10.14445/22315373/ijmtt-v67i9p506

Englis, B. G., & Frederiks, A. J. (2024). Using Experimental Designs to Study Entrepreneurship Education: A Historical Overview, Critical Evaluation of Current Practices in the Field, and Directions for Future Research. In Entrepreneurship Education and Pedagogy (Vol. 7, Issue 1, pp. 93–149). https://doi.org/10.1177/2515 12 74231161102.

Estrada-Díaz, J. A., Elías-Zúñiga, A., Martínez-Romero, O., Rodríguez-Salinas, J., & Olvera-Trejo, D. (2021). A mathematical dimensional model for predicting bulk density of inconel 718 parts produced by selective laser melting. Materials, 14(3), 1–20. https://doi.org/10.3390/ma14030512

Florence, F., Toyin, J., Olugbenga, O., Sunday, B., & Ezekiel, I. (2023). Changes in soil physical and mechanical properties under different tillage and cropping systems in al fi sol soil of southwestern Nigeria. Farming System, 1(3), 100050. https:// doi. org/ 10.1016/j.farsys.2023.100050

Friendly, M., & Denis, D. (2005). The early origins and development of the scatterplot. Journal of the History of the Behavioral Sciences, 41(2), 103–130. https://doi. org/ 10.1002/jhbs.20078

Garré, A. (2022). Farming with Draft Animals : Using Retro Innovations for Sustainable Agrarian Development. A case study of organic small-scale farming in Northern Italy. 1–94.

Gebregziabher, S., De Swert, K., Saeys, W., Ramon, H., De Ketelaere, B., Mouazen, A. M., Gebrehiwot, K., Deckers, J., & De Baerdemaeker, J. (2016). A mobile, in-situ soil bin test facility to investigate the performance of maresha plough. Biosystems Engineering, 149, 38–50. https://doi.org/10.1016/j.biosystemseng.2016.05.013

Gebregziabher, S., Mouazen, A. M., Van Brussel, H., Ramon, H., Nyssen, J., Verplancke, H., Behailu, M., Deckers, J., & De Baerdemaeker, J. (2006). Animal drawn tillage, the Ethiopian ard plough, maresha: A review. Soil and Tillage Research, 89(2), 129–143. https://doi.org/10.1016/j.still.2005.08.010.

Geiger M, Hockenhull J, Buller H, Tefera G, Getachew M, Burden FA and Whay H (2020)

understanding the attitudes of communities to the social, economic, and cultural importance of working donkeys in rural, peri-urban, and urban areas of Ethiopia. Frontiers in Veterinary Science 7. https://doi org/10.3389/fvets202000060.

Gelaw, A. M., & Ababa, A. (2018). Climate-Smart Agriculture in Ethiopia. January 2017.

Geza, M. (1969). Harnessing techniques and work performance of draft horses in Ethiopia.

Gowers, W. (1895). This is a reproduction of a library book that was digitized by Google as part of an ongoing effort to preserve the information in books and make it universally accessible. https://books.google.com. Oxford University, I, 60.

Guadie, A. F., Degu, Y. M., & Firew Guadie, Y. (2018). Design, Fabrication and Testing of Animal Drawn Multiple Mouldboard Plough. World Journal of Agricultural Sciences, 14(5), 151–162. https://doi.org/10.5829/idosi.wjas.2018.151.162

Guthiga, P. M., Karugia, J. T., & Nyikal, R. A. (2007). Does use of draft animal power increase economic efficiency of smallholder farms in Kenya? Renewable Agriculture and Food Systems, 22(4), 290–296. https://doi.org/10.1017/S174217050700186X

Hajiahmadi, S., Elyasi, M., & Shakeri, M. (2019). Investigation of a new methodology for the prediction of drawing force in deep drawing process with respect to dimensionless analysis. International Journal of Mechanical and Materials Engineering, 14(1). https://doi.org/10.1186/s40712-019-0110-9

Hales, T. C., & Miniat, C. F. (2017). Soil moisture causes dynamic adjustments to root reinforcement that reduces slope stability. Earth Surface Processes and Land forms, 42(5), 803-813.

Higgins, T. J., & Moran, M. J. (1968). Similitude: Theory and applications. Journal of the Franklin Institute, 285(6), 495–497. https://doi.org/10.1016/0016-0032 (68)90058-6

Hocking, R. R. (2013). Methods and applications of linear models: regression and the analysis of variance. John Wiley & Sons.

Hormazabal, C. C.-T. & E. (2018). Computational tools for the determination of factors of safety and location of the critical circular failure surface for slopes in Mohr-Coulomb dry ground. Slope Stability Analysis in Mohr-Coulomb Dry Ground, 1–18.

Imhoff, S., Da Silva, A. P., Ghiberto, P. J., Tormena, C. A., Pilatti, M. A., & Libardi, P. L. (2016). Physical quality indicators and mechanical behavior of agricultural soils of Argentina. PLoS ONE, 11(4), 1–21. https://doi.org/10.1371/journal.pone.0153827

Jiang, Q., Cao, M., Wang, Y., Wang, J., & He, Z. (2021). Estimation of Soil Shear Strength Indicators Using Soil Physical Properties of Paddy Soils in the Plastic State. Applied

Sciences, 11(12), 5609. https://doi.org/10.3390/app11125609

Jiang, X., Tong, J., Ma, Y., & Sun, J. (2020). Development and verification of a mathematical model for the specific resistance of a curved subsoiler ScienceDirect Development and verification of a mathematical model for the specific resistance of a curved subsoiler. Biosystems Engineering, 190(31970454), 107–119. https://doi.org/ 10.1016/j.biosystemseng.2019.12.004

Jiménez, P. G., Fish, A., & Bosch, C. E. (2022). Unlocking Scientific Knowledge with Statistical Tools in JMP Benefits and challenges of new statistical tools. Johnson Matthey Technology Review, 66(2), 198–211. https://doi.org/10.1595/ 20565 1322 X16445719154043

Karmakar, S., & Lal Kushwaha, R. (2005). CFD simulation of soil forces on a flat tillage tool. 2005 ASAE Annual International Meeting, January 2005. https://doi.org/ 10. 13 031/2013.18880

Kenny, D. A., & Editor, S. (2007). Confirmatory factor analysis for applied research. In Choice Reviews Online (Vol. 44, Issue 05). https://doi.org/10.5860/choice.44-2769

Kim, Y. S., Lee, S. D., Baek, S. M., Baek, S. Y., Jeon, H. H., Lee, J. H., Kim, W. S., Shim, J. Y., & Kim, Y. J. (2022). Analysis of the Effect of Tillage Depth on the Working Performance of Tractor-Moldboard Plow System under Various Field Environments. Sensors, 22(7). https://doi.org/10.3390/s22072750

Kirchner, S. (2022). The World Bank Aids Smallholder Farmers in Ethiopia. In World Bank. https://doi.org/10.1016/j.gecco.2019.e00539 0A

Kome, G. K., Enang, R. K., Tabi, F. O., & Yerima, B. P. K. (2019). Influence of Clay Minerals on Some Soil Fertility Attributes: A Review. Open Journal of Soil Science, 09(09), 155–188. https://doi.org/10.4236/ojss.2019.99010

Koolen, A. J., & Kuipers, H. (1983). Agricultural soil mechanics. In Agricultural soil mechanics. https://doi.org/10.1016/0308-521x(84)90019-2

Kotrocz, K., Mouazen, A. M., & Kerényi, G. (2016). Numerical simulation of soil-cone penetrometer interaction using discrete element method. Computers and Electronics in Agriculture, 125(July), 63–73. https://doi.org/10.1016/j.compag.2016.04.023

Kyalo, N., & Nairobi, O. (2019). University of Nairobi School of Engineering. 2011 (July).

Labuz, J. F., & Zang, A. (2012). Mohr-Coulomb failure criterion. Rock Mechanics and Rock Engineering, 45(6), 975–979. https://doi.org/10.1007/s00603-012-0281-7

Liu, K., Benetti, M., Sozzi, M., Gasparini, F., & Sartori, L. (2022). Soil Compaction under

Different Traction Resistance Conditions—A Case Study in North Italy. Agriculture (Switzerland), 12(11). https://doi.org/10.3390/agriculture12111954

Ma, L., Qi, J., Yu, F., & Yao, X. (2016). Experimental study on variability in mechanical properties of a frozen sand as determined in triaxial compression tests. Acta Geotechnica, 11(1), 61–70. https://doi.org/10.1007/s11440-015-0391

MacLaren, C., Storkey, J., Menegat, A., Metcalfe, H., & DehnenSchmutz, K. (2020). An ecological future for weed science to sustain crop production and the environment. A review. Springer Science Business Media. https://doi.org/10.1007/s13593-020-006316

Mahmood, M. S., & Abrahim, M. J. (2021). A Review of Collapsible Soils Behavior and Prediction. IOP Conference Series: Materials Science and Engineering, 1094(1), 012044. https://doi.org/10.1088/1757-899x/1094/1/012044

Mahoney, J. F., & Yeralan, S. (2019). Dimensional analysis. Procedia Manufacturing, 38 (2019), 694–701. https://doi.org/10.1016/j.promfg.2020.01.094

Makange, N. R., Ji, C., Nyalala, I., Sunusi, I. I., & Opiyo, S. (2021). Prediction of precise subsoiling based on analytical method, discrete element simulation and experimental data from soil bin. Scientific Reports, 11(1), 1–12. https://doi.org/10.1038/s41598-021-90682-w

Makange, N. R., Okinda, C., Soomro, S. A., & Ji, C. (2020). Approaches used to model prediction of cutting forces for tillage tools: A review. International Agricultural Engineering Journal, 29(2), 34–44.

Malvajerdi, A. S. (2023). Wear and coating of tillage tools: A review. Heliyon, 9(6), e16669. https://doi.org/10.1016/j.heliyon.2023.e16669

Mckyes E. (1989). McKyes Agric Soil Mechamnics (pp. 192–193).

Midi, H., Sarkar, S. K., & Rana, S. (2010). Collinearity diagnostics of binary logistic regression model. Journal of Interdisciplinary Mathematics, 13(3), 253–267. https://doi.org/10.1080/09720502.2010.10700699

Misic, T., Najdanovic-Lukic, M., & Nesic, L. (2010). Dimensional analysis in physics and the Buckingham theorem. European Journal of Physics, 31(4), 893.

Moinfar, A. M., & Shahgholi, G. (2018). Dimensional Analysis of the Tractor Tractive Efficiency Parameters. Acta Technologica Agriculturae, 21(3), 94–99. https:// doi. org/10.2478/ata-2018-0017

Mwiti, F. M., Gitau, A. N., & Mbuge, D. O. (2023). Effects of soil-tool interaction and mechanical pulverization of arable soils in tillage-a comprehensive review. Agricultural

Engineering International: CIGR Journal, 25(3), 75–94. https://doi.org/10.2139/ssrn.4891651

Naji Al-Dosary, N. M., Aboukarima, A. M., Al-Hamed, S. A., Zayed, M. F., Marey, S. A., & Kayad, A. (2023). Modification of Values for the Horizontal Force of Tillage Implements Estimated from the ASABE Form Using an Artificial Neural Network. Applied Sciences (Switzerland), 13(13), 1–22. https://doi.org/10.3390/app13137442

Nebiolo, A. (1958). Regression in Spss. None, 49(16), 697–699.

Neuberger, A., Peles, S., & Rittel, D. (2007). Scaling the response of circular plates subjected to large and close-range spherical explosions. Part I: Air-blast loading. International Journal of Impact Engineering, 34(5), 859–873. https://doi.org/ 10. 10 16/ jimpeng. 2006.04.001

Nikiforova, A. A. (2019). Soil classification. Knowledge Organization, 46(6), 467–488. https://doi.org/10.5771/0943-7444-2019-6-467

Oduma, O., Oluka, S. I., & Eze, P. C. (2018). Effect of soil physical properties on performance of agricultural field machinery in southeastern Nigeria. AgricEngInt: CIGR Journal, 20(1), 25–31.

Ogunnigbo, C. O., Adetan, D. A., & Morakinyo, T. A. (2022). A study on the mathematical model for predicting the peel removal efficiency of a cassava peeler. Research in Agricultural Engineering, 68(1), 18–26. https://doi. org/ 10. 17 221/ 32/ 2021-RAE

Okoko, P., Ajav, E. A., & Olosunde, W. A. (2018). Draft and power requirements for some tillage implements operating in clay loam soil. Agricultural Engineering International: CIGR Journal, 20(1), 95–102.

Okyere, F. G., Qasim, W., Basak, J. K., Khan, F., Lee, Y. J., Park, J., Arulmozhi, E., Yoon, Y. C., Kang, D. S., & Kim, H. T. (2019a). Analysis of Draft Force Requirement of a Compact Disc Harrow and Model Development for Future Predictions. Journal of Biosystems Engineering, 44(2), 47–56. https://doi.org/10.1007/S42853-019-00003-3

Ortopan, M., Simonović, V., Tasić, N., Veg, E., Zlatanović, I., & Gubeljak, N. (2024). Analyzing Site-Specific Tractor Draft Force in Different Passes during Plowing. Tehnicki Vjesnik, 31(1), 228–232. https://doi.org/10.17559/TV-20230614000733

Pan, Q., Reitmayr, G., & Drummond, T. (2009). ProFORMA: Probabilistic feature-based on-line rapid model acquisition. British Machine Vision Conference, BMVC 2009 - Proceedings, May. https://doi.org/10.5244/C.23.112

Pandey, M. (2006). Present status and future requirement of farm equipment for crop

production. Made Avail by Central Institute of Agricultural 95, 69–113. http:// agric oop.nic.in/farm mech. pdf/05024-05.pdf

Patel, R. R., Thompson, D. S., Riveros, G. A., Hodo, W. D., Peters, J. F., & Acosta, F. J. (2020). Dimensional analysis of structural response in complex biological structures. Mathematics and Computers in Simulation, 172, 305–320. https: //doi.org/ 10.1016/ j. matcom.2019.12.001

Pratap, S., Datta, S., & Sharma, V. (2023). Determination of surface roughness of micro rods fabricated by reverse μEDM using dimensional analysis. International Journal of Advanced Manufacturing Technology, 128(7–8), 3649–3659. https://doi.org/ 10.1007 /s00170-023-12131-4

R.K. Gupta, R. K. N., Ashish Dwivedi, R. S. R., Vineet Kumar, M. K., Amit Kumar, A. K. S., S.P. Singh, V. S., Yogesh Kumar, S. T., & Mahajan, N. C. (2017). Crop Residue Management and Soil Health with Changing Climate in Smallholders Farming: A Subtropical Indian Perspective. International Journal of Current Microbiology and Applied Sciences, 6(2), 1591–1609. https://doi.org/10.20546/ijcmas.2017.602.178

Ranjbar, I., Rashidi, M., Najjarzadeh, I., Niazkhani, A., & Niyazadeh, M. (2013). Modeling of moldboard plow draft force based on tillage depth and operation speed. Middle East Journal of Scientific Research, 17(7), 891–897. https://doi.org/10. 5829/ idosi. mejsr. 2013.17.07.12232

Regassa, A., et al. (2023): "Major Soil Types" in The Soils of Ethiopia (Springer) details soil diversity and distribution.

Reichert, J. M., da Rosa, V. T., Vogelmann, E. S., da Rosa, D. P., Horn, R., Reinert, D. J., Sattler, A., & Denardin, J. E. (2016). Conceptual framework for capacity and intensity physical soil properties affected by short and long-term (14 years) continuous no-tillage and controlled traffic. Soil and Tillage Research, 158, 123–136. https://doi.org/10.10 16/j.still.2015.11.010

Reicosky, D. C. (2001). Effects of Conservation Tillage on Soil Organic Carbon Dynamics: Field Experiments in the U.S. Corn Belt. Sustaining the Global Farm. Selected Papers from the 10th International Soil Conservation Organization Meeting, 1, 481–485. http://www.sdsoil.com/wp-content/uploads/2014/11/Carbon.pdf

Riaz, M., Ahmad, S., Ashraf, H., Awais, M., Hussain, G., & Saeed, M. (2023). Structural Optimization of Chisel Plough. AMA-Agricultural Mechanization in Asia Africa and Latin America, 54(04), 12625–12638.

RiazSalman, N. D. (2020). Effect of bulk density and moisture content of soil on the penetration resistance and penetration depth. June.

Sadek, M. A., Chen, Y., & Zeng, Z. (2021). Draft force prediction for a high-speed disc implements using discrete element modelling. Biosystems Engineering, 202, 133–141. https://doi.org/10.1016/j.biosystemseng.2020.12.009

Saunders, C., Godwin, R. J., Dogherty, M. J. O., & Mk, B. (2007). Prediction of Soil Forces Acting on Mouldboard Ploughs. Journal of Terramechanics, 44(1968), 3–14.

Schweitzer, F., Bitsch, G., & Louw, L. (2023). Choosing Solution Strategies for Scheduling Automated Guided Vehicles in Production Using Machine Learning. Applied Sciences (Switzerland), 13(2). https://doi.org/10.3390/app13020806

Shafii, S., Upadhyaya, S. K., & Garrett, R. E. (1996). Empirical prediction equations : a case study. 39(2), 377–384.

Shahhosseini, M., Hu, G., Huber, I., & Archontoulis, S. V. (2021). Coupling machine learning and crop modeling improves crop yield prediction in the us corn belt. Nature Portfolio. https://doi.org/10.1038/s41598-020-80820-1

Simonyan, K. J., Y. D. Yiljep and O. J. Mudiare (2006). Modelling the Cleaning Process of a Stationary Sorghum Thresher. Agricultural Engineering International: the CIGR Ejournal: Modeling the Grain Cleaning Process of a Stationary Sor. January 2006.

Slezingr, M., & Purcz, P. (2013). Sciences A model based on dimensional analysis for prediction of nitrogen and phosphorus concentrations at the river station Iˇ. 201–209. https://doi.org/10.5194/hess-17-201-2013

Smith, T. W., & Strahan, D. (2004). Toward a prototype of expertise in teaching: A descriptive case study. Journal of Teacher Education, 55(4), 357–371. https://doi.org/10.1177/0022487104267587

Smolders, S. (2017). Measurement of draught requirement of ard plough working in vertisol of ethiopian highlands. July 2006. https://doi.org/10.13140/ RG.2.2. 29638. 06723

Sousseau, Y., Elachachi, S. M., Chaplain, M., Faye, C., Catterou, T., & Garcia, P. (2021). Characterization of timber connection behaviour from reduced scaled experiments based on similitude laws. World Conference on Timber Engineering 2021, WCTE 2021.

Szirtes, T., & Rozsa, P. (2007). List of titled examples and problems. In Applied Dimensional Analysis and Modeling (Issue December). https://doi.org/10.1016/b978-012370620-1/50000-9

Takele, A., & Selassie, Y. G. (2018). Socio-economic analysis of conditions for adoption of tractor hiring services among smallholder farmers, Northwestern Ethiopia of tractor hiring services among smallholder. Cogent Food & Agriculture, 4(1), 1–15. https://doi.org/10.1080/23311932.2018.1453978

Tariku, G. D., Biza, T. D., Tesfaye, S. K., & Kebede, S. A. (2025). Working animal welfare and their multidimensional roles on livelihood improvement in Ethiopia: A systematic review and meta-analysis. Animal Welfare, 34. https:// doi.org/ 10.1017/ awf.2024.68

Tegegn, H., Senbetie, T., Abrham, S., Tagese, A., & Sisay, B. (2024). Socio-Economic Determinants of Smallholder Farmers' Coffee Production in Wolaita Zone, Ethiopia. African Journal of Food, Agriculture, Nutrition and Development, 24(6), 26798–26818. https://doi.org/10.18697/ajfand.131.24465

Tekeste, M. Z., Way, T. R., Syed, Z., & Schafer, R. L. (2020). Modeling soil-bulldozer blade interaction using the discrete element method (DEM). Journal of Terra mech anics, 88, 41–52. https://doi.org/10.1016/j.jterra.2019.12.003

Temesgen, M., Rockstrom, J., Savenije, H. H. G., Hoogmoed, W. B., & Alemu, D. (2008). Determinants of tillage frequency among smallholder farmers in two semi-arid areas in Ethiopia. Physics and Chemistry of the Earth, 33(1–2), 183–191. https://doi.org/ 10.1016/j.pce.2007.04.012

Thorp, K. R., Malone, R. W., & Jaynes, D. B. (2007). Simulating long-term effects of nitrogen fertilizer application rates on corn yield and nitrogen dynamics. Transactions of the ASABE, 50(4), 1287–1303.

Tsige, M., Synnevåg, G., & Aune, J. B. (2020). Gendered constraints for adopting climate-smart agriculture amongst smallholder Ethiopian women farmers. Scientific African, 7, e00250. https://doi.org/10.1016/j.sciaf.2019.e00250

Turner, P. (2020). Critical values for the Durbin-Watson test in large samples. Applied Economics Letters, 27(18), 1495–1499. https://doi.org/10.1080/ 13504851. 2019. 16 91711

Twomlow, S., Riches, C., O'Neill, D., Brookes, P., & Ellis-Jones, J. (1999). Sustainable Dryland Smallholder Farming in Sub-Saharan Africa. Annals of Arid Zone, 38(2), 93–135.

Usaborisut, P., & Ampanmanee, J. (2015). Compaction properties of silty soils in relation to soil texture, moisture content and organic matter. American Journal of Agricultural and Biological Science, 10(4), 178–185. https://doi.org/10.3844/ajabssp.2015.178.185

V. I. O. Ndirika. (2006). a Mathematical Model for Predicting Output Capacity of Selected Stationary Spike-Tooth Grain Threshers. Applied Engineering in Agriculture, 22(2), 195–200. https://doi.org/10.13031/2013.20281

Wang, C., Gao, F., Tan, X., & Xu, W. (2022). A modified method for improving the prediction accuracy of the tunnel shaking table model test based on non-direct similarity technique. Systems Science and Control Engineering, 10(1), 104–114. https:// doi.org/ 10.1080/21642583.2022.2040061

Wang, H., Zhuang, J., Qi, H., & Yu, J. (2020). Effects of bionic curves on penetration force under different soils. Multidisciplinary Digital Publishing Institute. https:// doi.org/ 10. 3390/app10020529

Wittwer, R., Bender, S. F., Hartman, K., Hydbom, S., Lima, R. A. A., Loaiza, V., Nemecek, T., Oehl, F., Olsson, P. A., Petchey, O. L., Prechsl, U. E., Schlaeppi, K., Scholten, T., Seitz, S., Six, J., & Heijden, M. G. A. V. D. (2021). Organic and conservation agriculture promotes ecosystem multi-functionality. American Association for the Advancement of Science. https://doi.org/10.1126/sciadv.abg6995

Zerssa, G., Feyssa, D., Kim, D., & Eichler-löbermann, B. (2021). Challenges of Smallholder Farming in Ethiopia and Opportunities by Adopting Climate-Smart Agriculture. 1–25

Zhang, X., Zhang, L., Hu, X., Wang, H., Shi, X., & Ma, X. (2022). Simulation of soil cutting and power consumption optimization of a typical rotary tillage soil blade. Multidisciplinary Digital Publishing Institute. https://doi.org/10.3390/app12168177

APPENDICES

APPENDIX I: Samples of soil engineering properties, Ard Plow Geometry and Operating Conditions in silt clay soil

The samples of soil engineering properties and operating condition in silt clay soil of implement mass (m_s), soil moisture content (M), bulk density (ρ), soil cohesion (Ca), soil internal friction angle (φ), operating depth (d), velocity (v), distance between leather stripe (metal loops) and share (p), operator operating angle (λ) and rack angle (α) are shown in the following table.

Operating condition			Plow Geometry			Physical property		Mechanical property			Measured force
d (m)	v (m/s)	λ (^{0})	α (0)	P (cm)	M_s (kg)	ρ (g/cm^3)	M (%)	φ 0	Ca (KPa)	CI (KPa)	F_d
0.1	0.61	57	20	0.15	14	12	24.84	27.18	19.44	1.58	436
0.1	0.61	57	20	0.15	14	12	25.36	27.16	19.47	1.61	426
0.1	0.61	57	20	0.15	14	12.1	26.4	27.21	19.49	1.63	439
0.15	0.61	60	21	0.15	14	12.2	26.9	27.22	19.54	1.66	423
0.15	0.61	60	21	0.15	14	12.2	26.79	27.25	19.55	1.63	428
0.15	0.61	60	21	0.15	15	12.2	27.2	27.25	19.58	1.75	445
0.2	0.63	63	23	0.15	15	12.3	28.1	27.48	19.58	1.74	450
0.2	0.63	63	23	0.15	15	12.3	29.19	27.52	19.62	1.8	447
0.2	0.63	63	23	0.15	15	12.3	29.2	27.55	19.64	1.89	449
0.1	0.63	57	20	0.18	14	12.5	29.42	27.66	19.75	1.92	450
0.1	0.63	57	20	0.18	14	12.7	29.29	27.72	19.79	1.92	452
0.1	0.63	57	20	0.18	14	12.9	29.7	27.77	19.88	1.94	459
0.15	0.65	60	21	0.18	14	12.9	29.7	27.78	19.95	1.96	467
0.15	0.65	60	21	0.18	14	13.3	30.07	27.76	19.98	1.97	538
0.15	0.65	60	21	0.18	15	13.5	30.21	27.81	19.99	1.98	588
0.2	0.65	63	23	0.18	15	13.8	29.6	27.88	20.11	2.01	596
0.2	0.65	63	23	0.18	15	14.8	30.12	27.91	20.27	2.09	602
0.2	0.65	63	23	0.18	15	14.9	23.1	27.93	20.33	2.1	605

APPENDIX II: Samples of soil engineering properties, Ard Plow Geometry and Operating Conditions in silt clay soil

The samples of soil engineering properties and operating condition in silt loam soil are shown in the following table.

Operating condition			Plow Geometry			Physical property		Mechanical property			Measured force
d (m)	v (m/s)	λ (^{0})	α (0)	P (cm)	M_s (kg)	ρ (g/cm^3)	M (%)	φ 0	Ca (KPa)	CI (KPa)	F_d
0.1	0.61	57	20	0.15	14	10.7	0.29	26.28	19.34	1.58	450.5
0.1	0.61	57	20	0.15	14	10.8	0.3	26.29	19.44	1.61	454.5
0.1	0.61	57	20	0.15	14	11.2	0.3	26.33	19.56	1.63	460.5
0.15	0.61	60	21	0.15	14	11.7	0.29	26.39	19.64	1.66	470.5
0.15	0.61	60	21	0.15	14	11.2	0.3	26.39	19.61	1.63	460
0.15	0.61	60	21	0.15	15	12.2	0.31	26.43	19.78	1.75	498
0.2	0.63	63	23	0.15	15	12.2	0.29	26.26	19.78	1.74	496.5
0.2	0.63	63	23	0.15	15	13.1	0.3	26.29	19.82	1.8	502
0.2	0.63	63	23	0.15	15	13.6	0.31	26.43	19.94	1.89	537
0.1	0.63	57	20	0.18	14	13.9	0.29	26.48	20	1.92	568.5
0.1	0.63	57	20	0.18	14	13.9	0.3	26.49	20	1.92	568
0.1	0.63	57	20	0.18	14	14.1	0.31	26.54	20.01	1.94	571
0.15	0.65	60	21	0.18	14	14.3	0.29	26.59	20.03	1.96	581
0.15	0.65	60	21	0.18	14	14..30	0.3	26.62	20.11	1.97	586
0.15	0.65	60	21	0.18	15	14.3	0.31	26.65	20.21	1.98	593.5
0.2	0.65	63	23	0.18	15	14.7	0.29	26.66	20.31	2.01	602
0.2	0.65	63	23	0.18	15	14.8	0.3	26.69	20.47	1.98	612
0.2	0.65	63	23	0.18	15	14.9	0.31	26.72	20.59	2.01	615

APPENDIX III: Amount of shear stresses in silt soil on selected draft forces

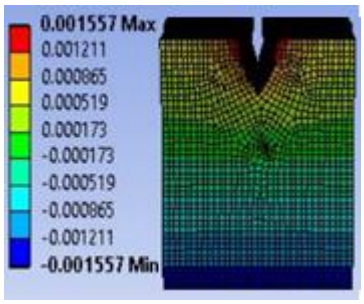

615 N

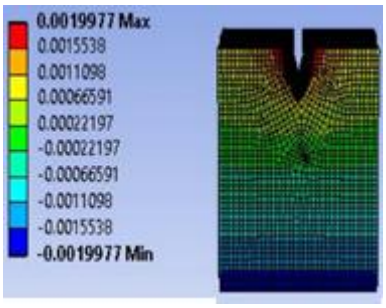

815 N

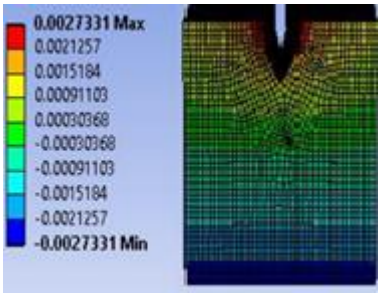

1115 N

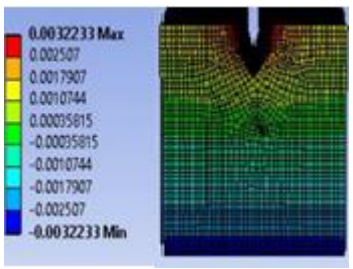

1315 N

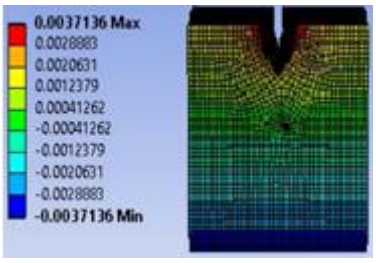

1515 N

APPENDIX IV: Amount of Shear stresses in the sand soil under selected draft forces

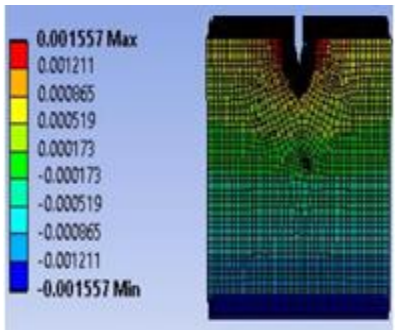

615 N

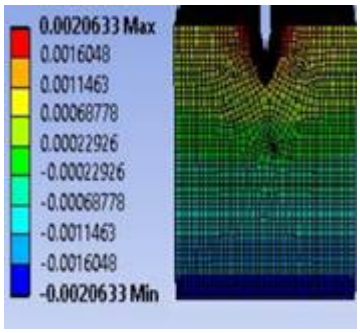

815 N

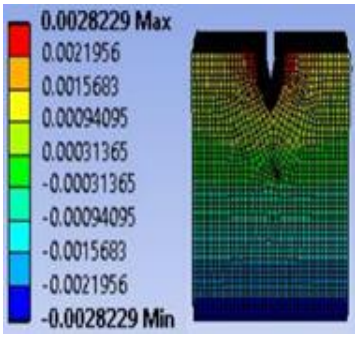

1115 N

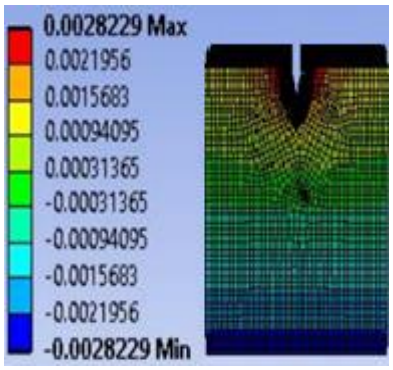

1315 N

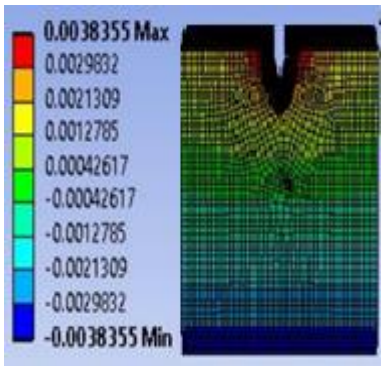

1515 N

APPENDIX V Amount of deformation in silt soil on selected draft forces

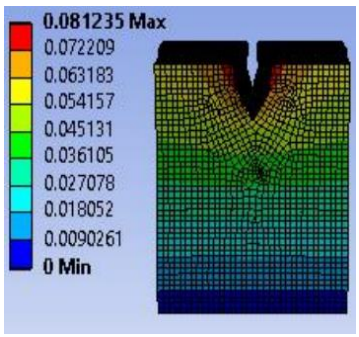

615 N

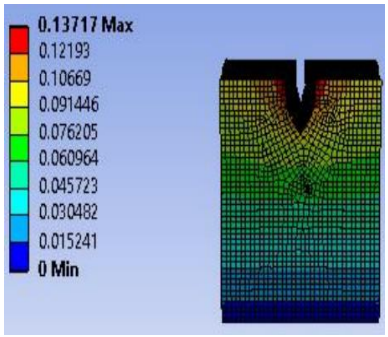

815 N

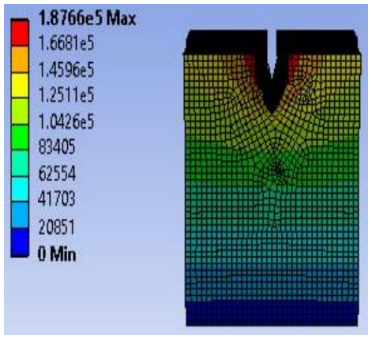

1115 N

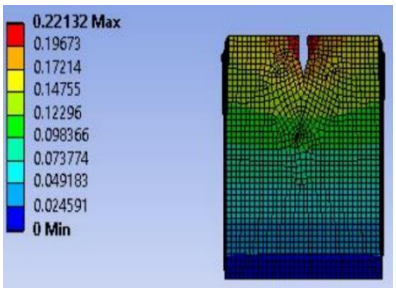

1315 N

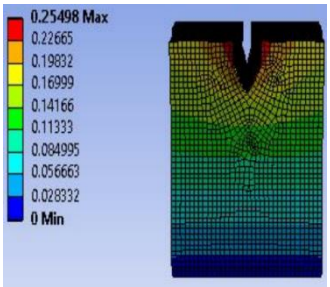

1515 N

APPENDIX VI Amount of deformation in the sand soil under selected draft forces

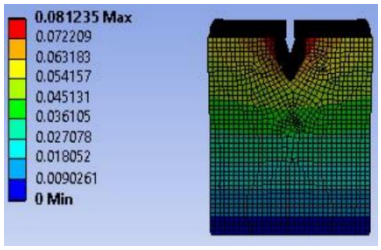

615 N

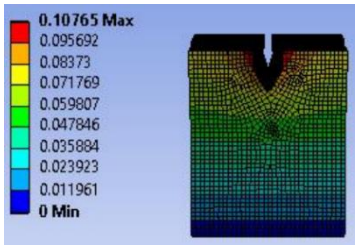

815 N

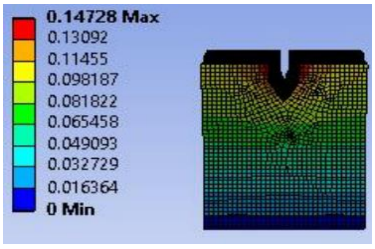

1115 N

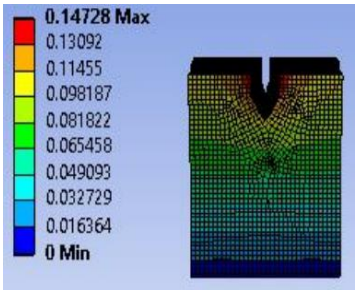

1315 N

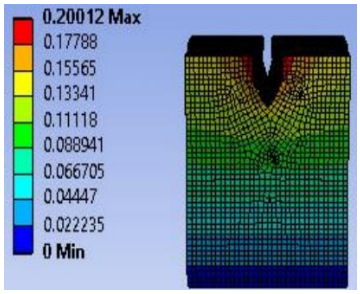

1515 N